

Evaluation of contained ilmenite in the Franklin sills and dykes of the Steensby Land and Moriusaq

Troels F. D. Nielsen, Thomas F. Kokfelt & Samuel M. Weatherley



Evaluation of contained ilmenite in the Franklin sills and dykes of the Steensby Land and Moriusaq

Troels F. D. Nielsen, Thomas F. Kokfelt & Samuel M. Weatherley

Contents

Summary of observations and recommendations	4
Introduction	6
Scope of the investigation	6
Regional geology	8
The Thule Basin	8
Geological setting.	9
Age.....	9
Thickness of formations.....	9
Metamorphism and structure.	10
Location.	10
The Steensby Land Sill Complex.....	11
Constructed cross sections	12
Moriusaq East.....	12
Constructed profile.....	16
Moriusaq West.....	18
Constructed profile.....	20
Stratigraphic proportions of sills in the Dundas Formation	22
Franklin dykes	23
Evaluation of volumetric proportions of sill material	23
Regional (blocks A-K)	24
Mineralogical investigation	26
Petrography on basis of backscatter images.....	26
Sample GGU 166673, east coast of Granville Fjord.....	26
Sample GGU 166672, east coast of Granville Fjord	28
Sample GGU 166624, Sill on shore NW of Booth Sund	29
Sample GGU 166671: Granville Fjord	31
Sample GGU 166635, E-shore of Booth Sund	32
Sample 166670, western shore inner Granville Fjord.....	35
Sample 243559, Dundas Fjeld, Thule.....	36
Sample 212513, N-shore Northumberland Ø East	39
Sample GGU 166143, S-shore Olrik Fjord	41
Sample 212556, Northumberland and Ø N-shore	43
Sample 243410, western Inglefield Land.....	47
Summary of petrographic observation.....	48
Compositions of ilmenite, titanomagnetite and magnetite.	49
Ilmenite	49
Titanomagnetite and magnetite	49
Compositional diagrams	51
<i>Ilmenite, titanomagnetite and magnetite.</i>	51

<i>Ilmenite diagrams</i>	52
<i>Titanomagnetite and magnetite diagrams</i>	51
Laser ICP-MS compositions of ilmenite.....	52
Observed compositions relative to specifications for ilmenite	53
Bulk rock compositions	56
Evaluation of primary magnetite and ilmenite content and proportions	56
Ilmenite made available by erosion	58
Regional evaluation	58
Northern Moriusaq block	61
Model 1	61
Model 2	62
Dykes	63
Total ilmenite for Moriusaq Block south of watershed:	64
Summary of calculated ilmenite	64
References	65
Appendixes 1-5	

Summary of observations and recommendations

- Bulk rock and mineral compositions suggest that the Franklinian magmatism in the Steensby Land Sill Complex and the slightly younger but related dykes represent a suite of tholeiitic magmas characterized by elevated FeO* (all Fe as FeO), TiO₂ and P₂O₅. Most likely, they are representatives of a major magmatic event through thick crust below the Thule basin.
- The dykes as well as the sills contain magnetite or replaced magnetite and fresh ilmenite. Primary titanomagnetite is extensively exsolved and resulting Ti-poor magnetite is commonly altered. Some sill samples have no magnetite at all, despite high V and Cr contents that would suggest the presence of magnetite. Calculated CIPW mineral norms suggest that the sill and dyke rocks on average originally contained c. 6 wt% titaniferous magnetite and had an ilmenite to titanomagnetite ratio of 1±0.4.
- The CIPW norms suggest a potential for ca. 9 wt% ilmenite in the rock. The number would be a little lower as some Ti-magnetite remains in some samples and the most plausible average ilmenite content in the sill and dyke rocks is 7 wt. %.
- The absence or very low concentrations of magnetite in the sill and dyke rocks reflect the alteration of the rocks. This is probably the result of (i) the emplacement of the magma in a water-bearing sedimentary succession, (ii) the accumulation of heat and (iii) a long cooling period in the heavily sill injected shales of the Dundas Formation. This mode of emplacement appears critical for the style alteration of the FeTi-oxides and for the formation of the ilmenite deposits at Moriusaq. Secondary alteration processes caused primary titanomagnetite to exsolve into low-Ti magnetite and secondary ilmenite. The primary and secondary ilmenite have different trace element characteristics. In many samples the secondary magnetite was then partially replaced by hydrous silicate phases.
- High TiO₂ in the emplaced magmas is a contributing factor to generating ilmenite-rich deposits in Steensby Land, but the exsolution and formation of “cleaned” ilmenite by exsolution and the subsequent loss of the magnetite is a prerequisite for the development of the ilmenite deposits along the south coast of Steensby Land.
- Concentrations of FeTi-oxide minerals in beach deposits would be dominated by ilmenite, as most magnetite was altered to silicate minerals or oxidized and readily subjected to dissolution during erosion and re-deposition in the fluvial or marine environment
- The volumes of magmatic rocks are difficult to estimate with high precision, but gigatons (Gt) of basalt have been eroded, and dependent on chosen constraints at least 5-9 Gt tons of ilmenite have been made available for redistribution in the fluvial and marine environment.
- The shore and near shore deposits within the presently investigated Moriusaq block are derived from sills and dykes south of the watershed some 5 km inland and are estimated to have fed up to 0.7 Gt ilmenite into the coastal environment.
- North of the watershed the Moriusaq Block is eroded and the broad E-W valley represents an eroded volume of Dundas Formation and included sills. Calculated to

the northern margin valley more than 1.6 Gt of ilmenite were made available for deposition in the valley or in Granville Fjord in post-glacial times. Calculated to the fault between Dundas and Qaanaaq Formations as much as ~3 Gt ilmenite may have been supplied to the E-W valley and the eastern shore of Granville Fjord.

- The sediment-rich shores west and northwest of Granville Fjord and in Booth Sund are situated next to a large number of sills, and as such would seem to be areas in which large tonnages of ilmenite could have been deposited.

Introduction

The present investigation aims at an evaluation of the potential resource of ilmenite hosted in the shore sediments along the coast of the Thule district and in particular along the southern shore of Steensby land. The investigation was conducted in cooperation with the present concession holder, Bluejay Mining (formerly FinnAust Mining), in accordance with the contract between FinnAust Mining Plc and GEUS (January 24th, 2017). This report gives: i) evaluated volumes of titanium-rich host rocks in the Steensby Land Sill Complex and Franklin dykes, ii) provides an estimate of the primary contents of titanomagnetite and ilmenite in the host rocks, iii) gives measured and modelled vanadium and niobium concentrations in titanomagnetite and ilmenite as tests for the calculated proportions of titanomagnetite and ilmenite, iv) provides petrographic information for the evaluation of the degree of alteration of titanomagnetite, and v) provides evaluated volume of basaltic material that was eroded, and from this also the tonnages of ilmenite made available for re-deposition along the shores of Steensby Land.

Scope of the investigation

A first order estimate of the volumes of host rocks of the ilmenite in the Steensby Land Sill Complex and in the Franklin dykes is based on previously published stratigraphic profiles and evaluations of the relative proportions of sill rock, and newly constructed N-S geological profiles on either side of Granville Fjord. They are referred to as Moriusaq East and Moriusaq West profiles. The profiles are based on compiled field maps in 1:100 000 (GEUS archive) and downloaded satellite images (Google Earth).

A first order estimate of the contents of primary titanomagnetite and ilmenite in host rocks is based on CIPW norms (Cross, Iddings, Pirsson, and Washington norms) calculated from bulk rock major element compositions. Bulk rock trace element compositions were used to calculate the concentrations of vanadium in titanomagnetite and niobium in ilmenite, in order to test for the proportions of primary titanomagnetite and ilmenite calculated using the CIPW norm.

Calculated vanadium and niobium concentrations in titanomagnetite and ilmenite are then compared to observed trace element concentrations using electron microprobe (EMP, superior analyses: 96 ilmenite, 36 titanomagnetite; appendixes 1 and 2) and laser ablation - inductively coupled plasma - mass spectrometry (LA-ICP-MS). The trace element modelling supports the modelled proportions of primary titanomagnetite and ilmenite calculated in CIPW norms and provides constraints for the calculation of the potential resources of ilmenite. The database includes 21 full bulk rock analyses (appendix 3).

The extent of exsolution and alteration of the primary FeTi-minerals, and thus the contents of magnetite and ilmenite (including ilmenite formed as the result of exsolution from titanomagnetite) were evaluated in backscattered electron images (BSE). In combination the normative contents of titanomagnetite and ilmenite and the observed proportion of ilmenite

formed from titanomagnetite allows a first order evaluation of the weight % of ilmenite that could be derived from given host rock, i.e., sill rock. An average potential for ilmenite from the basaltic sills and dykes of the Steensby Land and the Steensby Land Sill Complex is then obtained by combining data from many samples. Not all sills are eroded and only a fraction of the available ilmenite is made available for re-deposition. It is not possible with the available data to make a detailed and reliable evaluation of the amounts of eroded sill material, but an average of 40% was adopted for the regional modeling.

The Moriusaq East profile, however, allows a first order calculation of the mass of eroded sill rock. Calculations are based on extrapolation of sills and their host rocks into areas where they have been eroded. Some of these have a potential of eroded ilmenite in the Gigaton (Gt) range. Evidently eroded ilmenite will not be evenly distributed and would have concentrated in coastal deposits where rivers reach the coast and the here given numbers are averages for the defined sectors along the Steensby Land coast.

Regional geology

The Thule Basin

The Thule Basin is a Proterozoic depositional basin straddling northern Baffin Bay and Smith Sound. It is defined by the Thule Supergroup. This comprises a several kilometre thick unmetamorphosed faulted succession of multicoloured sedimentary and basaltic strata, characterised by red beds, that overlies the Archaean–Palaeoproterozoic Greenland–Canadian shield with profound unconformity. Present exposures define a depocentre about 300 km across. In both Greenland and Canada (Ellesmere Island), outcrops are lost to the sea but geophysical data confirm that the Thule Supergroup underlies the seaway. Contrary to conventional kinematic modelling, the Thule Basin is a product of within-plate evolution. Its geometry is pristine and not due to a late Phanerozoic convergent regime involving an independent Greenland plate.

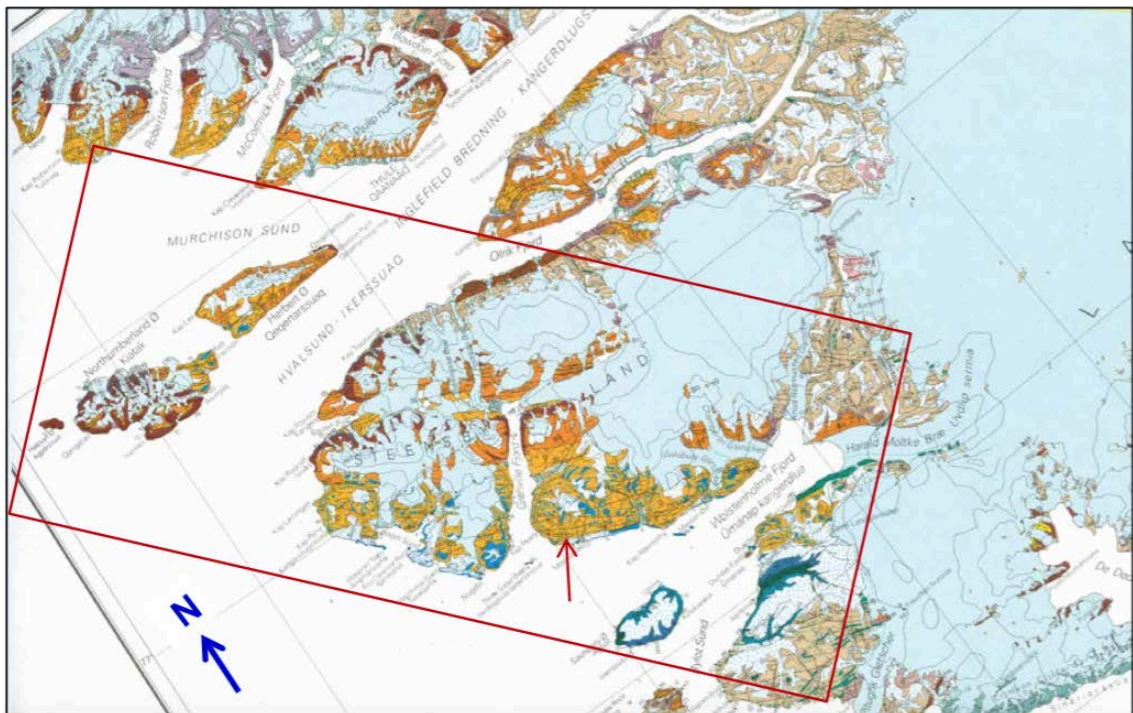


Fig. 1: The area of interest in the Thule District. The Steensby Land Sill Complex (bright blue) is hosted in the Dundas Formation (yellow). The red arrow points to exposures of the Dundas Formation and the Steensby Land Sill Complex. At least 15 sills with an estimated average thickness of 20-50 meter and up to 100 m in thickness are hosted in the ~1000 m thick Dundas formation. The sills constitute a minimum of 30% of the volume of the Dundas Formation.

Geological setting

The Thule Basin is part of a belt of Proterozoic depocentres along the northern margin of the North Atlantic craton. Its nearest counterpart is the Borden Basin of Baffin Island, Can-

ada. Dominated by continental, littoral and shallow marine sedimentary rocks, coupled with continental tholeiitic magmatism, the Thule Supergroup is an expression of the evolution of a rifted continental margin or intracratonic basin. Spatial relationships and thicknesses define two major structural margins, one in the north across Smith Sound and the other on land in Greenland in the south-east. Over these faulted margins, basinal strata are cut out with younger strata overlapping onto the shield. This indicates a geological setting for the Thule Supergroup as the fill of a restricted or semi-restricted intracratonic fracture–sag basin rather than a one-sided wedge on the continental margin.

Age

The precise age of the Thule Supergroup is uncertain. Any regional unconformities within the basin remain undocumented. The succession is bracketed by the Palaeoproterozoic shield with its basic dykes of Statherian age (1670 Ma); northern exposures (Inglefield Land) are unconformably overlain by Lower Cambrian strata. Based on the evidence of microfossils (acritarchs) and radiometric dates of basaltic rocks (sills and dykes), the succession is of Mesoproterozoic–?Neoproterozoic age, more specifically Ectasian/Stenian–?Tonian. Basal strata are older than Mackenzie sills of Ectasian age (c. 1270 Ma); uppermost strata are older than Franklin sills and dykes of Cryogenian age (c. 720 Ma). Correlation with the Borden Basin of Canada suggests that the entire Thule Supergroup could be of Mesoproterozoic age.

Thicknesses of formations

The first regional lithostratigraphic subdivision of the Thule succession made during the mapping for the 1:500 000 map sheet concluded that it was “*at least 6 km thick*” and “*possibly as much as 8 km*”. This uncertainty stems from three conditions: (1) the reconnaissance nature of the mapping, (2) the upper part of the Supergroup (Dundas and Narssâr-suk Groups) lacks regional marker beds and (3) the outcrop pattern of Thule strata is strongly controlled by regional faults (Thule half-graben system). Structural and stratigraphical (sedimentological) studies are needed for a more accurate thickness assessment.

Lithostratigraphy. The Thule Supergroup is presently divided into 36 formal lithostratigraphic units: 5 groups, 15 formations and 16 members. The five groups are Smith Sound, Nares Strait, Baffin Bay, Dundas and Narssâr-suk. They are listed here in younging order except that the Smith Sound Group is the marginal equivalent of the Nares and Baffin Bay Groups of the central basin (see Fig. 120; Dawes 1997, p.139)

The Smith Sound Group represents an overall shelf environment with stable conditions for shallow water to subaerial deposition; supratidal to marginally marine and intermittently lacustrine sedimentation prevailed. Up to 700 m thick and cut by basic sills, varicoloured sandstones and shales including red beds dominate, with subordinate stromatolitic carbonates.

The Nares Strait Group, up to 1200 m thick, comprises the basal strata of the central basin. It is composed of sandstones and basaltic volcanics, including flows, sills and volcanoclastic deposits, as well as shale- and carbonate-dominated intervals. It represents deposition in alluvial plain, littoral and offshore environments, with accompanying terrestrial tholeiitic volcanicity.

The Baffin Bay Group is the most widespread Thule strata. Conformably overlying the previous group, it reaches a thickness of 1300 m. Multicoloured, sandstones and quartz-pebble conglomerates, with intervals of shales and siltstones, indicate mixed continental to marine shoreline environments. Upper strata represent a gradually deepening depositional regime into the Dundas Group.

The Dundas Group is estimated to be 2 to 3 km thick. Dominated by dark weathering, thin to medium bedded variously laminated, sandstones, siltstone and shale, with lesser amounts of dolomitic limestone, chert and evaporitic rocks, deposition was in an overall deltaic to offshore environment. Dark shales can be pyritic. Basaltic sills of Franklin age are common in many parts of the group, including Steensby Land, where the so-called 'Steensby Land Sill Complex' contains some 15 master sills, the thickest being more than 100 m. Basaltic rock can form 30–40% of the stratigraphic section.

The Narssârssuk Group, estimated to be 1.5 to 2.5 km thick, supposedly contains the youngest sediments of the basin. The group is confined to the Pituffik half-graben; its southern extent being limited by the Narssarsuk Fault, with northern exposures lost to the Quaternary deposits of the Pituffik valley (that support the U.S. airbase). The carbonate – red bed siliciclastic sequence with evaporates represent cyclic deposition in a hypersaline peritidal environment in conditions analogous to modern coastal sabkhas.

Metamorphism and structure

Thule strata form predominantly homoclinal, shallow-dipping sections, with anomalous inclinations caused by block faulting, drag folding and regional flexing. The rocks are regionally unmetamorphosed but they are indurated and locally altered. Apart from fault crushing and gouge formation, the main types of alteration are contact metamorphic effects, for example, baking of shales/siltstones and bleaching of red beds adjacent to basaltic intrusions. The outcrop pattern of Thule strata is controlled by regional faults, mainly WNW–ESE- to NW–SE-trending that split the central part of the basin (south of Inglefield Land) into six major half grabens composing 'The Thule half-graben system' (Fig. 35 with caption from Dawes 2006, p. 55). The half-grabens are characterised by shallow south-westerly dipping successions that overlie the shield in the north and that are down-faulted in the south and juxtaposed against the shield of the adjoining block. Displacements along the bounding faults are measureable in kilometres. Five of the six half-grabens contain successions that top in the Dundas Group; the Pituffik half-graben preserves both the Dundas and Narssârssuk Groups.

Location

The Moriussaqa black sands are located within in the Moriussaqa half-graben which is supposedly bounded offshore by the Moltke Fault. The sands have accumulated at the coastal termination of the Steensby Land Formation (Dundas Group) comprising a monotonous succession of shallow-dipping shales and siltstones invaded by numerous titanium-rich Franklin basaltic sills (Steensby Land Sill Complex).

The Steensby Land Sill Complex

The Steensby Land Sill Complex comprises a suite of ~15 sills emplaced concordantly into the Dundas Formation in Neoproterozoic times around 700 Ma. The Neoproterozoic magmatism is described in some detail in Dawes (2006). The sills are up to 100m thick with most between 20 and 50 m in thickness. They show age as well as compositional variations and more magmatic events may have occurred. The sills outcrop as marked buttresses and ledges and are easily identified from the air. Sills exposed on dip-slope can be intensely weathered and turned into gravel. All the sills and related dyke rocks are high-TiO₂ and -P₂O₅ basalts with mostly low mg# and are suggested to reflect considerable fractionation *en route* through thick lithosphere of a continental rifting environment (Dawes, 2006).

The by far largest concentration of the sills is found through southern Steensby Land to Northumberland Ø and Herbert Ø to the northwest and to Dundas Fjeld in the southeast (Fig. 1).



Fig. 2: Dundas Fjeld near Thule Airbase. The charismatic mountain is composed of the Dundas Formation that hosts the Steensby Land Sill Complex. One of these sills cap the mountain (front piece in Dawes, 2006)

Constructed cross sections

An evaluation of the volumes of ilmenite that can have been made available for re-deposition along the south coast of Steensby Land requires, as one of many constraints, an estimate of the volume of sill material in the Steensby Land region. Dawes (1997 and 2006) mentions on several occasions a figure of 30-40% of sill in the Dundas Formation. The sills are mostly conformable with the lithologies of the Dundas Formation and the stratigraphic proportion would be equivalent to the volumetric proportions. Based on these suggestions the integrated thickness of sills could be as much as 300-400m or more. In the Moriusaq region on either side of Granville Fjord the Dundas formation is at least 700m and probably more than 1000 m thick and the enclosed sills would following Dawes (1997 and 2006) amount to more than 300m.

An alternative approach is to assume a conservative average thickness of the sills of 20 m. As many as 15 sills have been recorded and as above the total thickness of sill material in the Dundas Formation in the Moriusaq region is suggested to be 300 meters or more.

A test for this proportion of sill material has been attempted in the Moriusaq area. The field maps in scale 1:100 000 (Fig. 3), which in part are based on mapping from oblique aerial photographs, are used for the reconstruction of stratigraphic profiles east and west of Granville Fjord (Fig. 3). On to the profiles are also, within the limits of the available information, projected sills exposed in the coastal cliffs. Support for stratigraphic correlations and corrections to earlier maps have been carried out using satellite images. The presentation of the profiles includes maps that show the sections along which the profiles have been constructed. The Moriusaq East profile is a single N-S profile, whereas the Moriusaq West profile is a combination of 4 sections in order to maintain a profile perpendicular to the regional dip of the formations of the Thule Group.

Moriusaq East

The Moriusaq East profile is located along the Eastern shore of Granville Fjord. The profile includes the Precambrian basement, the Northumberland Formation, the Clarence Head and Borden Formation, the Robertson Formation and the Qaannaq Formation to the fault that separates these formations from the overlying Dundas Formation and the sills of the Steensby Land Sill Complex. The profile is approximately 25 km in length and hosts ~13 sills of the Steensby Land Sill Complex. Minor uncertainties are due to the large amounts of surface cover that hide contacts and small faults.

The satellite images that have been used for guidance include figures 4-7.

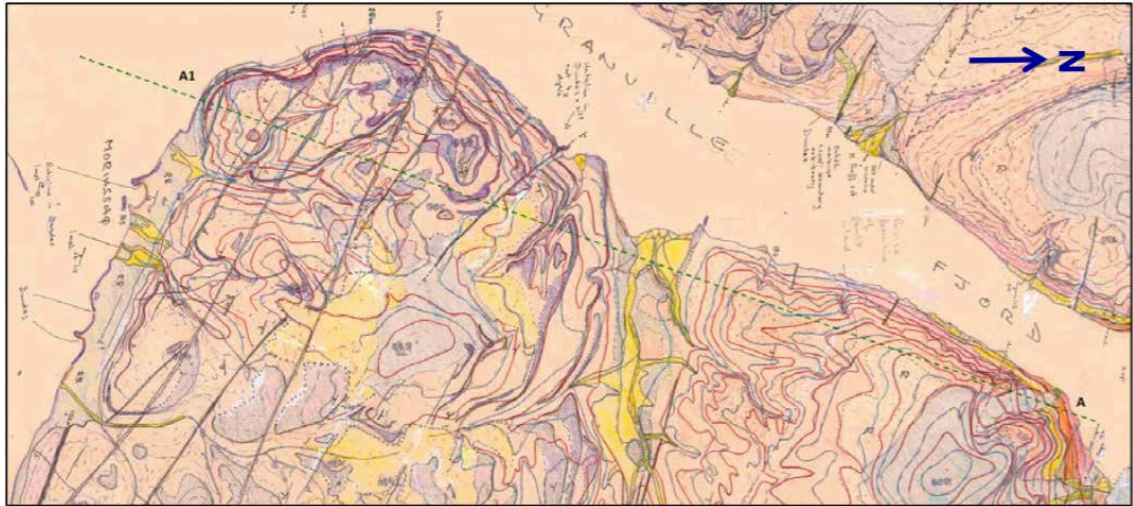


Fig. 3: Compiled geological field map in scale 1:100 000. The green stippled line shows the Moriusaq East profile (A-A1) starting inland (N) and to the coast (S)



Fig. 4: Satellite image from the Moriusaq area. Note that north is to the right to comply with the map of the the Moriusaq East Profile. Red arrows show the sills mapped by Dawes (1997 and 2006) and in blue the Franklin dykes. In this part the Dundas Formation would host at least 4 sills with an integrated stratigraphic thickness of ca. 80 meters.



Fig. 5: Satellite image from the Moriusaq area. Note that north is to the right to comply with the map of the Moriusaq East Profile (Fig. 3). The image shows the eastern shore of outer Granville Fjord. As above: red arrows point to sills and blue to dikes that are clearly visible in the satellite images. The section seems to contain 10 sills equivalent to a total thickness of basaltic material of at least 200 meters.



Fig.6: The outer coast of Granville Fjord seen from west. The sills form escarpments in the softer sediments, mainly shales. Note that the escarpments commonly are composed of a lower and darker rock (the basaltic sill rocks) and a lighter colored bench that are metamorphosed sediments. The escarpments include both of these lithologies. As above: red arrows point to sills and blue to dikes that are clearly visible in the satellite images. Observed sills and dykes can be found in the field map in Fig. 3.



Fig. 7: Middle part of the eastern shore of Granville Fjord with numerous and marked basaltic sills in the shales of the Dundas Formation. As above: red arrows point to sills and that are clearly visible in the satellite images. Observed sills and dykes can be found in the field map in Fig. 3.

Constructed profile

The Moriusaq East profile is divided into nine sections for illustrative reason (Figs 8-10). Scales are in meters and no vertical exaggeration is applied. Formations have colours relating to those of the field maps (e.g. Fig. 3). Sills and dikes are cross hatched and left uncoloured. Sills projected onto the profile are shown as short cross-hatched boxes (e.g., Moriusaq East 3, lower section, Fig. 8). Dykes are made vertical – often due to lack of information on the dip of the dykes and the sills are, where data has been insufficient, shown with the common 2 degrees of southward dip.

The nine sections are arranged with the top of the stratigraphy to the basement some 25 km inland. The profile is arranged in the opposite order, starting at the coast (A1) and ending inland (A, Figure 10).

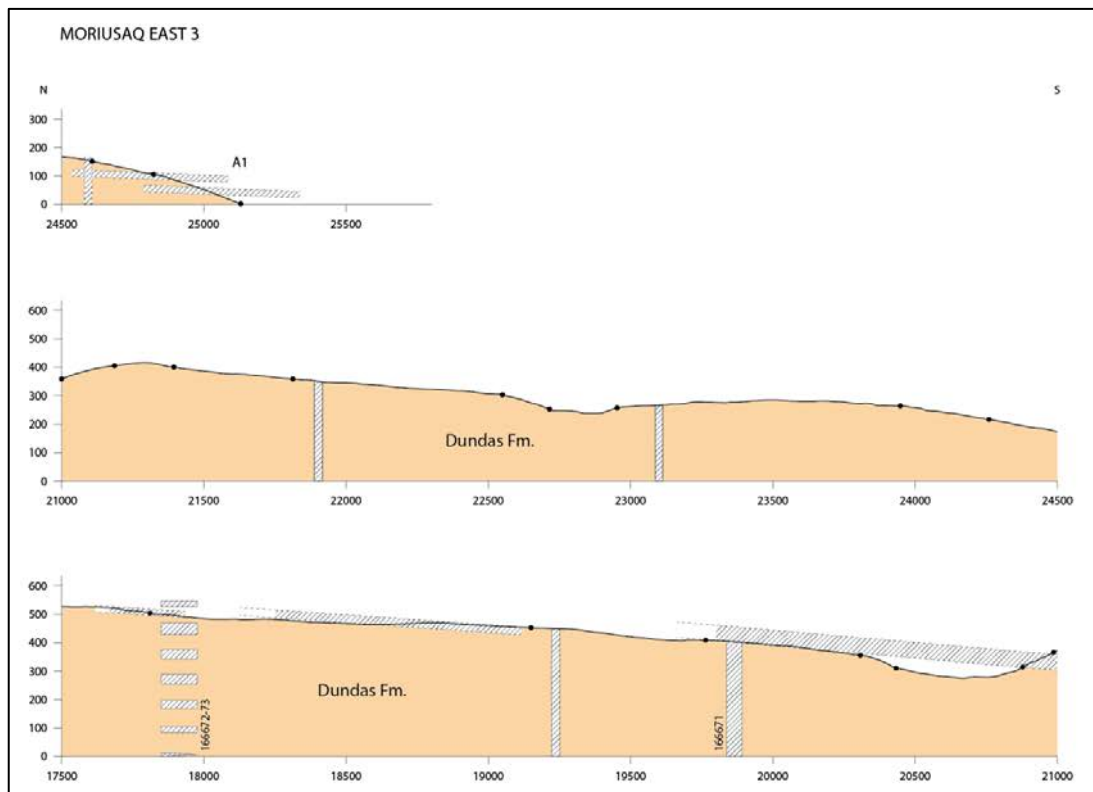


Fig. 8: Constructed profile starting from the coast at A1 (top of figure) and moving north down the figure. Distance in profile measured in meters from the northern and inland end of the profile. Steensby Land sills are projected on the the profile at 18000 m. Formation names are shown

The total thickness of sills in the A-A1 profile is estimated to 280 meters in reasonable agreement with the assumes proportion of 30% and an average thickness of 20 m for the sills (see above).

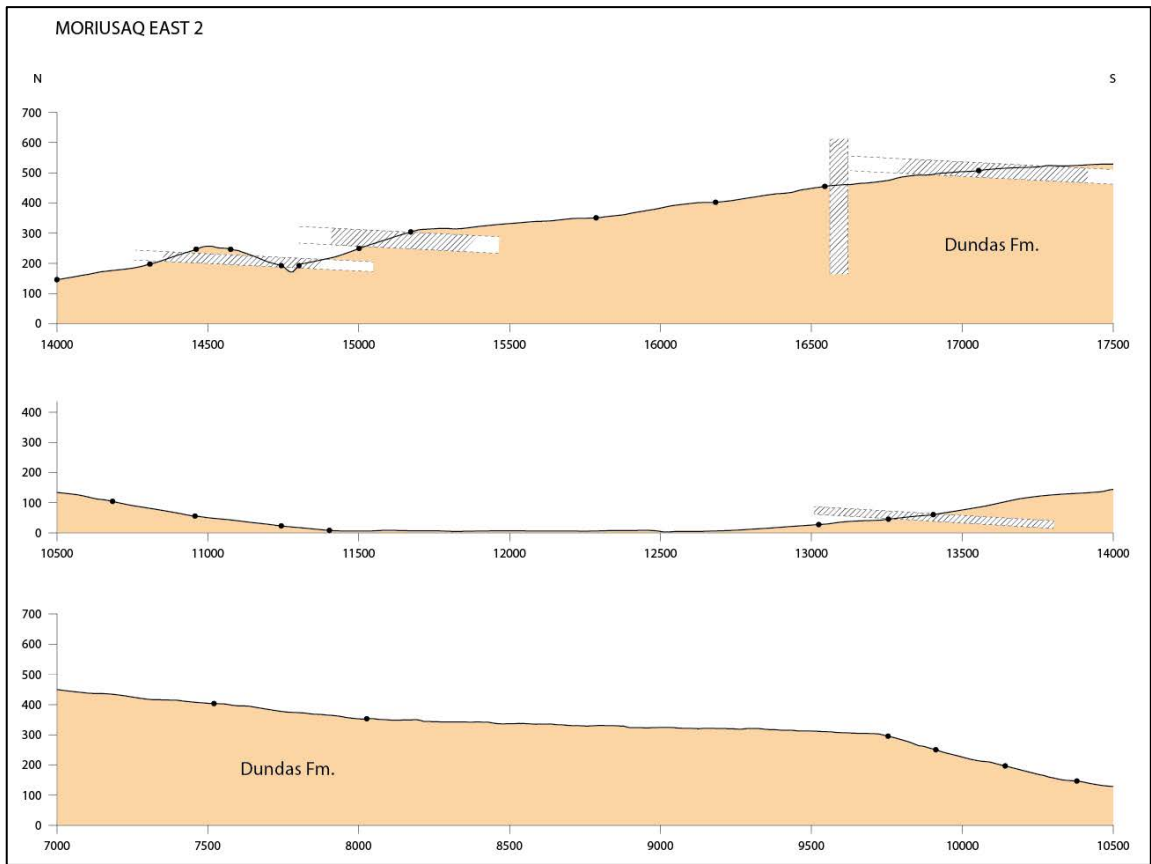


Fig. 9: Middle section of the Moriusaq East profile. See caption to Fig. 8 for further information.

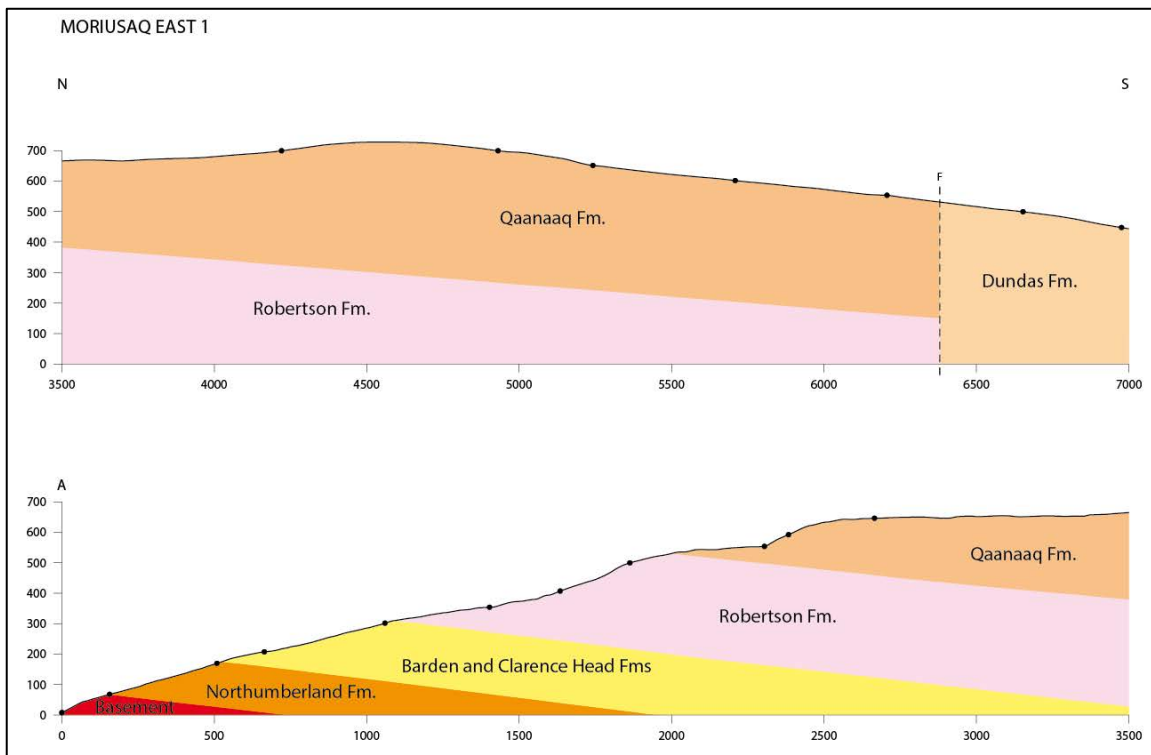


Fig. 10: Northern part of the Moriusaq East profile. See caption to Fig. 8 for further information.

Moriusaq West

The Moriusaq West profile is subdivided into four separate profiles (Fig. 11) due to icefields and the general orientation of the profile (perpendicular to the strike of the sedimentary succession). The profiles were located to allow for the coverage of all sills on the western shore of Granville Fjord.

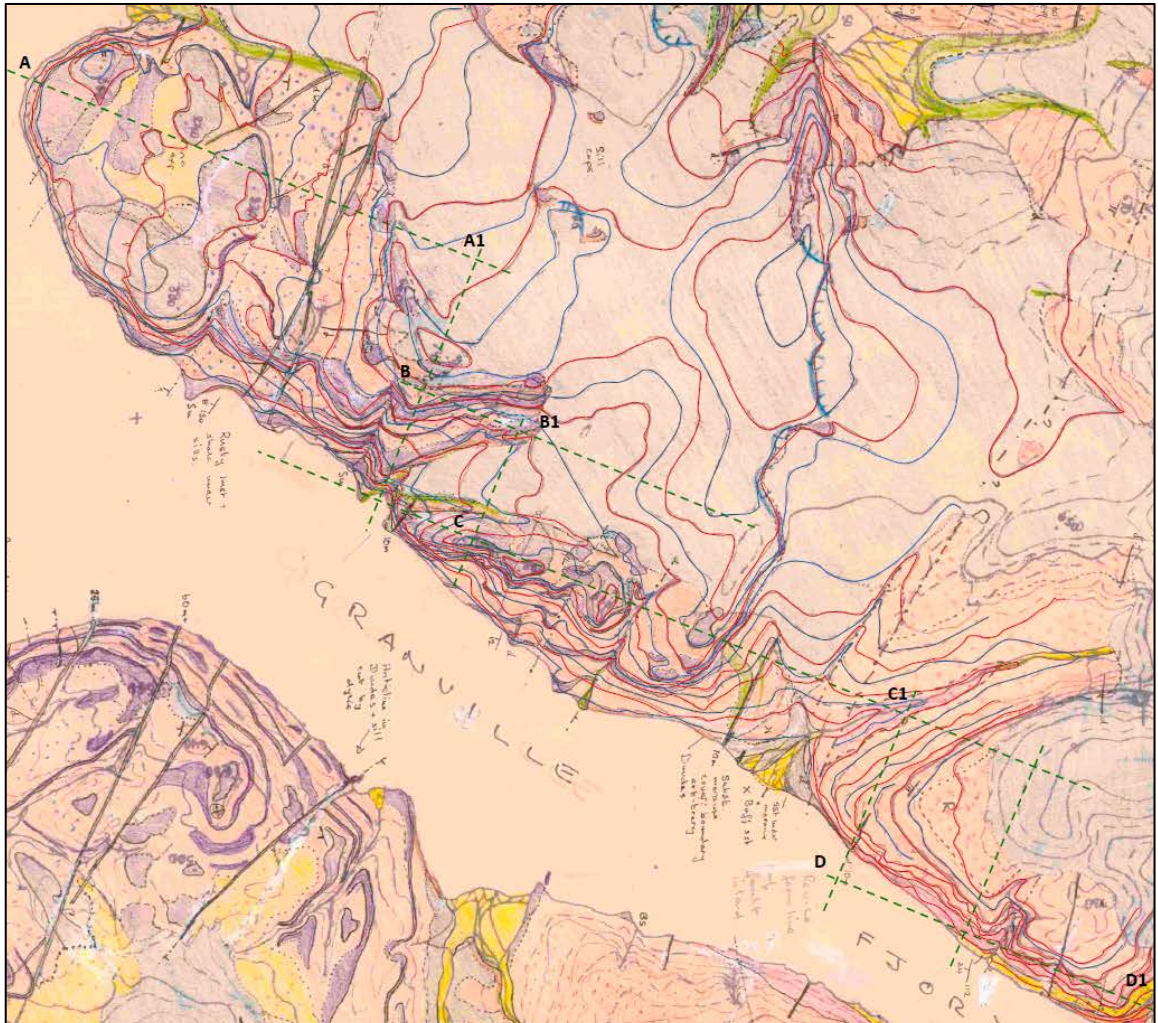


Fig. 11: The four sub-profiles on the western side of Granville Fjord (A-A1, B-B1, C-C1 and D-D1). The Moriusaq West profile starts from the top of the stratigraphy in Dundas Formation and near the coast of Steensby Land (A)

The satellite images that were used for correlation of sills (Figs 12-14) focus on the middle reaches of the western shore of Granville Fjord where the entire section of sills seems to be exposed. The constructed profiles are shown in Figs. 15-17.



Fig. 12: Satellite image from Google Earth showing the middle part of Granville Fjord. Sills are easily identified in the coastal sections (red arrows). The coast is seen from the south.

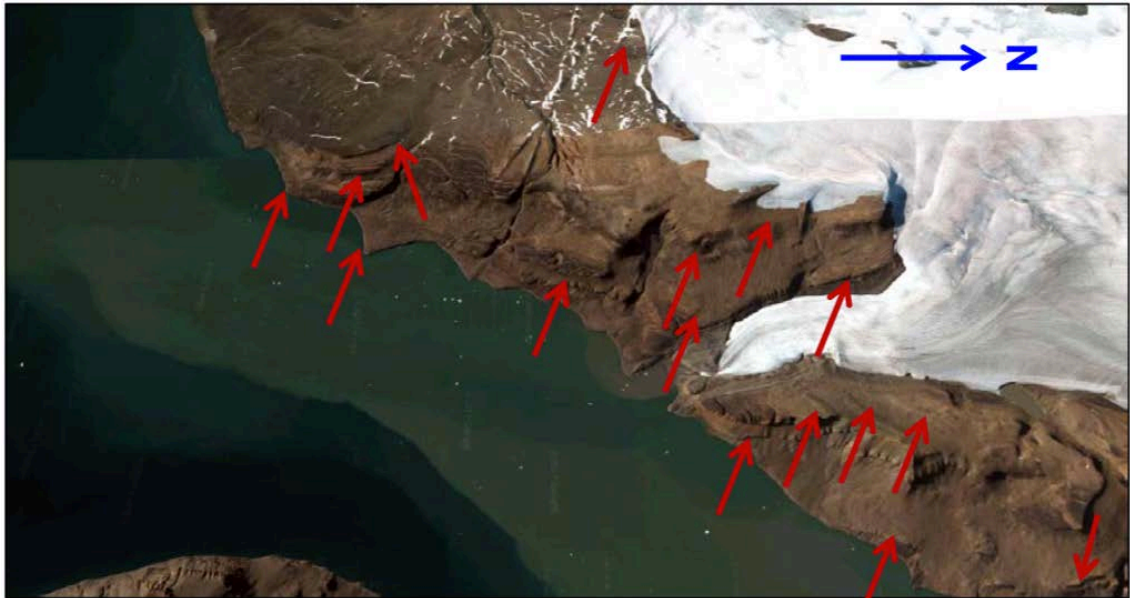


Fig. 13: Same as Fig. 12 but seen from the east.

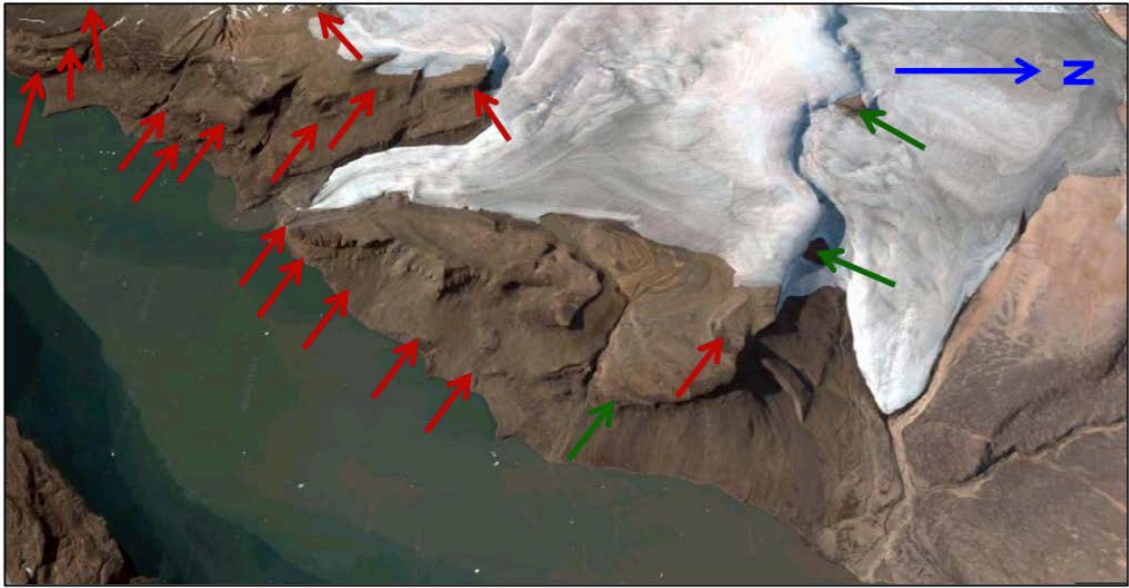


Fig. 14: Inner part of Granville Fjord in oblique satellite image (Google Earth) showing in addition to many sills, the northernmost ~100 meter sill that forms the sharp escarpment in the icefield and continues down to the fjord (green arrows).

Constructed profile

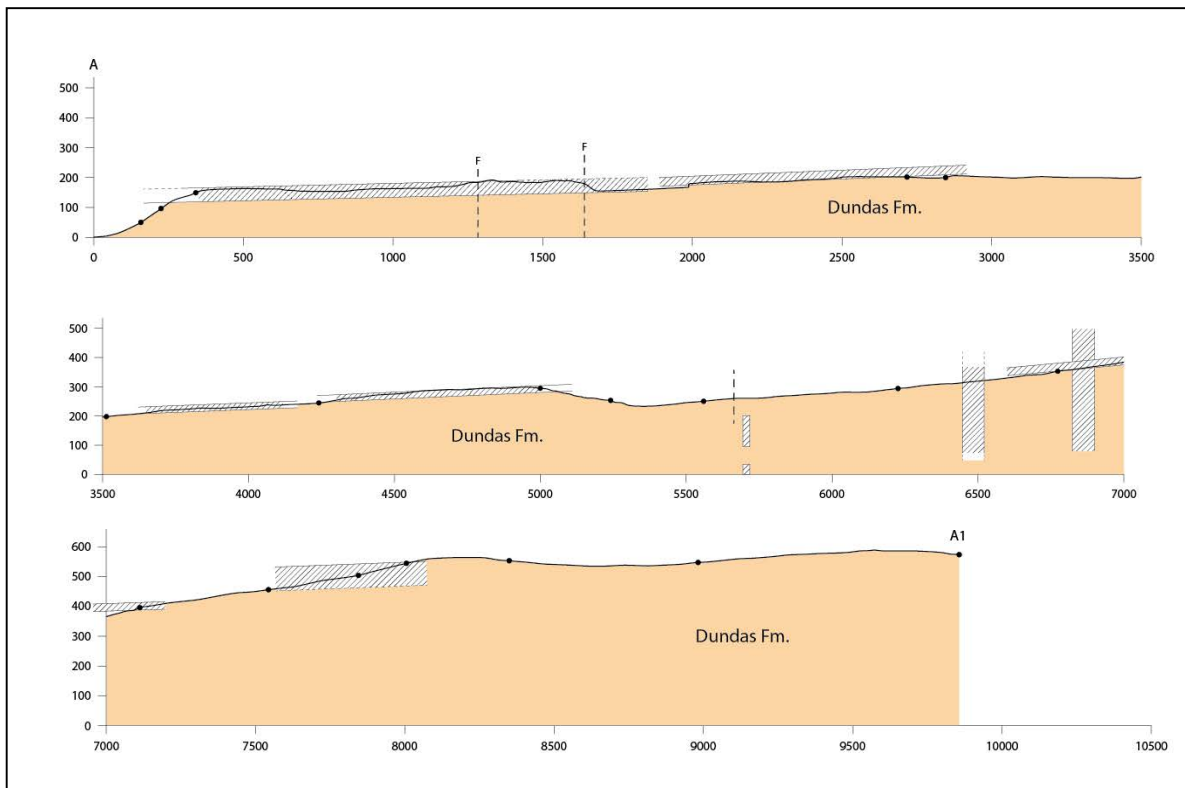


Fig. 15: Outer part of Moriusaq West profile (A-A1, see Fig. 11) starting in top left corner of the figure and going north toward the lower right corner. Sills and dykes are shown.

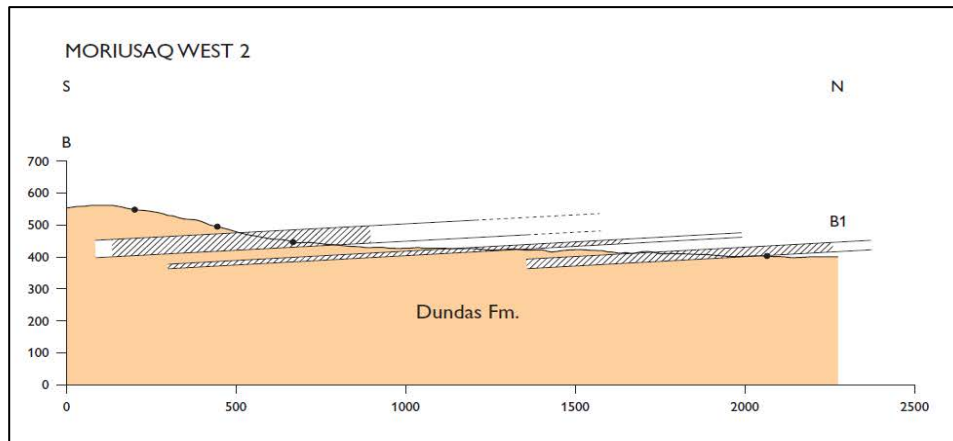


Fig. 16: Section B-B1 of Moriusaq West profile (see Fig. 11) with three prominent sills (50-100 m of sill).

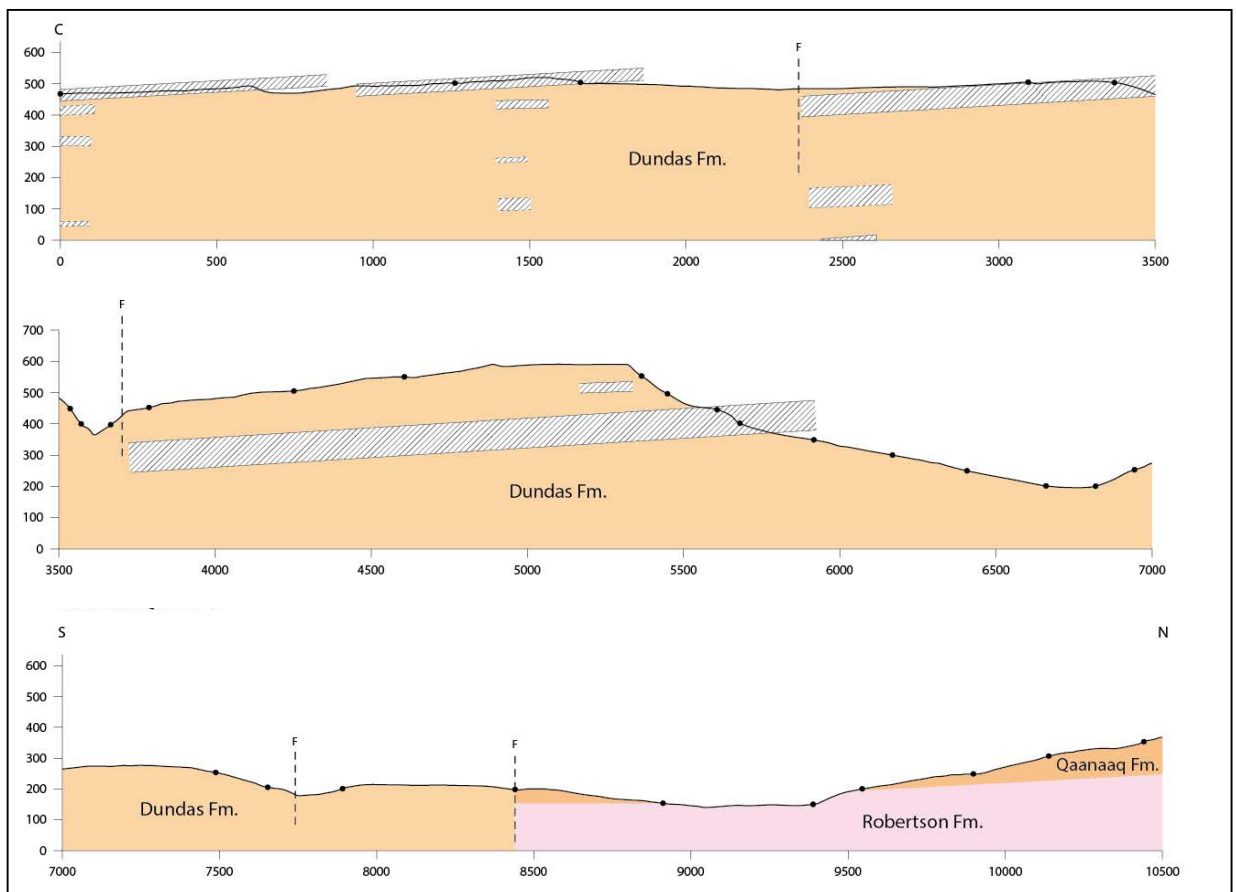


Fig. 17: Section C-toward C1 (see continuation below) of Moriusaq West profile (see Fig. 11). Sills are projected on to the profile at 0, 1500, 2500, and 5300 meters in C-C1.

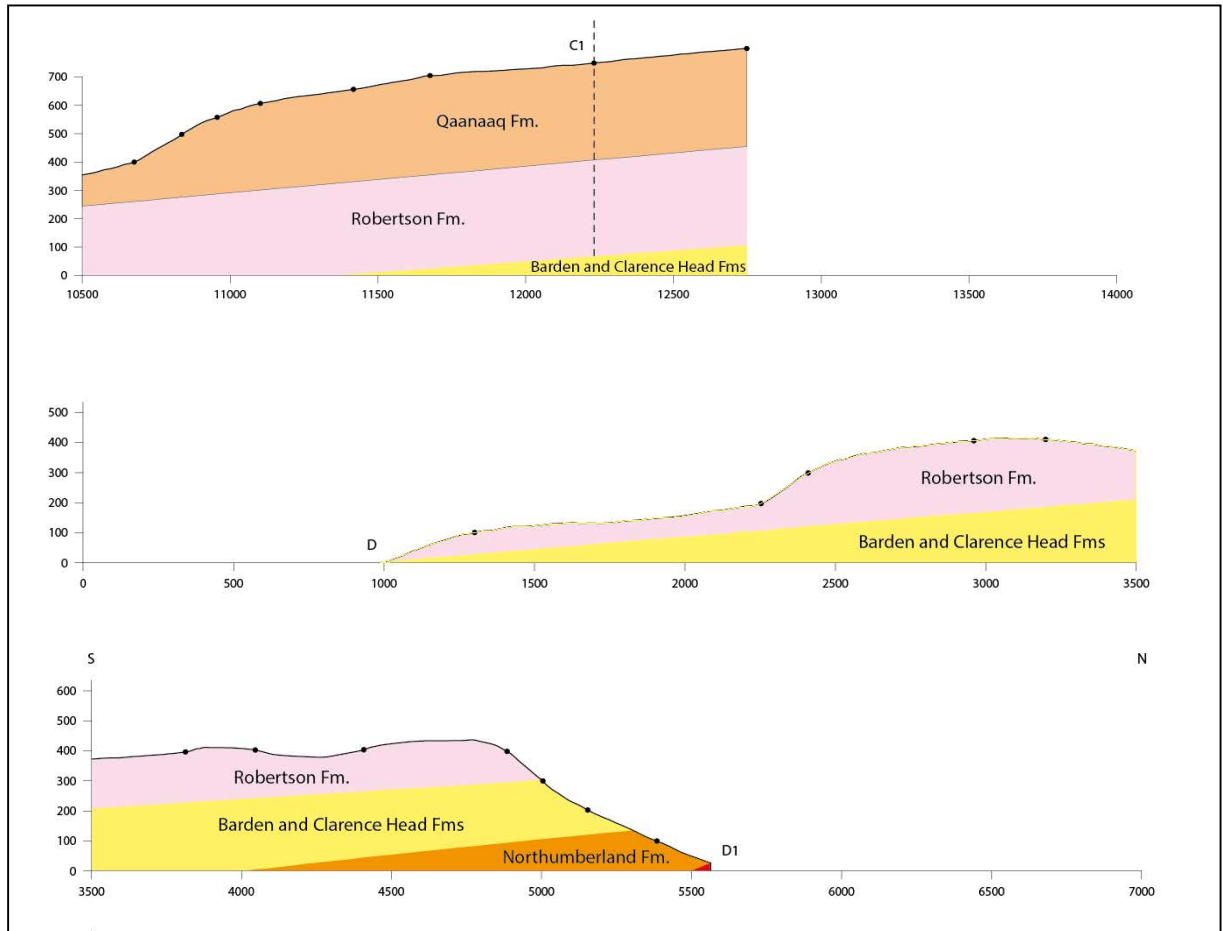


Fig. 18: The inland end of section C-C1 and section D-D1 of the Moriusaq West profile (see Fig. 11). No sills are recorded in lower and northernmost part of the sedimentary succession.

Stratigraphic proportions of sills in the Dundas Formation

The stratigraphic proportions of sills in the Dundas formation in southern Steensby Land is based on the two profiles along Granville Fjord and the regional estimate of 30-40 vol. % sill material in the Dundas Formation (Dawes, 1997 and 2006).

Estimates of the number of sills as well as their thicknesses are limited to the resolution in the compiled 1:100 000 field maps and the geological sections in this report. The number and total thickness of sills in the Moriusaq West profile are uncertain and reduces the certainty with which the stratigraphic proportions of sill material can be evaluated.

The frequency of sills is high in the parts of Dundas formation exposed along the Steensby Land coast and sills do in some parts of the exposures constitute > 50 of the exposed sections. However, the conservative estimates in Table 1 supports that the Steensby Land Sill Complex constitutes 30-40 vol. % of the Dundas Formation in the Steensby Land – Pitufik region of the Thule District (Dawes, 1989).

Table 1: Estimated accumulated thickness of sills in Moriusaq East and West profiles and comparison to Dawes (1997 and 2006)

	Moriusaq East	Moriusaq West	Dawes (1997, 2006)
Total stratigraphic thickness	~900 m	~1000m	
Number of sills	~14	12-14	
Measured thickness of sill material	~280	300-350 m*	
Thickness assuming a 20 m thickness of sills	~280	240-280**	
Vol. % sill measured	~31	30-35	30-40
Vol. % modelled	~31	Min. 24-28**	

* Two and maybe three sills are between 50 and 100 m in thickness or may represent several sills separated by little host rock

** Probably underestimated due to the presence of thick or multiple sills

Franklin dykes

The Franklin dykes in Steensby Land have according to Dawes (pers. com, 2017) thicknesses up to 100 meter and in the Moriusaq area between the coast and 10 km inland an total thickness of 150 to 200 m for 5 dykes. With similar chemistry and general mineralogy they too contribute to the tonnage of ilmenite in the shore deposits of Steensby Land. The dykes are generally near vertical and two models are calculated (Table 18), one assuming erosion of a 100 m vertical section of the dykes and one assuming erosion of a 500 m vertical section.

Evaluation of volumetric proportions of sill material

The evaluation of the volumes of sill and dyke rocks in the Steensby Land region of the Thule district is based on the assumed average of 30 vol. % sill material (see above). The actual number may be higher, but 30 vol. % is, with the given information, regarded as a reasonable and conservative estimate.

The calculation of the volume of sill material originally available simply multiplies the area of the blocks shown in Fig.19 with the thickness of the stratigraphic section available for erosion and the volumetric proportion of sill material of 30%. More detailed calculations have been made for the Moriusaq block (see later section).

Regional (blocks A-K)

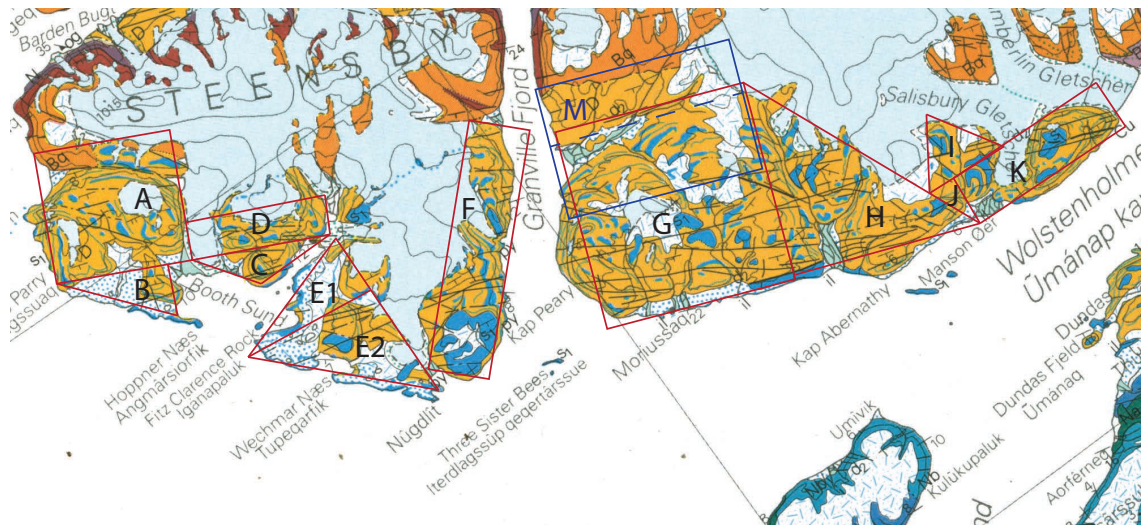


Fig. 19: Defined blocks of the Steensby Land for which the contained volume of sill material has been estimated. Red blocks: Regional evaluation; and blue: more detailed evaluations of the Moriusaq block. The areas and volumes of sill material in these blocks are used in subsequent section for evaluation of the ilmenite potential in the region and the Moriusaq blocks.

Table 2: Regional evaluation of the volumes of sill rock originally present in a 400 meter succession of the Dundas Formation (detailed calculation in appendix 5).*

Block	Area (km ²)	Calculated sill volume
A	116	13.9
B	18	2.2
C	13	1.5
D	33	4
E1	29	3.5
E2	58	6.9
F	95	11.4
g	233	27.4
H	112	13.5
I	19	3.9
J	4	0.5
K	46	5.5
Total	776	94.2

*A 400m section is chosen to as to ensure a conservative estimate of the calculated volume of sill rock.

Mineralogical investigation

The evaluation of the amount of ilmenite available for coastal and sedimentary deposits requires a petrographic and geochemical modeling of the mineralogical proportions of ilmenite and related FeTi-oxides. The aim of the mineralogical and textural investigation is to evaluate the extent of ilmenite exsolution in sill and dyke rocks and to evaluate to what extent ilmenite and magnetite and related FeTi-oxides have been affected by subsolidus alteration and dissolution.

The main method is electron microprobe back scatter imaging that provides textural evidence for the extent of dissolution and dissolution of FeTi-oxides in the sill and dyke rocks.

Petrography on basis of backscattered electron images

All investigated samples originate from the collections of P.R. Dawes (Dawes 1997, 1898, 2006) from which a selection of samples of sills (x) and dykes (x) were prepared for new polished thin sections. For each sample an overview image of the entire thin section is shown followed by several detailed BSE images that demonstrate the textural relations between ilmenite, titanomagnetite and related FeTi-oxides.

Sample GGU 166673, east coast of Granville Fjord (see Moriusaq East profile).

No magnetite or titanomagnetite was found in this sample. The primary titanomagnetite had exsolved into Ti-poor magnetite and ilmenite. Titanomagnetite was subsequently replaced by silicates (mainly sheet silicates – no detailed investigation). FeTi-oxide minerals are also in part re-crystallised to titanite, baddeleyite, anatase/rutile/brookite, and zircon, besides re-crystallised and equilibrated ilmenite.

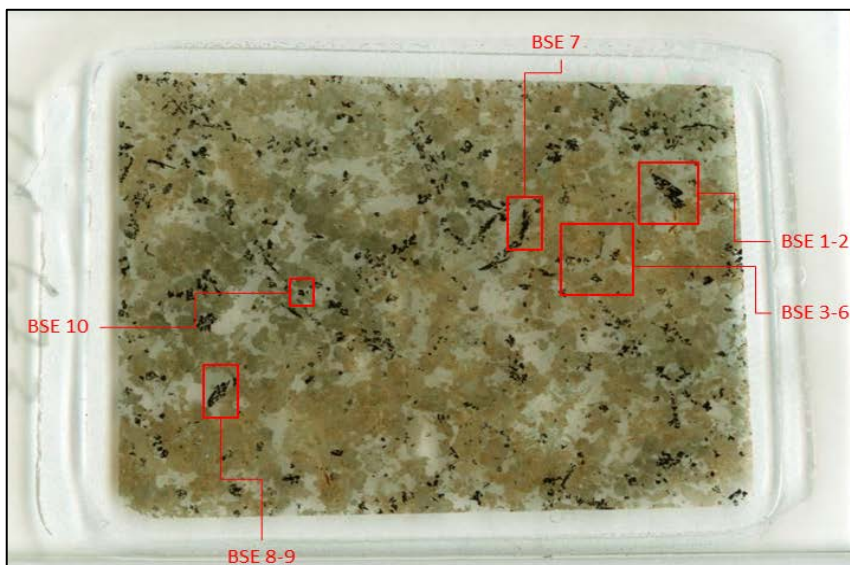


Fig. 20: Scan of thin section of sample 166673 (transmitted light) showing areas covered in backscatter images and location of grains analysed by EMP.

The enclosed BSE images show the general textural and mineralogical characteristics of FeTi-oxides paragenesis of the sample. Red spots represent point for which analyses were collected or where minerals were identified using energy dispersive spectroscopy (EDS) was performed.

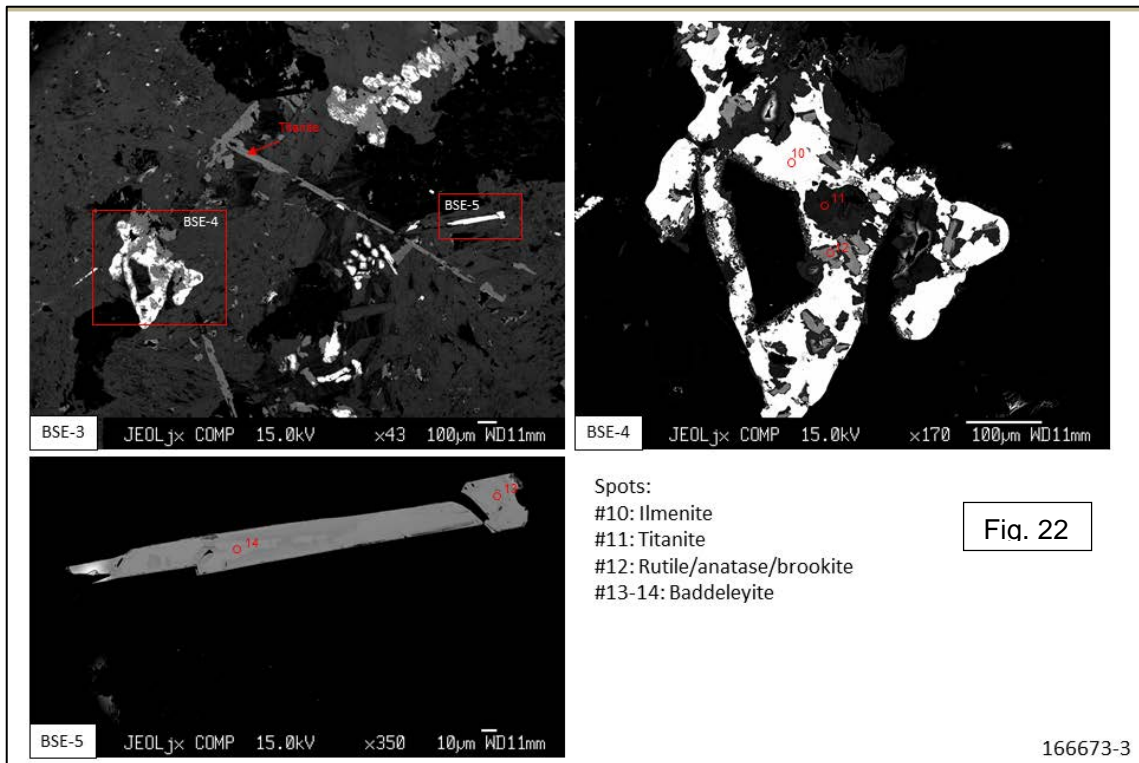
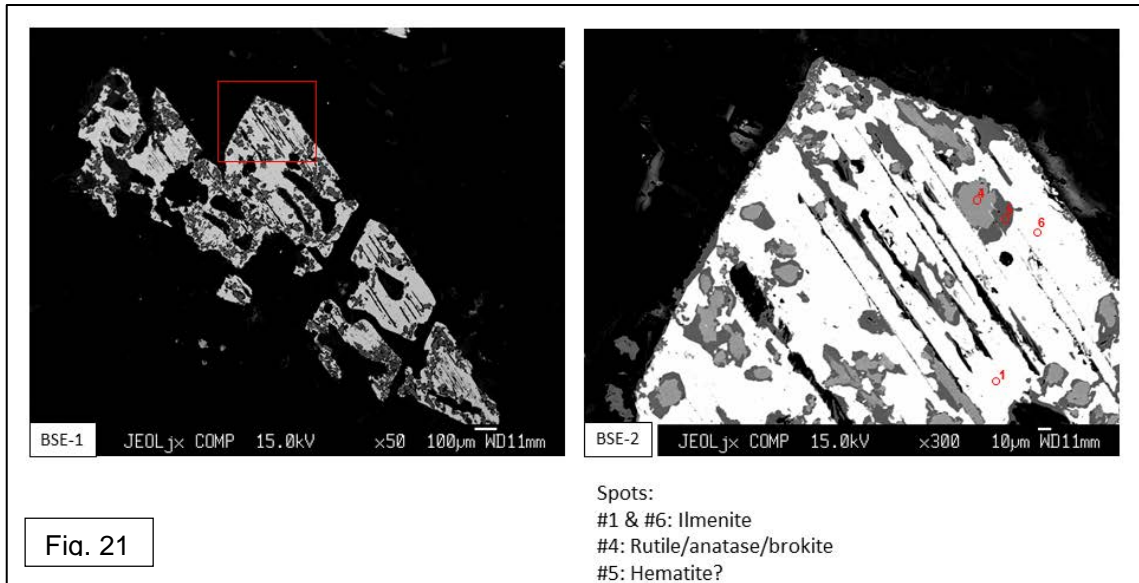


Fig. 21: and 22: Images of FeTi-oxides as found in sample 166673. The FeTi-oxides are partially dissolved after ilmenite exsolution in primary FeTi-oxides (BSE-1) or near euhedral ilmenite (BSE-2).

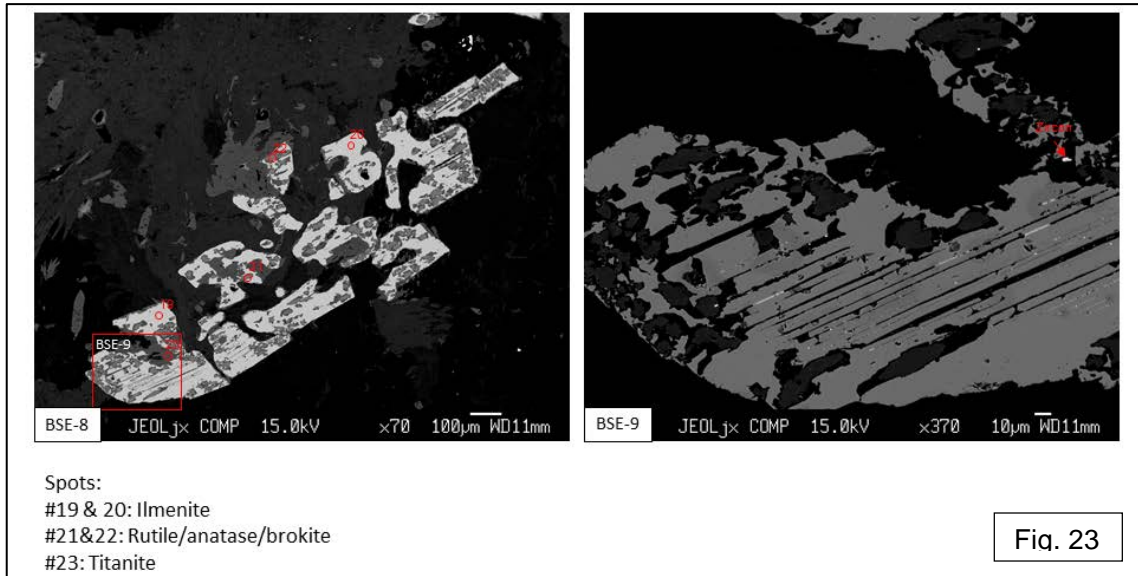


Fig. 23: Same as above. See caption to Figs 21 and 22.

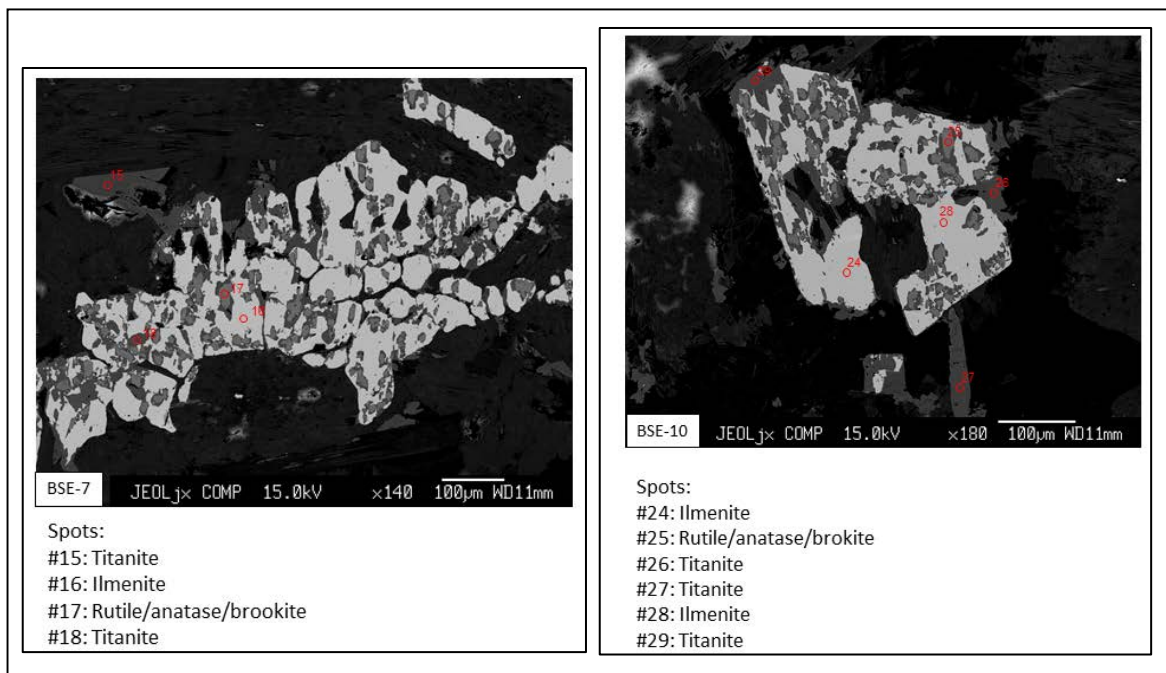


Fig. 24: Same as Fig. 23. Note that much of the former FeTi-oxides are replaced by titanite.

Sample GGU 166672, east coast of Granville Fjord (see Moriusaq East profile).

Very fine grained sill sample – presumably from near the contact of the sill. No magnetite or titanomagnetite was found in this first study of the sample. The primary titanomagnetite was subjected to exsolution into Ti-poor magnetite and ilmenite and subsequently replaced by silicates (mainly amphibole and sheet silicates – no detailed investigation). Note the complete dissolution of magnetite in BSE-3 (Fig. 26). Same observations as in sample 166673 (see above)



Fig. 25: Overview of sample 166672 with indication of studied sections. The FeTi-oxides are finely distributed throughout the sample.

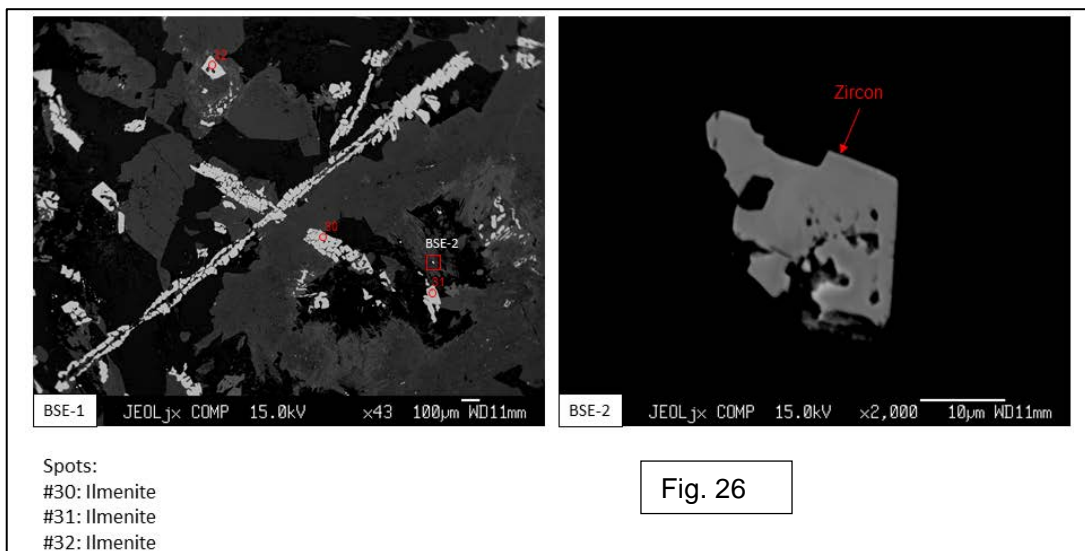
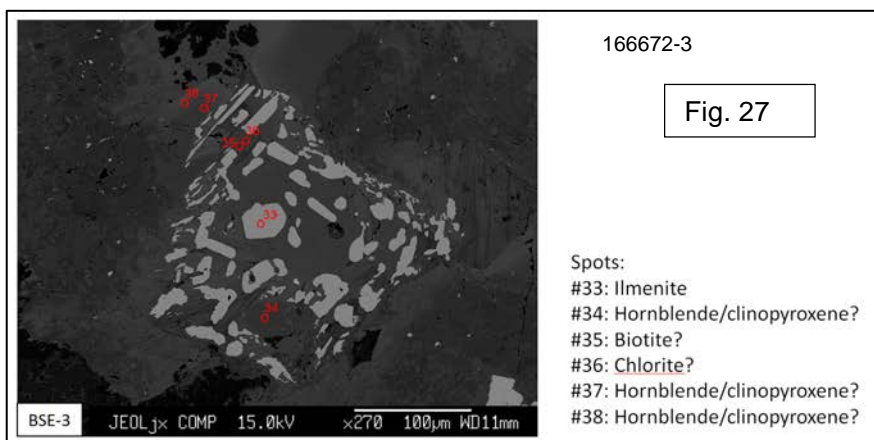


Fig. 26



166672-3

Fig. 27

- Spots:
- #33: Ilmenite
 - #34: Hornblende/clinopyroxene?
 - #35: Biotite?
 - #36: Chlorite?
 - #37: Hornblende/clinopyroxene?
 - #38: Hornblende/clinopyroxene?

Figs 26 and 27: Needles of ilmenite caused by rapid crystallisation near the margin of sill, zircon grains, and in fig. 26 titanomagnetite that was exsolved and totally re-crystallized into new ilmenite and silicate minerals (BSE-3).

Sample GGU 166624, shore NW of Booth Sund

Sill sample containing magnetite or titanomagnetite in addition to ilmenite and alteration products. The primary titanomagnetite was subjected to exsolution into Ti-poor magnetite and ilmenite and subsequently the magnetite was partially replaced by silicates (mainly amphiboles and sheet silicates – no detailed investigation).



Fig. 28: medium grained sill sample with evenly distributed FeTi-oxides grains. Greenish areas represent pyroxene replaced by amphiboles.

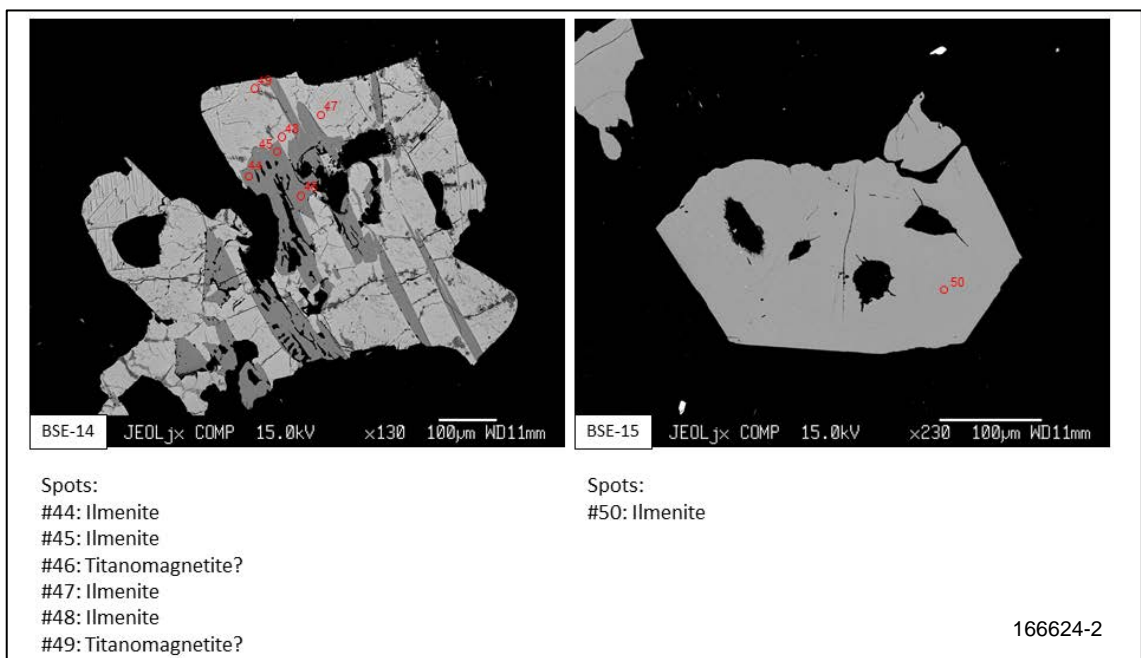


Fig. 29: Partially preserved titanomagnetite grains with ilmenite exsolutions and euhedral ilmenite grains. The sample preserves a near primary mineral paragenesis of FeTi-oxides affected by common exsolution and reactions in basaltic rocks.

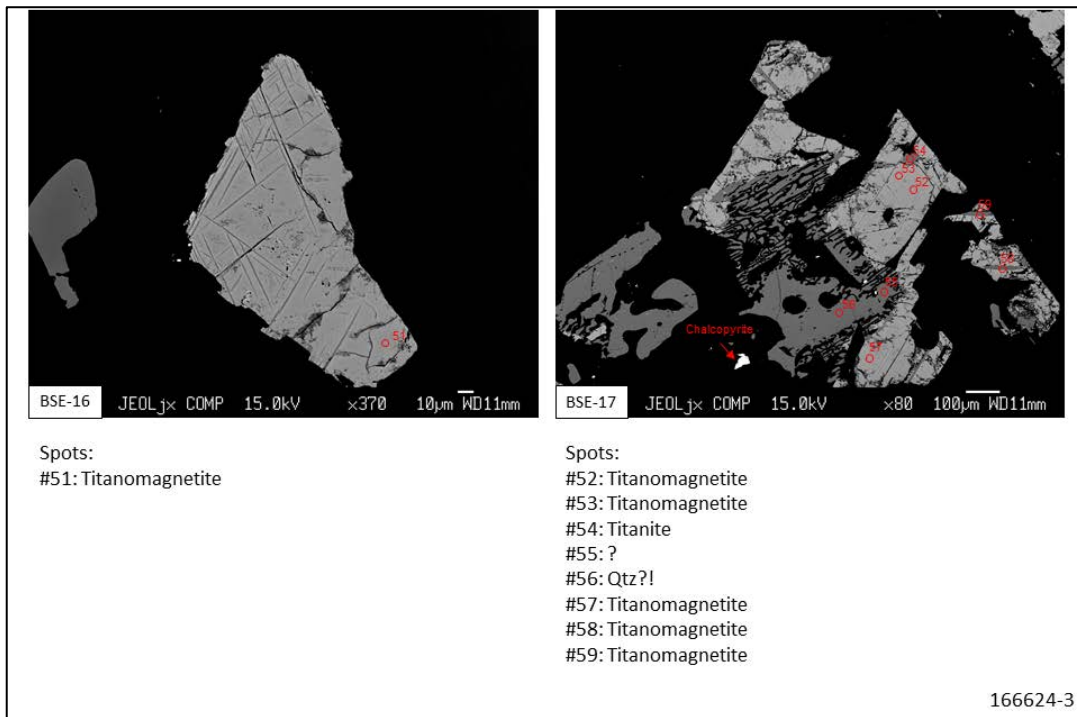


Fig. 30: Partially preserved titanomagnetite with ulvöspinel and ilmenite exsolutions common to “normal” basaltic rocks (BSE-16) and exsolved and partially dissolved titanomagnetite (BSE-17)

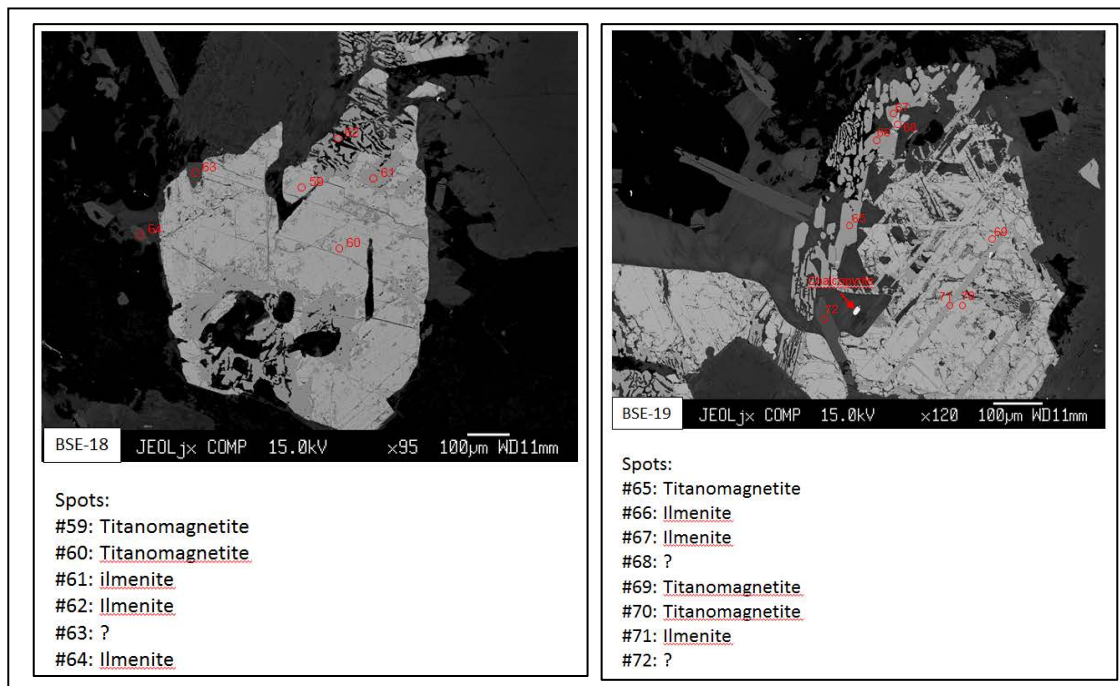


Fig. 31: Same as above (see caption to Fig. 30).

Sample GGU 166671: Granville Fjord

Dyke rock from eastern shore of Granville Fjord. Prominent wide dyke in Moriusaq East Profile.



166671-1

Fig. 32: Fragments of the sill rock (jaw crushed material) showing fine to medium grained basaltic rock. The sample contains partially preserved titanomagnetite. The titanomagnetite is exsolved into ilmenite and Ti-poor magnetite (Fig. 32).

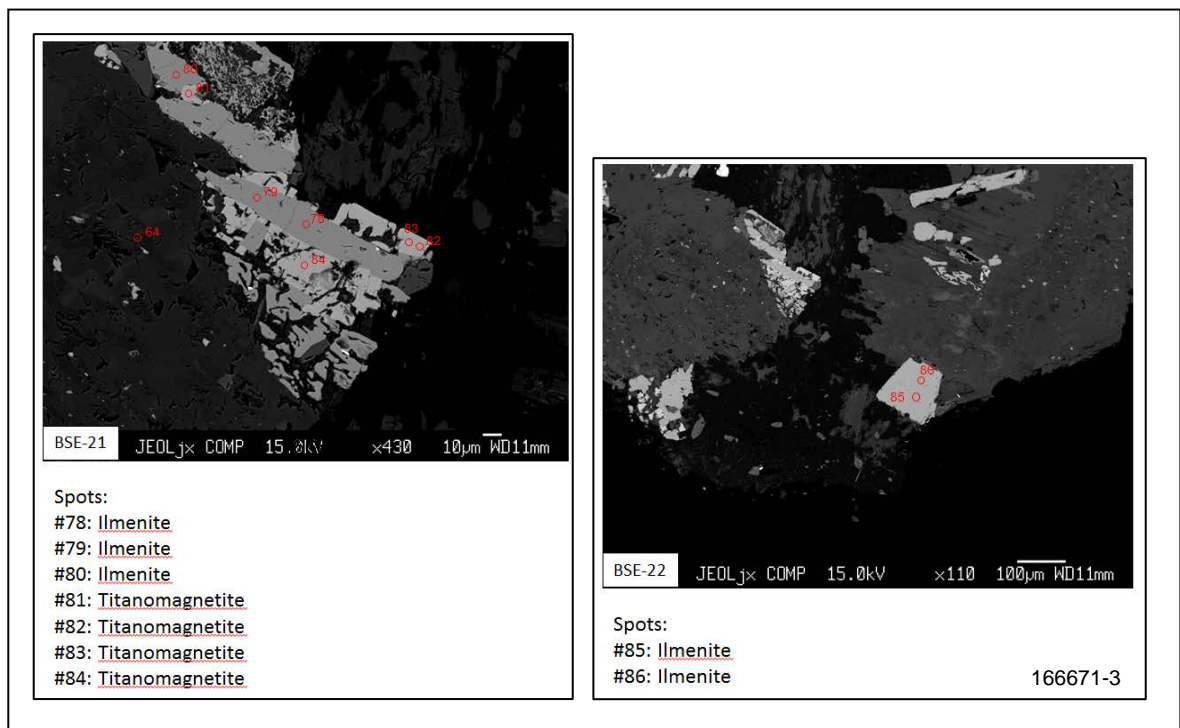


Fig. 33: Details of FeTi-oxides in dyke sample 166671 showing partial preservation of titanomagnetite with ilmenite exsolution and primary euhedral ilmenite.

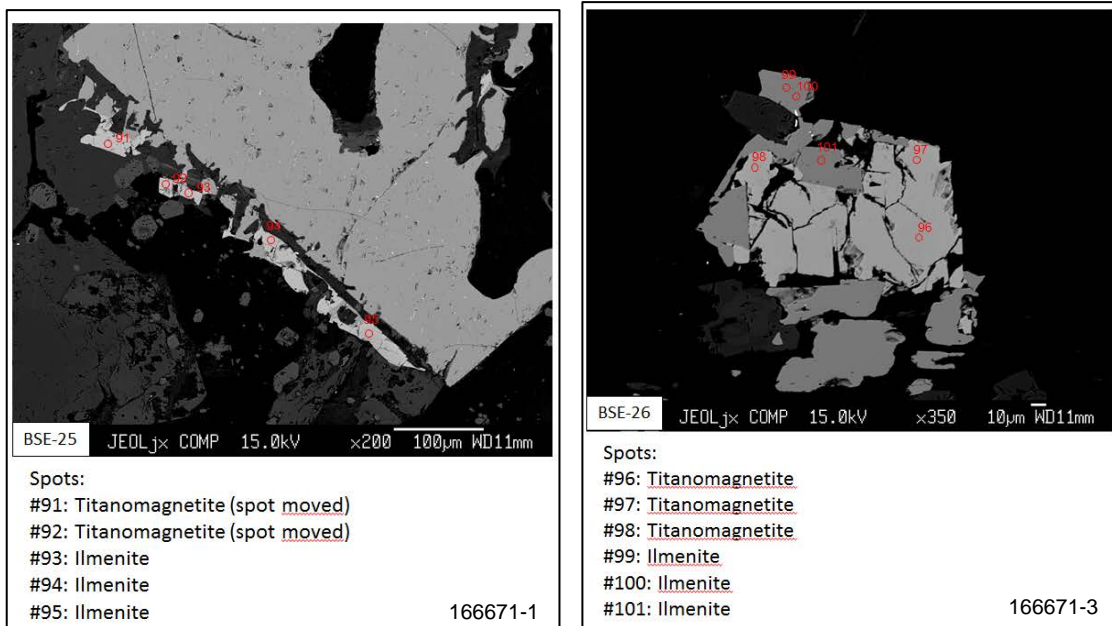


Fig. 34: Euhedral ilmenite with fine and skeletal overgrowth of ilmenite and magnetite and coarse intergrowth of ilmenite and titanomagnetite suggesting total recrystallization of the FeTi-oxide paragenesis.

Sample GGU 166635, eastern-shore of Booth Sund

Sill sample containing magnetite or titanomagnetite in addition to ilmenite and alteration products. The primary titanomagnetite was subjected to exsolution into Ti-poor magnetite and ilmenite and subsequently partially replaced by silicates (mainly amphiboles and sheet silicates – no detailed investigation).



Fig. 35: Sample from sill on out shore west of Booth Sund. The greenish taint and the comparatively large FeTi-oxide grains suggest alteration and recrystallization.

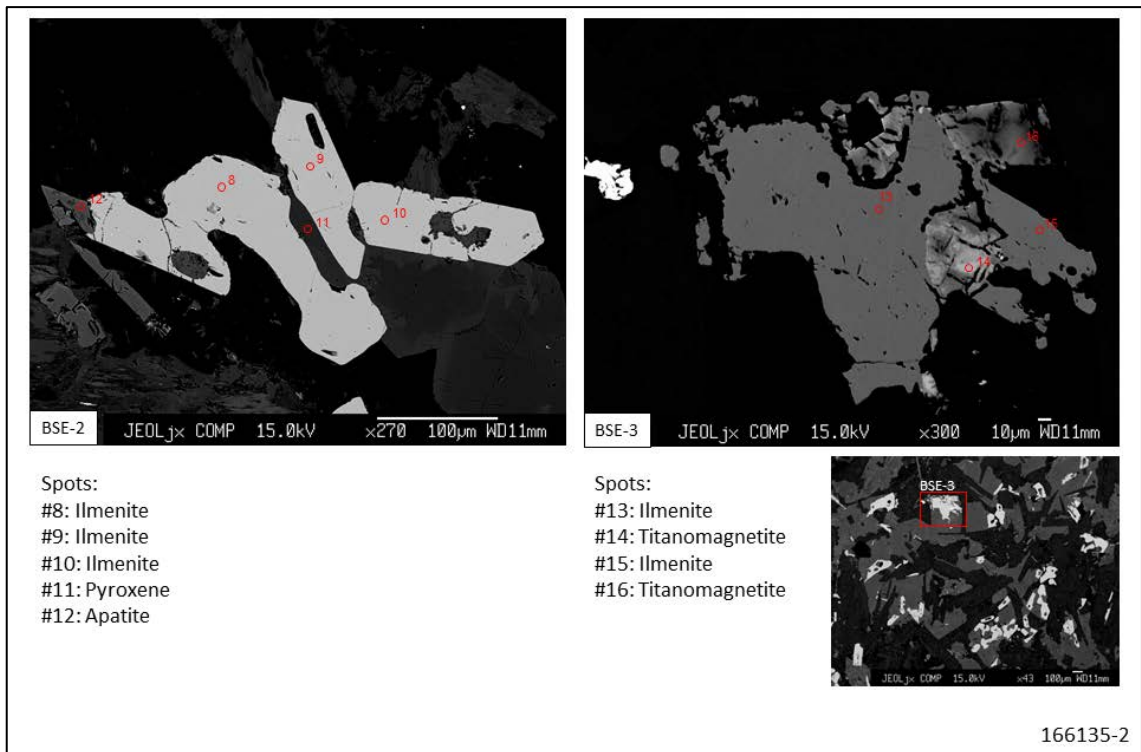


Fig. 36: Primary and later grown ilmenite (left) and grain of late crystallised ilmenite replacing titanomagnetite grain (right). Areas of magnetite and alteration products thereof have variable coloration from light to dark.

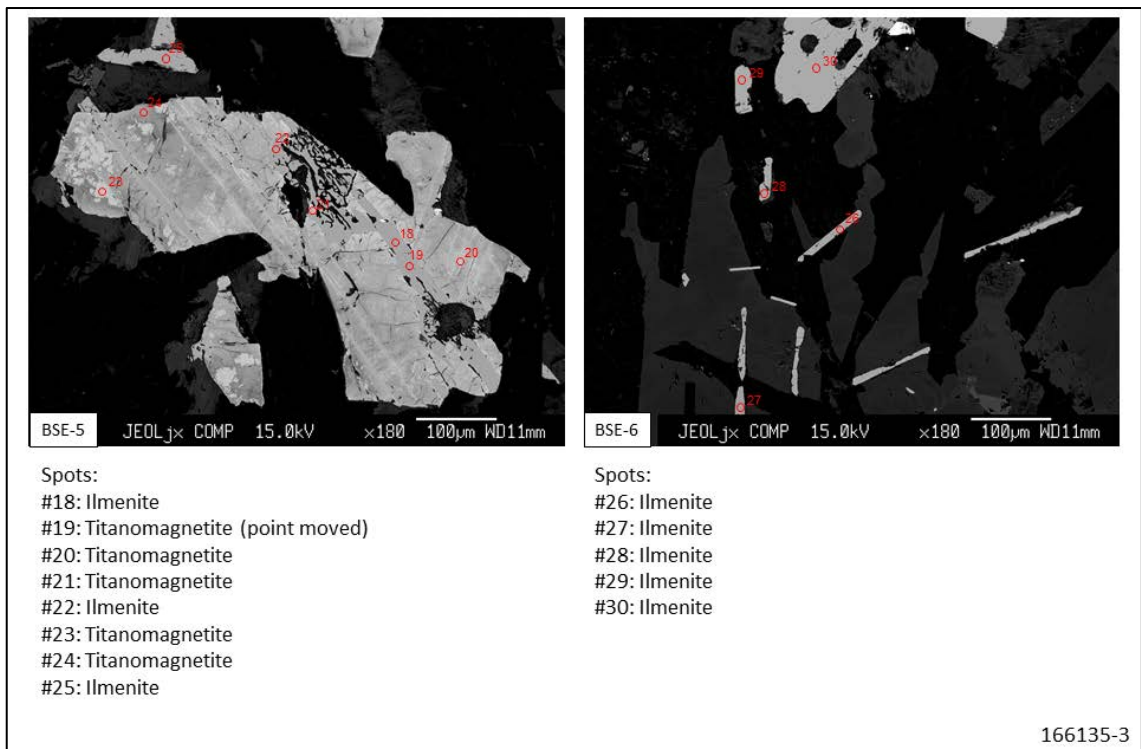


Fig. 37: Exsolved titanomagnetite under partial recrystallization and dissolution (left) and ilmenite needles characteristic of the Ti-rich basaltic rocks.

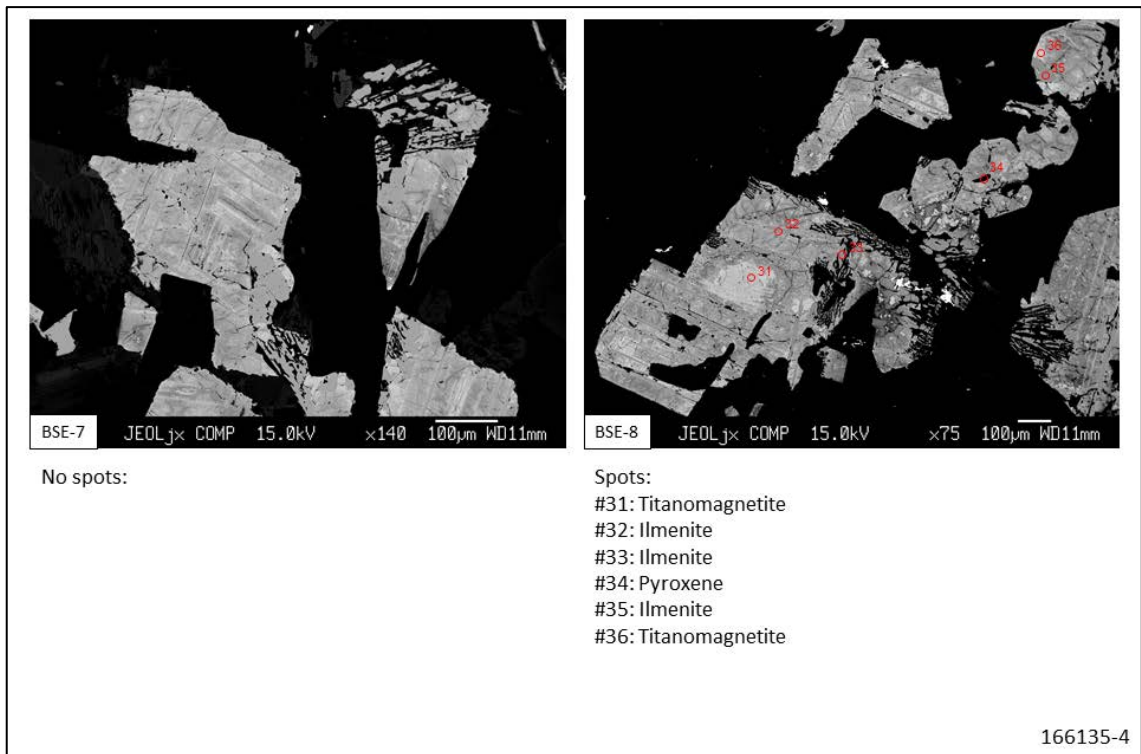


Fig. 38: Titanomagnetite with ilmenite exsolution undergoing alteration and initial replacement.

Sample 166670, western shore inner Granville Fjord

Dyke sample characterized by long skeletal needles of ilmenite in medium to fine grained basaltic rock. As most dykes the sample contains titanomagnetite and ilmenite. The titanomagnetite is exsolved and variably dissolved or replaced by Fe-bearing silicate minerals.



Fig. 39: Medium grained basaltic dyke with ilmenite needles characteristic of the high Ti-basalts.

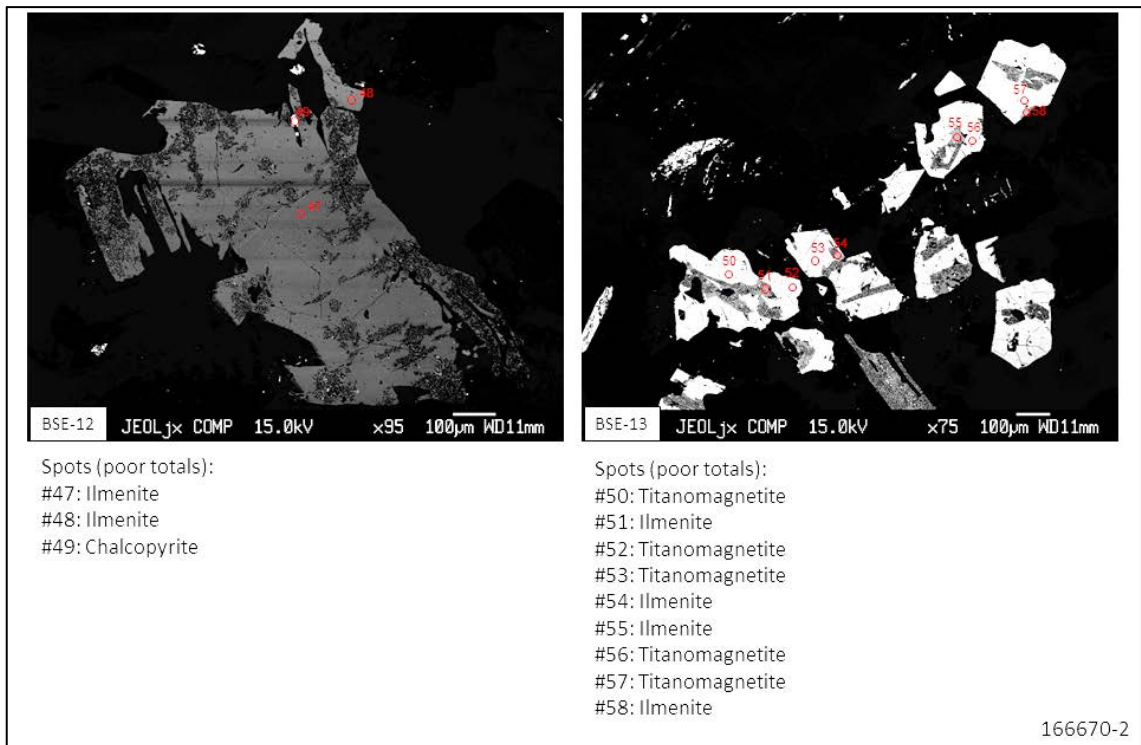


Fig. 40: Large grain of ilmenite (left) and right small euhedral titanomagnetite grains with ilmenite exsolution.

Sample 243559 , Dundas Fjeld, Thule

Very fine grained sill sample from the Dundas Formation on Dundas Fjeld near Thule Air-base.



Fig. 41: The sill sample is very fine grained and assumed collected from very thin sill or the margin of a sill. The greenish taint witnesses to the alteration of pyroxene to amphibole and sheet silicates.

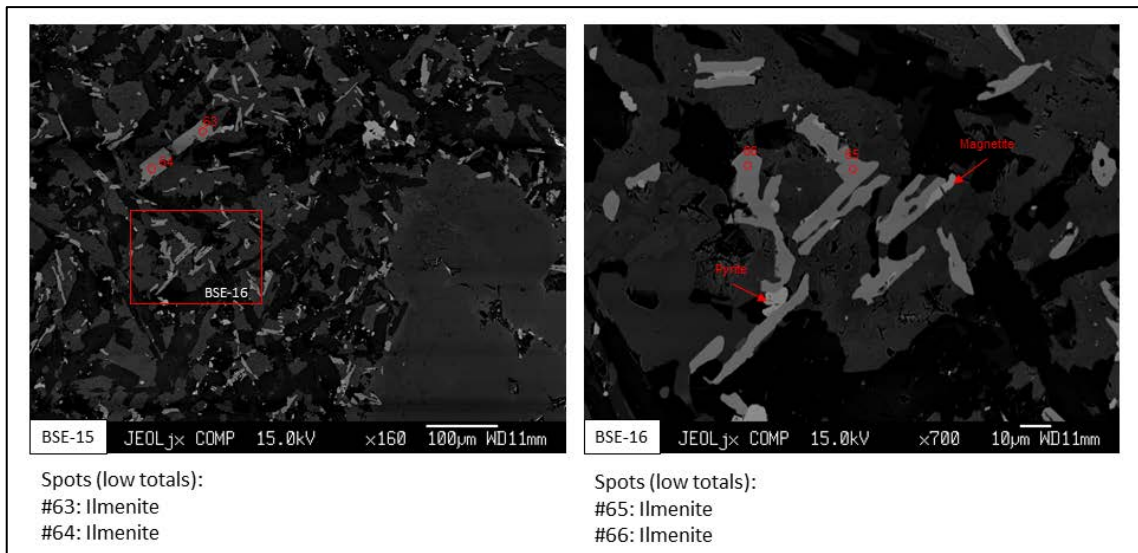


Fig. 42: Details of the mineralogy of the sill sample. The fine groundmass is characterized by elongated grains of ilmenite and few and small titanomagnetite grains (lighter grey).

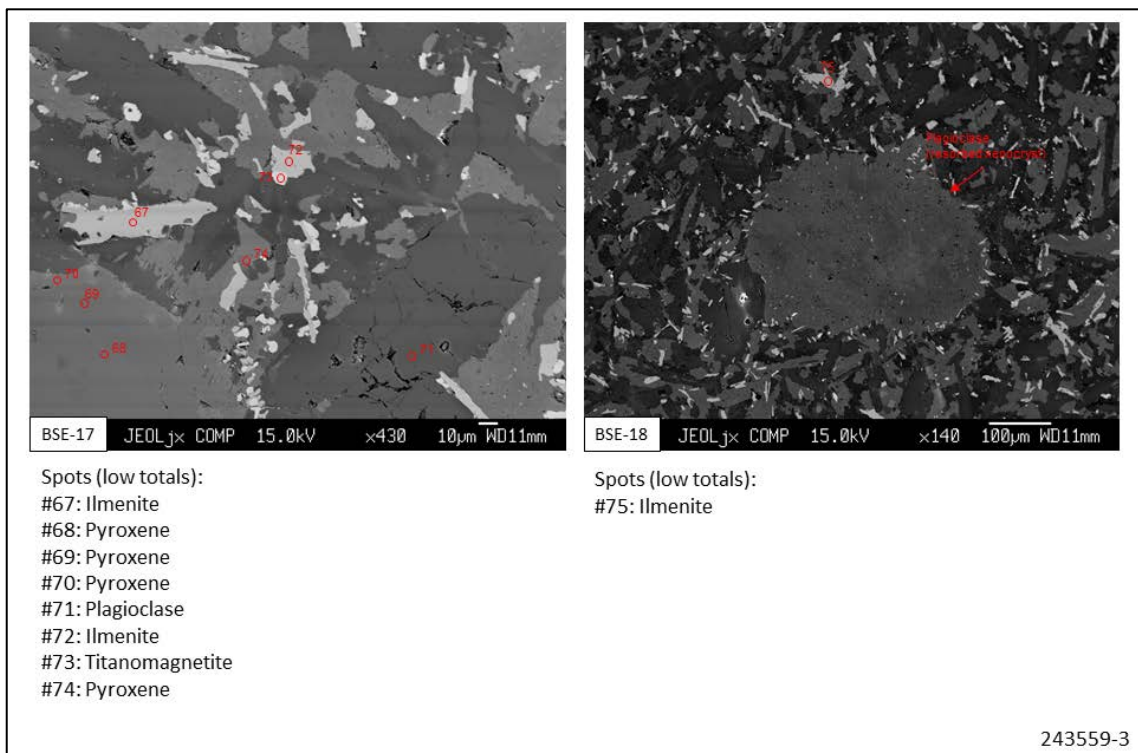


Fig.43: Further details of the FeTi-oxide mineralogy of the DundasFjeld sample. As in other samples with partially preserve primary paragenesis, ilmenite tends to form elongated or skeletal grains whereas magnetite forms more stubby grains in the groundmass. The rounded grain in the panel to the right is a resorbed and rounded feldspar grain with a rim with many small FeTi-oxide grains suggesting rimming of the resorbed grain in the basaltic host.

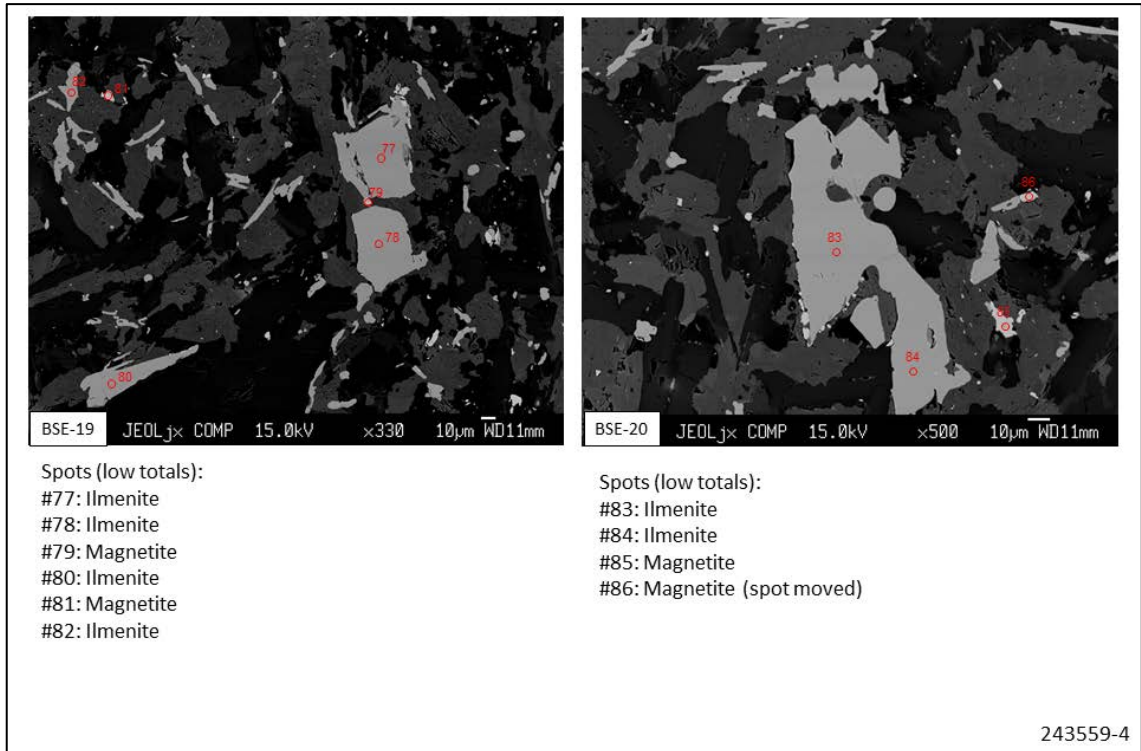


Fig. 44: Larger subhedral ilmenite grains in matrix with ilmenite needles. The larger grains may be primocrysts of ilmenite with irregular overgrowths.

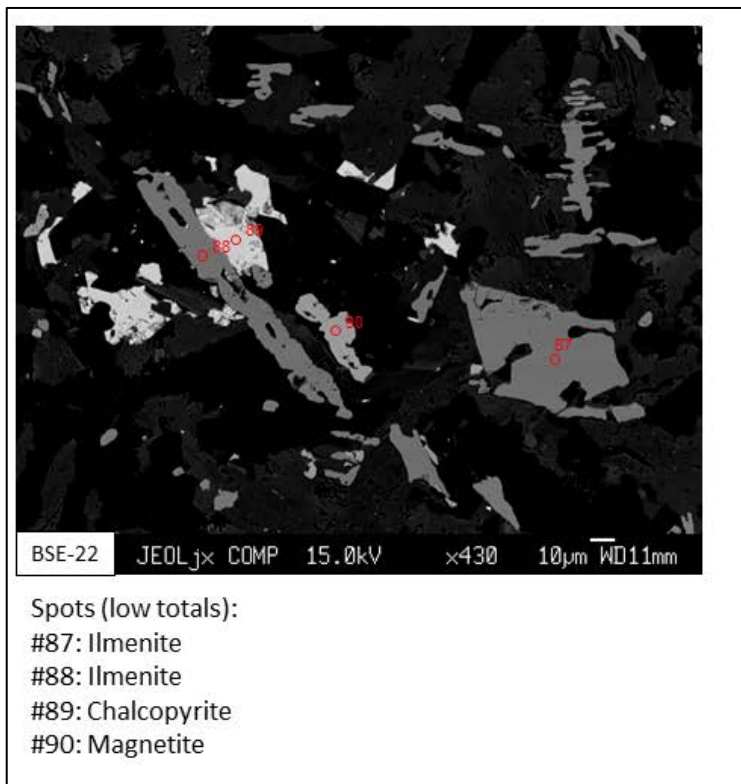


Fig. 45: Fine grained details of the FeTi-oxide mineralogy. Ilmenite forms elongated or plate like grains, whereas magnetite forms more stubby grains. The stubbier ilmenite grain may be a flake like grain seen perpendicular to its smallest width.

Sample 212513, northeastern shore of Northumberland Ø

The sample represents the sills in the northwestern part of the Steensby Land Sill Complex.



Fig. 46: Fine grained sill sample, probably near the margin of the sill. The sill is dotted by small FeTi-oxide grains.

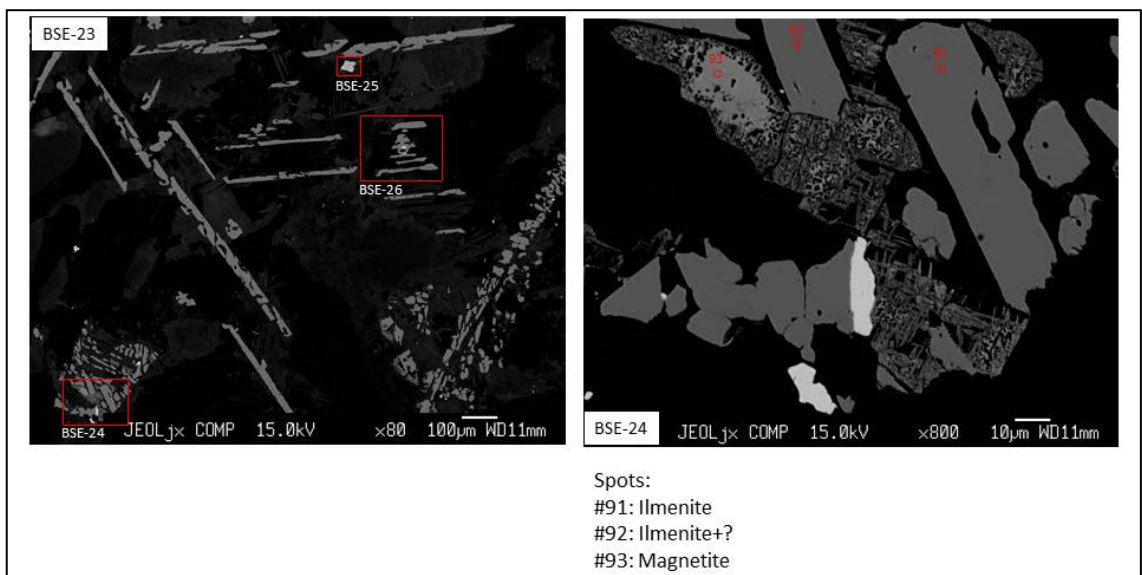


Fig. 47: Needle-like and skeletal ilmenite in groundmass (left) and in recrystallized ilmenite in the skeletal remains of titanomagnetite with ilmenite exsolution. Most magnetite is dissolved and replaced.

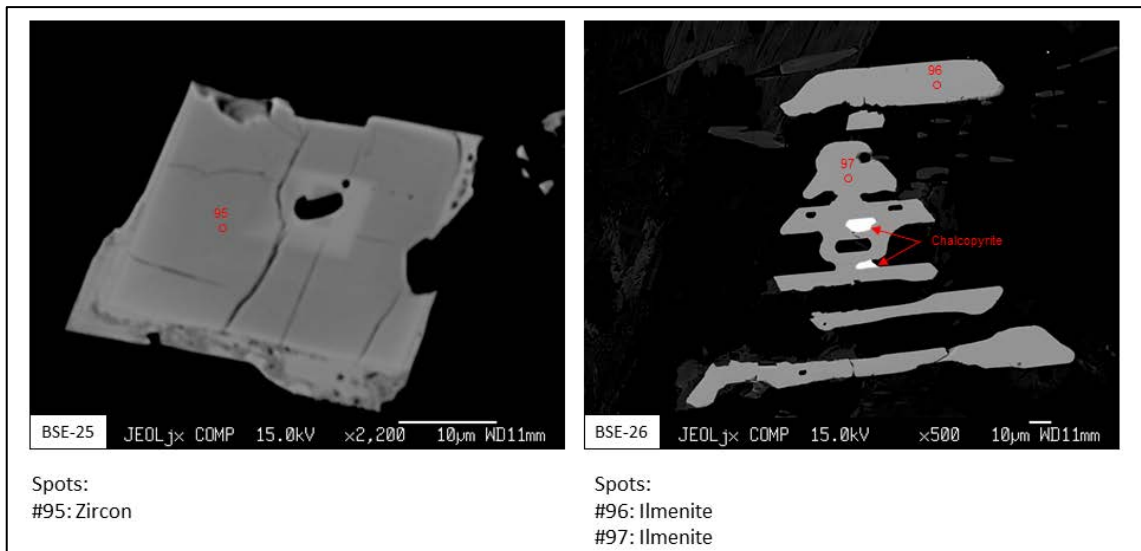


Fig. 48: Euhedral and zone zircon grain with late rims (left). Two small grains of chalcopyrite are enclosed in the ilmenite formed by exsolution from titanomagnetite. No magnetite remains.

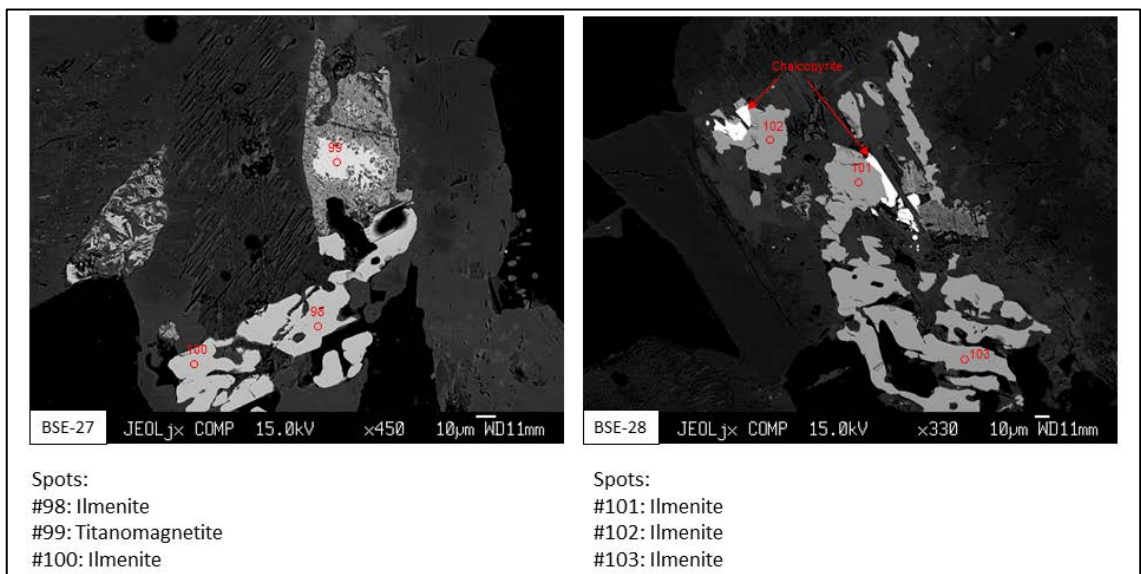


Fig. 49: Large blebby ilmenite grains and partially dissolved titanomagnetite grains with ilmenite exsolutions. Demonstrates the increase in ilmenite in the sill rocks by exsolution of ilmenite from titanomagnetite and the dissolution of the residual magnetite.

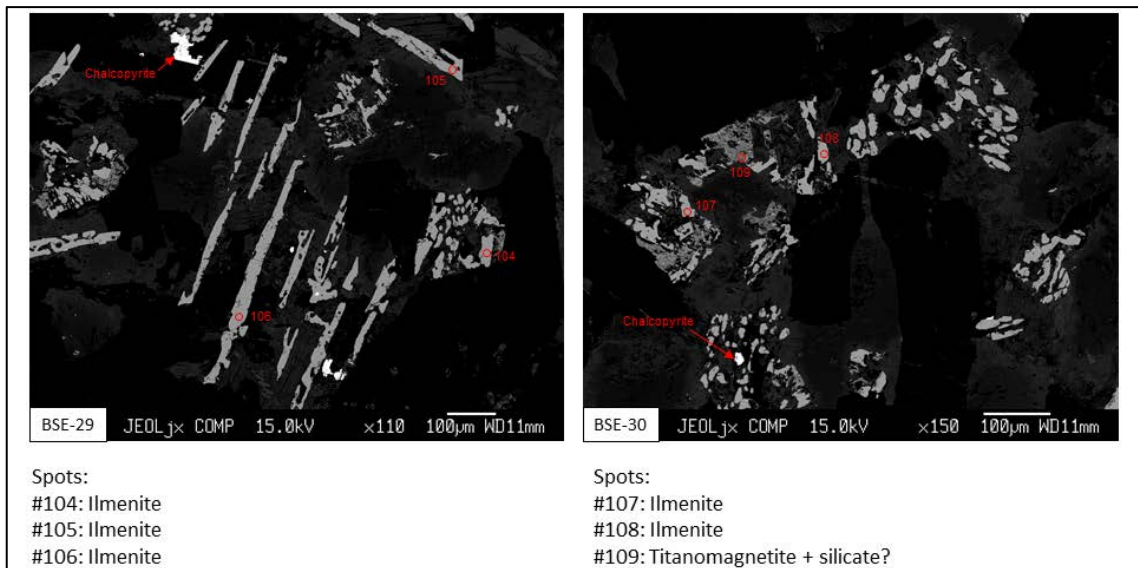


Fig. 50: Needle-like growth of ilmenite in the groundmass of the sill. Subhedral to euhedral titanomagnetite grains were subjected to ilmenite exsolution and subsequently to replacement of magnetite.

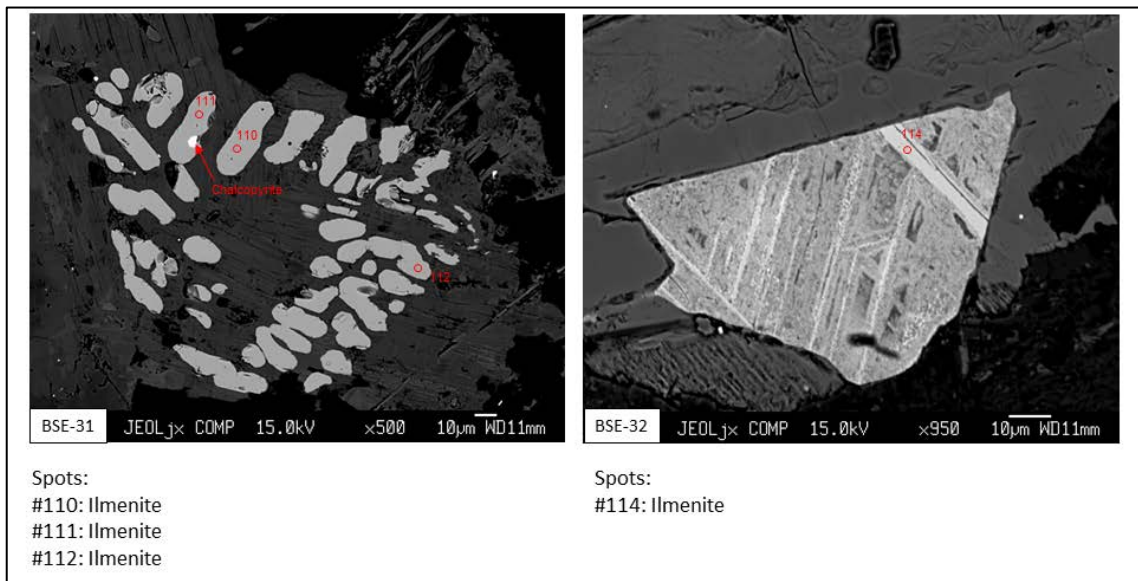


Fig. 51: Final and intermediate stage in the replacement of titanomagnetite. The rounded assemblage of ilmenite grains (left) shows the complete replacement of a subhedral to euhedral titanomagnetite grain by completely recrystallized ilmenite and silicate minerals. The assemblage probably formed from a euhedral titanomagnetite grain (right) that here is seen to have exsolved ilmenite and in which the residual magnetite is being replaced.

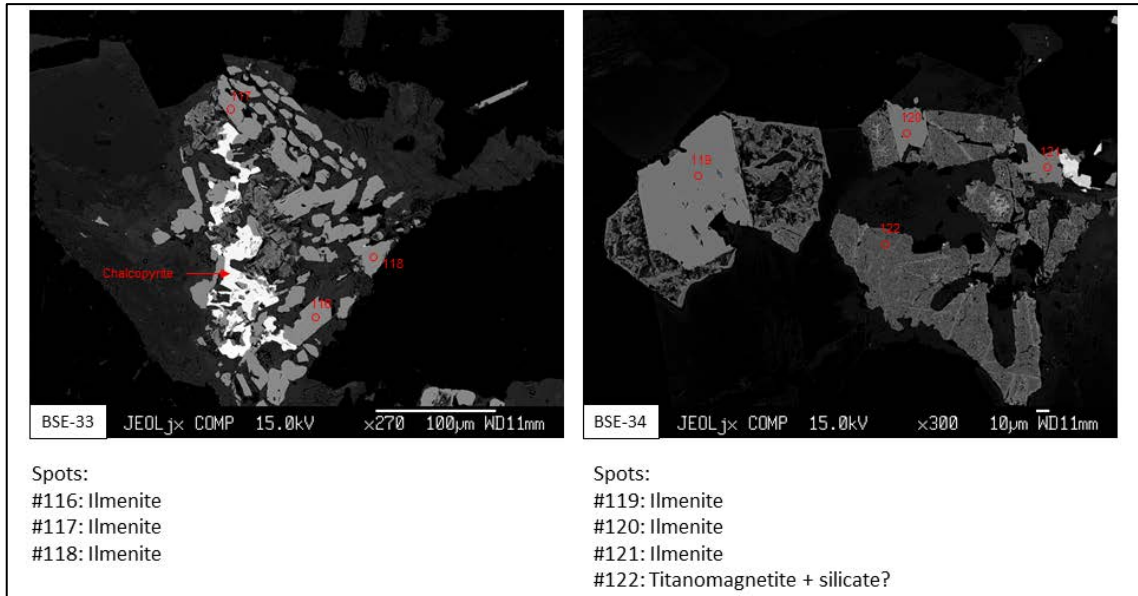


Fig. 52: Relict of titanomagnetite crystal as illustrated in the distribution of recrystallized ilmenite. The titanomagnetite was partially replaced by chalcopyrite and witness to extensive subsolidus reactions and equilibrations.

Sample GGU 166143, south shore of Olrik Fjord

The dyke sample has been prepared from jaw crushed material. The rock is fine to medium grained with partial replacement of pyroxene. FeTi-oxide grains are dotted throughout the sample.



Fig. 53: The rock is fine to medium grained with partial replacement of pyroxene.

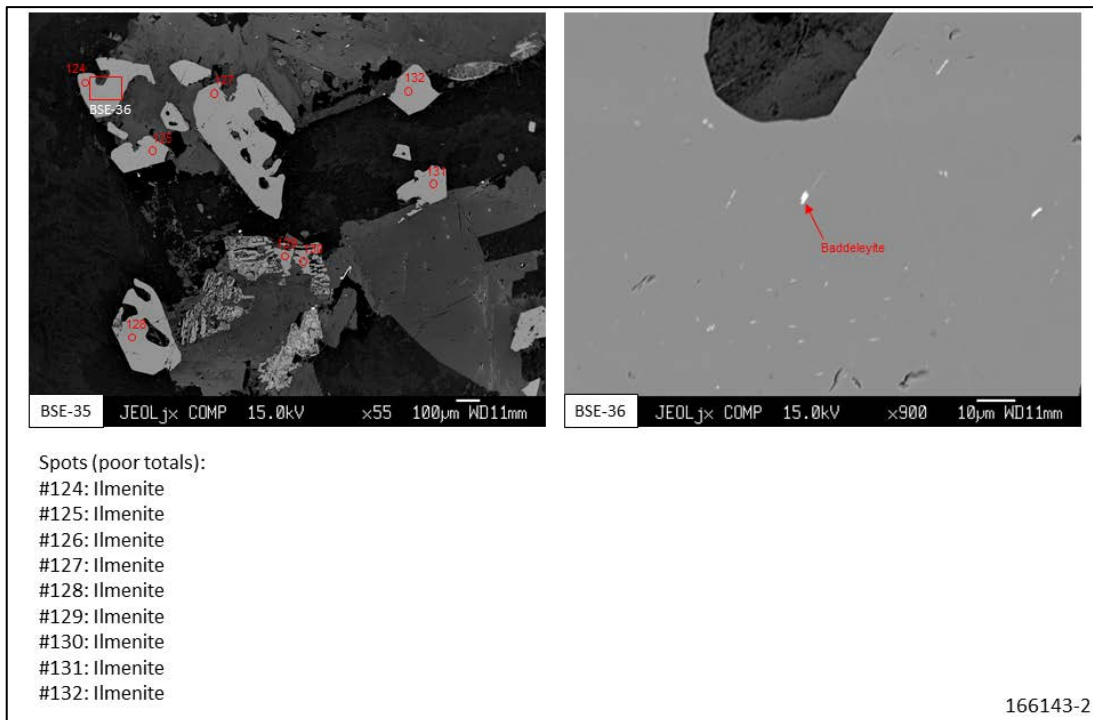


Fig. 54: The FeTi-oxide paragenesis is characterized by partially skeletal ilmenite grains and almost myrmecitic intergrowths of ilmenite and silicates that replace titanomagnetite. As in all previous samples the titanomagnetites are in variable stages of dissolution and leaving behind ilmenite formed from Ti originally contained in titanomagnetite.

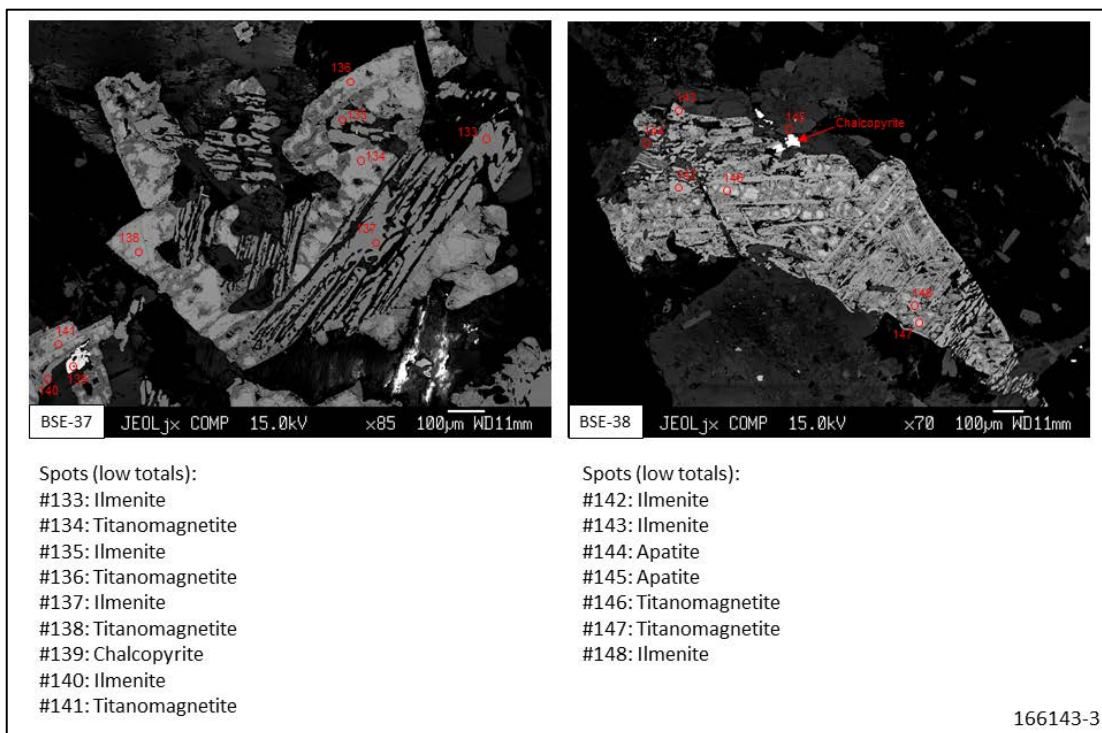


Fig. 55: The characteristic replacement of titanomagnetite with ilmenite exsolution. The residual magnetite is oxidized and eventually incorporated into Fe-bearing silicate minerals.

Sample 212556, northeastern of shore Northumberland Ø

The sample originates from a dyke and is just like sill sample 212513 a representative of the Ti-rich Franklin magmatism in the northwestern part of the Steensby land region.



Fig. 56: The dyke is fine grained and dotted with small grains of FeTi-oxides.

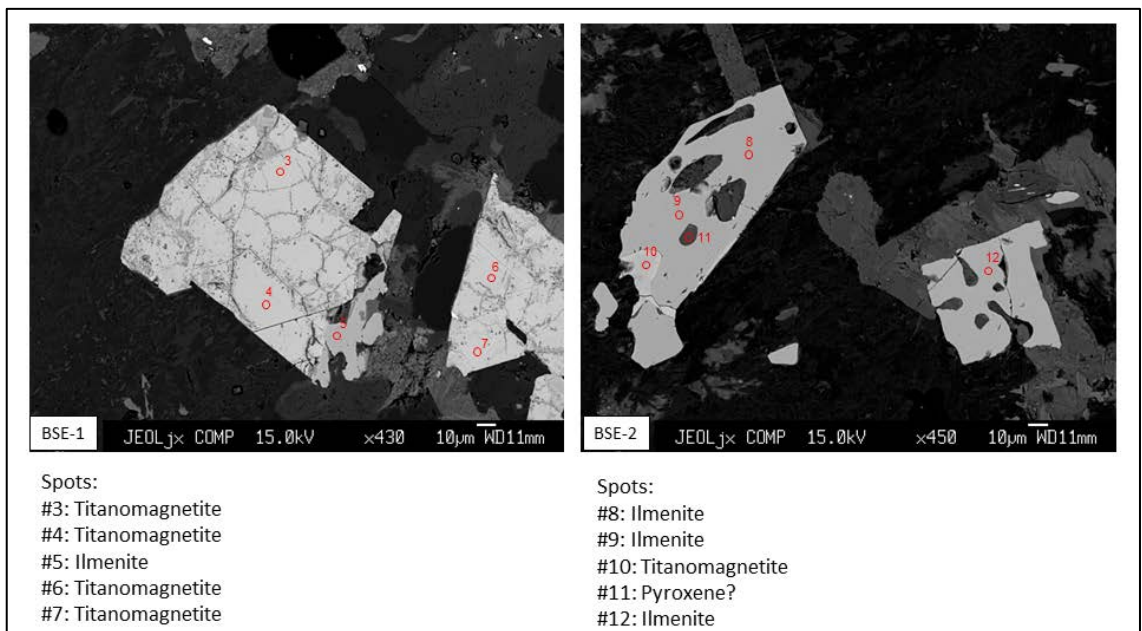


Fig. 57: As most dyke samples it contains primary ilmenite and titanomagnetite subjected to exsolution and alteration. Replacement of primary magnetite is seen along cracks in the titanomagnetite grain (left), whereas ilmenite with inclusions formed thickened skeletal crystals (right).

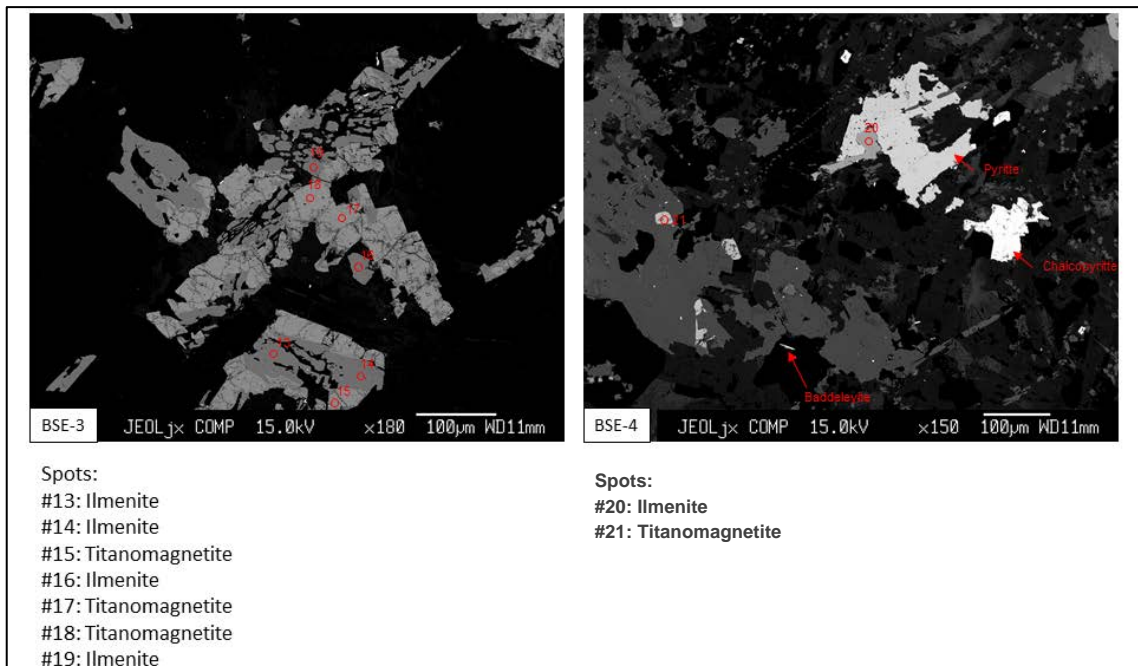


Fig. 58: Skeletal intergrowths of ilmenite and titanomagnetite (left). The intergrowth demonstrate the importance of titanomagnetite in the primary FeTi-oxide paragenesis of the dyke

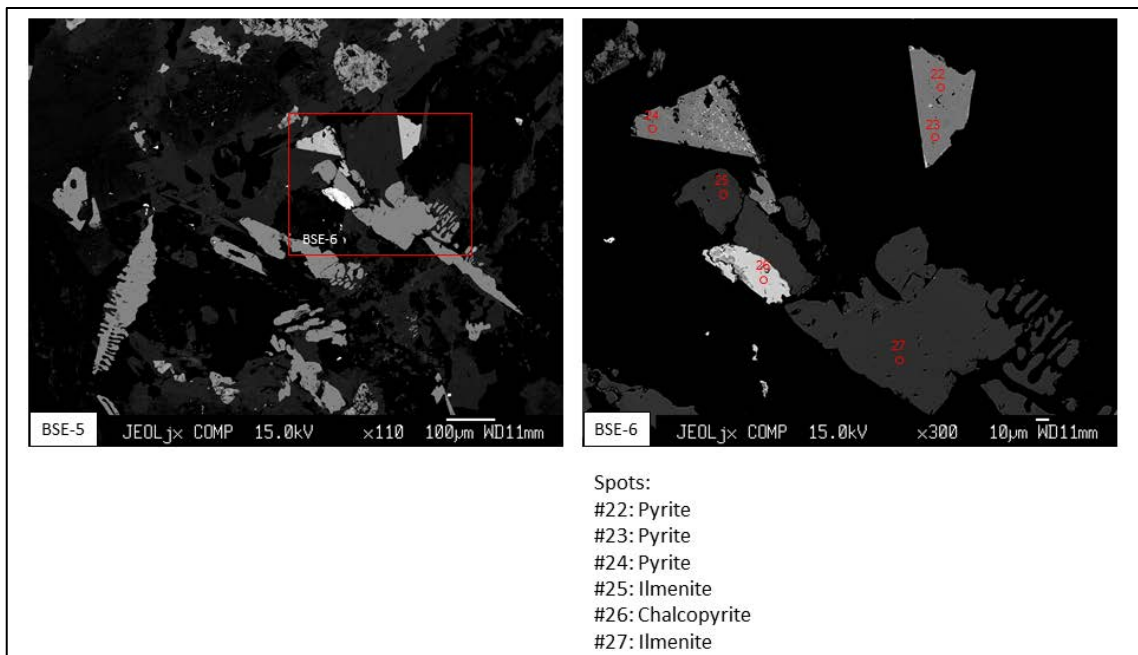


Fig. 59: Matrix with a FeTi-oxide paragenesis strongly dominated by ilmenite after dissolution of magnetite and with sulphide grains including pyrite and chalcopyrite.

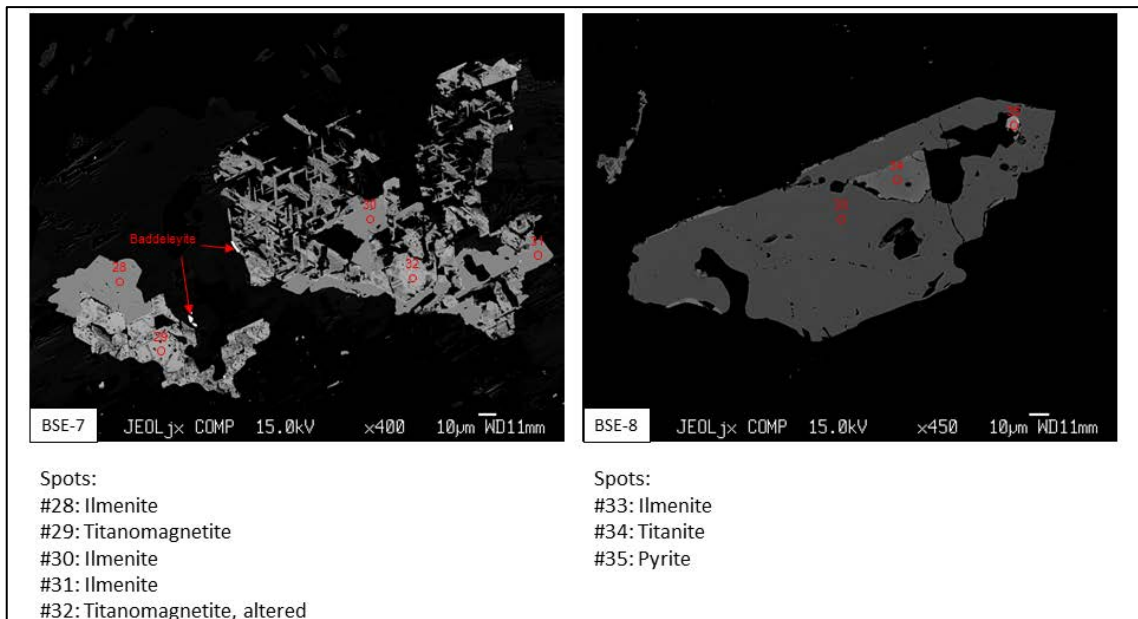


Fig. 60: Ghost of a titanomagnetite grain remaining after exsolution of ilmenite and dissolution of most of the residual magnetite (left) and ilmenite also subjected to re-equilibration leading to formation of titanite grain inside the ilmenite (right).

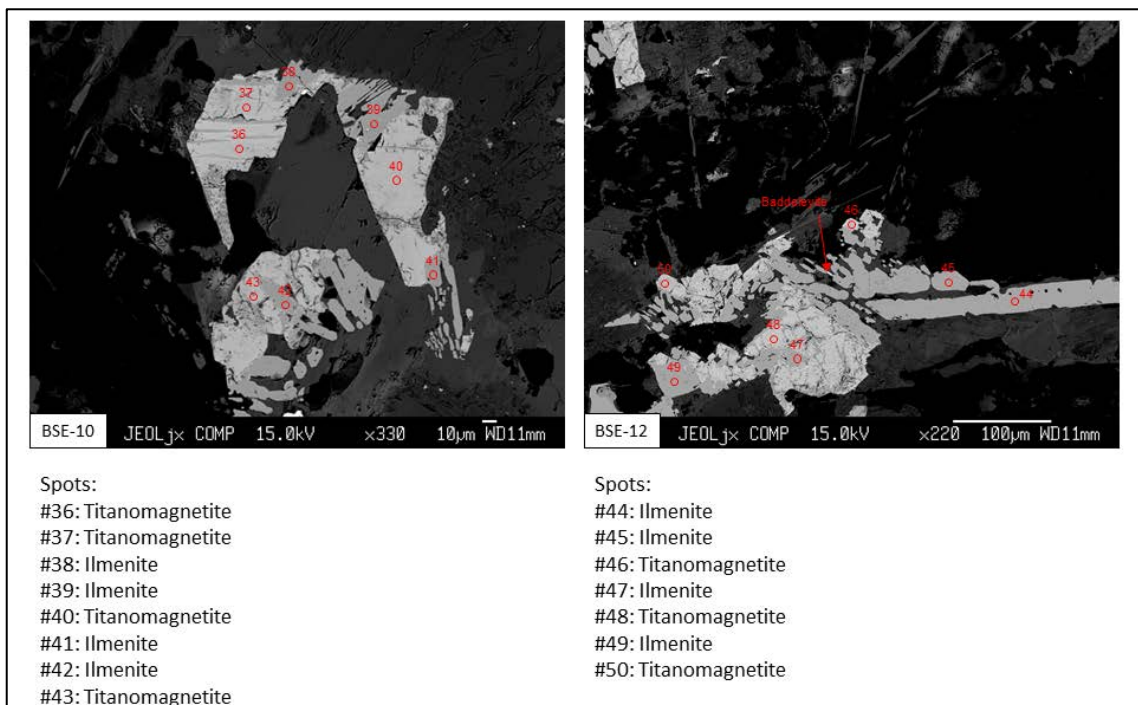


Fig. 61: Titanomagnetite with exsolution of ilmenite subjected to dissolution and loss of Fe.

Sample 243410, western Inglefield Land

The dyke is the most northerly representative of the Ti-rich Franklin magmatism. Only jaw crushed material remains in the collections.



Fig. 62: The dyke is fine grained and dotted with small FeTi-oxide grains and contains in addition conspicuous needles of FeTi-oxides.

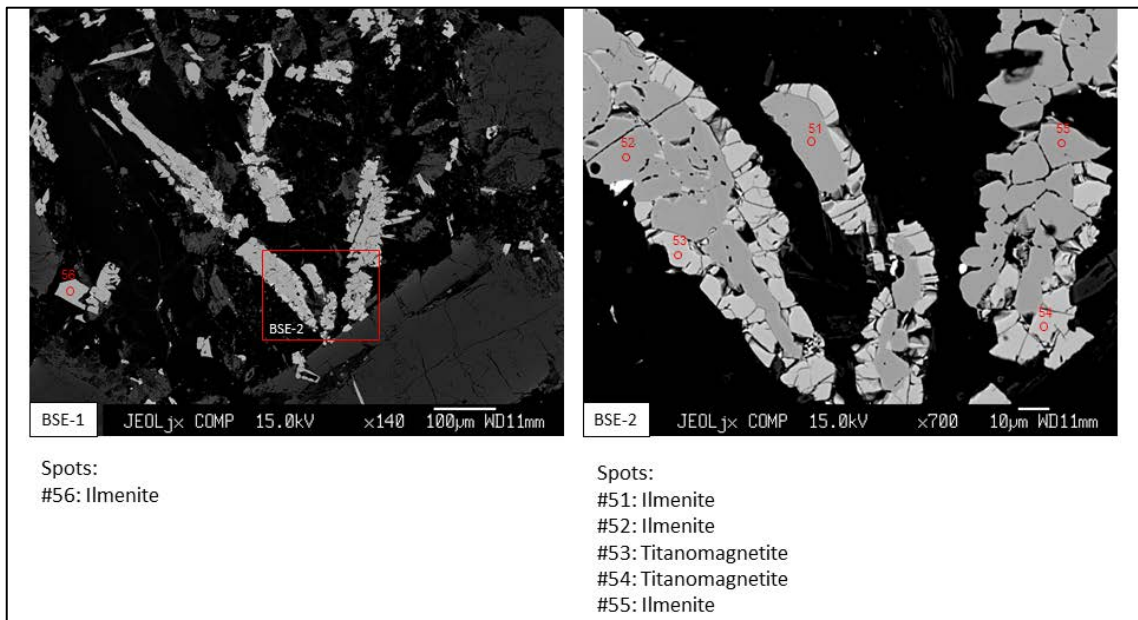


Fig. 60: FeTi-oxide needles (left) and enlargement (right). The needles are composed of a core of ilmenite surrounded by titanomagnetite. The spatial relationship suggests that ilmenite was first to crystallise in the basaltic melt in good agreement with the Ti-rich bulk composition.

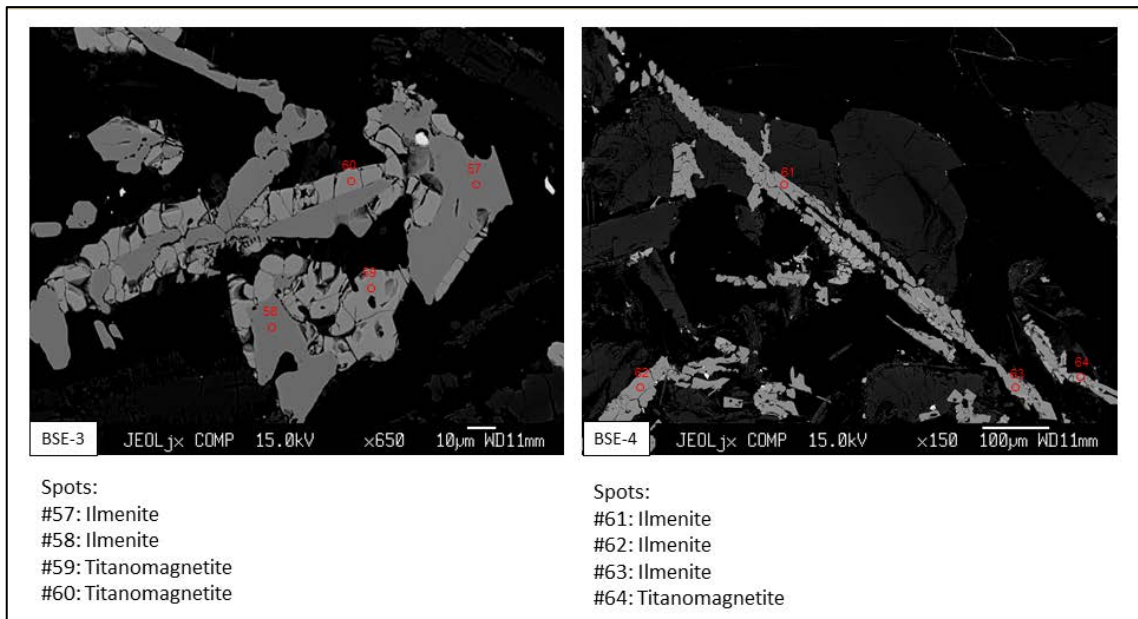


Fig. 64: Similar relations between ilmenite and titanomagnetite. Needles of ilmenite are nucleation hosts for later crystallisation of titanomagnetite.

Summary of petrographic observation

Ilmenite occurs in many forms due to exsolution and recrystallization in the basalts:

- 1) Primary euhedral crystals
- 2) Needles and rows of small crystals
- 3) Interrelated or detached groups of ilmenite grains, ghosts of exsolutions in titanomagnetite.

In some of the samples ilmenite appears to have preceded magnetite on the liquidus of the basaltic magma, a relationship that appears similar to that suggested for other TiO_2 -rich and evolved basaltic systems.

The samples of Franklin sills and dykes from the Steensby Land Sill Complex and the regional Franklin dyke swarm all demonstrate strong exsolution of ilmenite from titanomagnetite and often also complete dissolution of the residual magnetite. The net result of the exsolution and alteration of residual magnetite is a significant change in the titanomagnetite/magnetite to ilmenite ratio in the host rocks of the ilmenite deposits along the shores of Steensby Land. The primary magmatic ratios between titanomagnetite/magnetite and ilmenite and the present-day ratio that resulted from the exsolution and modifications of titanomagnetite/magnetite are in an later section modelled on the basis of the CIPW-norms of the bulk rock compositions and the bulk rock and EMP analyses of trace elements, especially vanadium and niobium provide a rational for the origin of the ilmenite-rich shore deposits and the composition of the ilmenite concentrate

Compositions of ilmenite, titanomagnetite and magnetite.

Ilmenite

The electron microprobe (EMP) single spot analyses show variations in elemental concentration. All superior analyses, as evaluated from stoichiometry and recalculated sums, are shown in Appendix 1. In general the ilmenites have low minor element concentrations. The minimum, maximum, mean, median and standard variations of the data set are shown in Table 3.

Table 3: Minimum, maximum, mean, median and standard variation for the composition of ilmenite.

	Weight%									Calculated		
	SiO ₂	TiO ₂	Al ₂ O ₃	Cr ₂ O ₃	FeO	MnO	NiO	MgO	CaO	Fe ₂ O ₃	FeO	Sum
Min	0.00	47.77	0.00	0.01	46.82	0.36	0.00	0.03	0.00	0.70	40.74	100.17
Max	1.00	53.25	0.30	0.10	51.94	2.11	0.12	2.54	0.33	11.60	46.52	104.79
Mean	0.04	50.74	0.06	0.04	49.89	0.87	0.02	0.39	0.08	6.49	44.05	102.74
Median	0.02	50.80	0.04	0.03	50.20	0.77	0.01	0.21	0.06	6.57	44.09	102.86
st. dev	0.11	1.13	0.07	0.03	1.22	0.37	0.03	0.41	0.07	2.12	1.16	0.89

Also the proportions of mineralogical end-members and the concentrations of vanadium and niobium are calculated. Trace element concentrations are maximum values and all samples with concentrations below detection limits have been omitted from the calculation. True average and median value are best obtained from a representative concentrate of ilmenite.

Table 4: Calculated mineral end-members and concentrations of V and Nb and oxides thereof for ilmenite; shown are minimum, maximum, mean, median and standard variation.

	Ilmenite	Gei- kilite	pyro- phaniite	Hae- matite	V ₂ O ₃	V ₂ O ₅	V ppm	Nb ₂ O ₅	Nb ppm
Min	84.01	0.10	0.76	0.65	0.00	0.00	0	0.01	0
Max	96.02	9.22	4.44	9.72	0.62	0.75	4618	0.45	3174
Mean	91.10	1.44	1.82	5.64	0.17	0.22	1301	0.06	395
Median	91.04	0.77	1.62	5.73	0.14	0.20	1181	0.05	339
st. dev	2.17	1.50	0.79	1.78	0.135	0.16	999	0.06	406

Titanomagnetite and magnetite

The compositions of preserved titanomagnetite/magnetite is a need constraint for estimation of the primary magmatic content of titanomagnetite and evaluation of the probable proportions of ilmenite derived from titanomagnetite in the beach deposits. Vanadium is an important tracer primary titanomagnetite and its concentration primary titanomanetite is a

priori assumed to reach 1-2 wt. % V₂O₅ with an average closer to 1 wt. %. This is based on a comparison the vanadium contents of titanomagnetite of e.g. the Bushveld Complex and the Skaergaard intrusion. The lower of the two concentrations is expected as the mg# of the basaltic rocks (see below) are low and that the basalts most likely already had experienced some titanomagnetite fractionation. Observed magnetite grains all have exsolved ilmenite and in many cases only the framework of exsolved ilmenite remains as a ghost after the former titanomagnetite grain. The average composition of titanomagnetite/magnetite is shown in Table 5.

Table 5: Average compositions of titanomagnetite/magnetite (wt. %)

										New	End-member prop.
SiO ₂	TiO ₂	Al ₂ O ₃	Cr ₂ O ₃	FeO	MnO	NiO	MgO	CaO	Sum*	Ulvöspinel	magnetite
0.211	14.62	1.227	0.025	77.14	0.596	0.031	0.025	0.257	99.88	43.39	56.61

*After calculation of Fe³⁺/Fe²⁺ ratio assuming stoichiometric composition, see appendix 2.

Maximum ulvöspinel component approaches 68% with 23-24 wt% TiO₂ in bulk compositions. Chromium contents are low conforming with the generally evolved nature of the basaltic compositions (low mg#). Maximum V₂O₅ contents reach 2 wt% with an average around 1 wt% (Table 6).

Table 6: V and Nb and oxides thereof in titanomagnetite/magnetite

V ₂ O ₃ *	V ₂ O ₅	V ppm	Nb ₂ O ₅	Nb max ppm
0.86	1.04	6539	0.19	134

*Oxides in weight %.

Compositional diagrams

The compositional variations in ilmenite and titanomagnetite/magnetite are illustrated in the following diagrams. They are all based on the EMP analyses in Appendixes 1 and 2.

Ilmenite, titanomagnetite and magnetite.

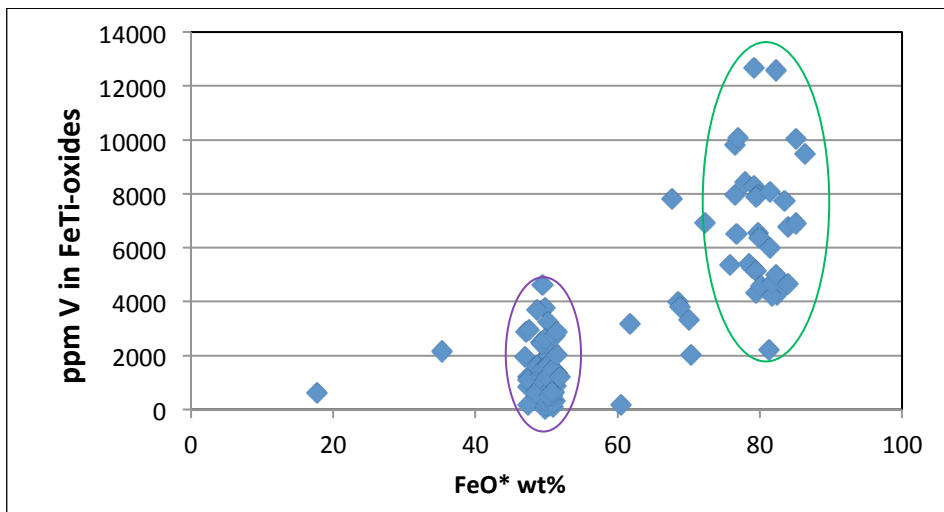


Fig. 65: Variation in vanadium (V) versus FeO* wt% in the FeTi-oxides of the Franklin sills and dykes (EMP data). The ilmenite grains (purple oval at 50 wt. % FeO*) have generally below 2000 ppm V and the titanomagnetite/magnetite grains (green oval at 80 wt. % FeO*) 4000->10000 ppm.

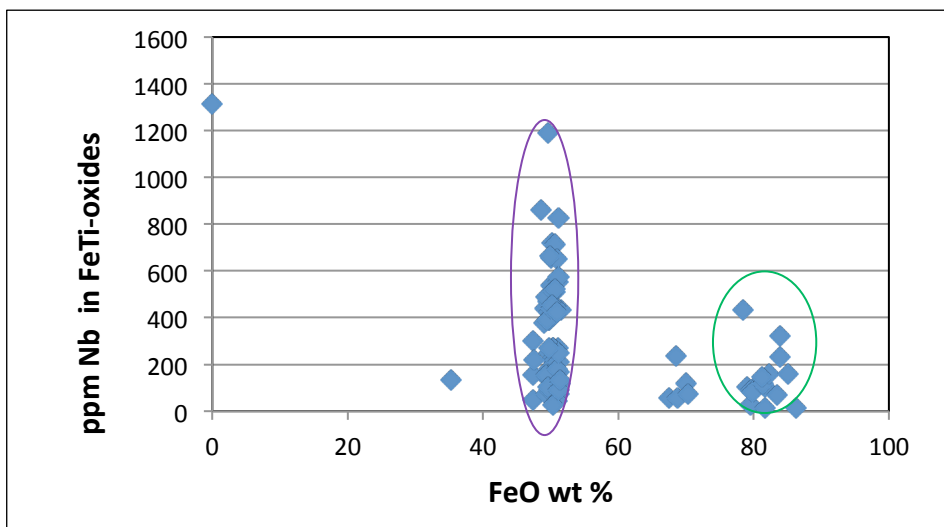


Fig. 66: FeO* versus Nb in FeTi-oxides. Ilmenite (purple oval) contain up to 1000 ppm Nb whereas titanomagnetite/magnetite mostly contain <200 ppm Nb (EMP data). The ilmenites separate into an Nb-rich group, assumed to be magmatic ilmenite (median 480 ppm Nb) and a low-Nb group assumed to represent ilmenite derived from titanomagnetite. One analysis with >3000 ppm Nb has been omitted as it is suspected to include Nb from a fragment of a Nb-rich phase, e.g., baddeleyite or zircon.

Ilmenite diagrams

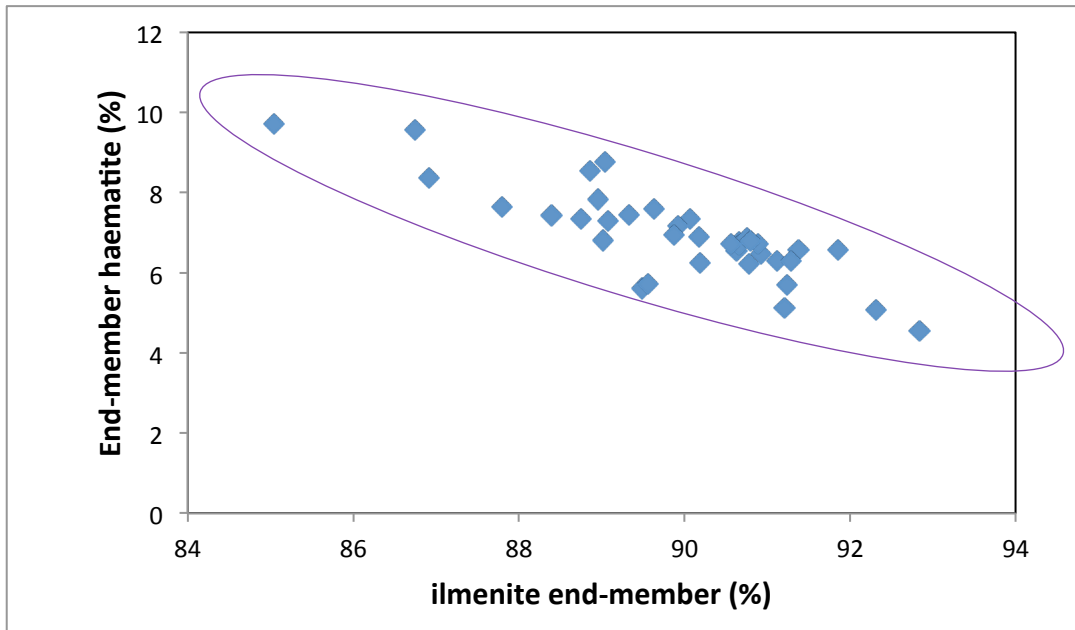


Fig. 67: Calculated ilmenite versus haematite end-members in ilmenite (*sensu lato*). Contents of haematite up to 10 atom % are not uncommon in ilmenite of igneous rocks of basaltic parentage.

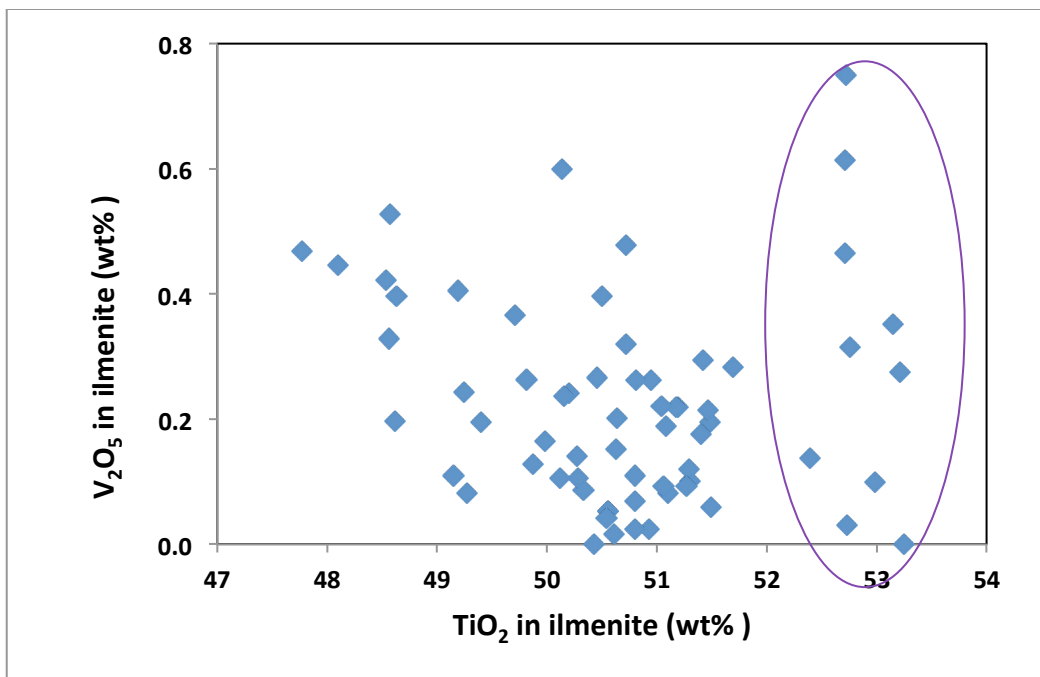


Fig. 68: V₂O₅ content in ilmenite (*sensu lato*). Note that TiO₂ rich ilmenites have a wide range of V₂O₅ contents (purple oval).

Titanomagnetite and magnetite diagrams

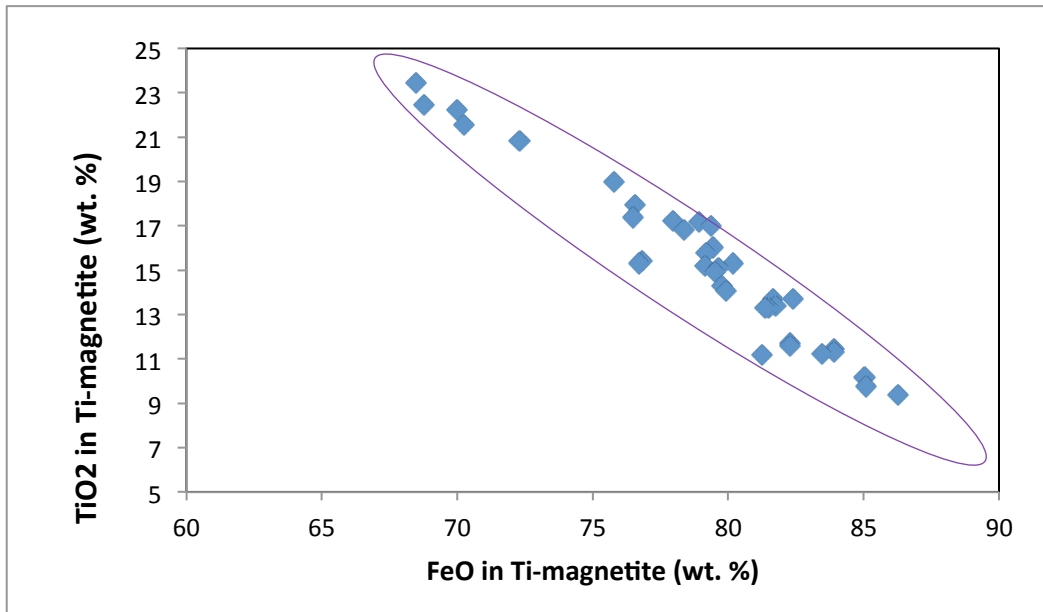


Fig. 69: FeO* versus TiO₂ in titanomagnetite/magnetite showing the normal negative correlation between the two.

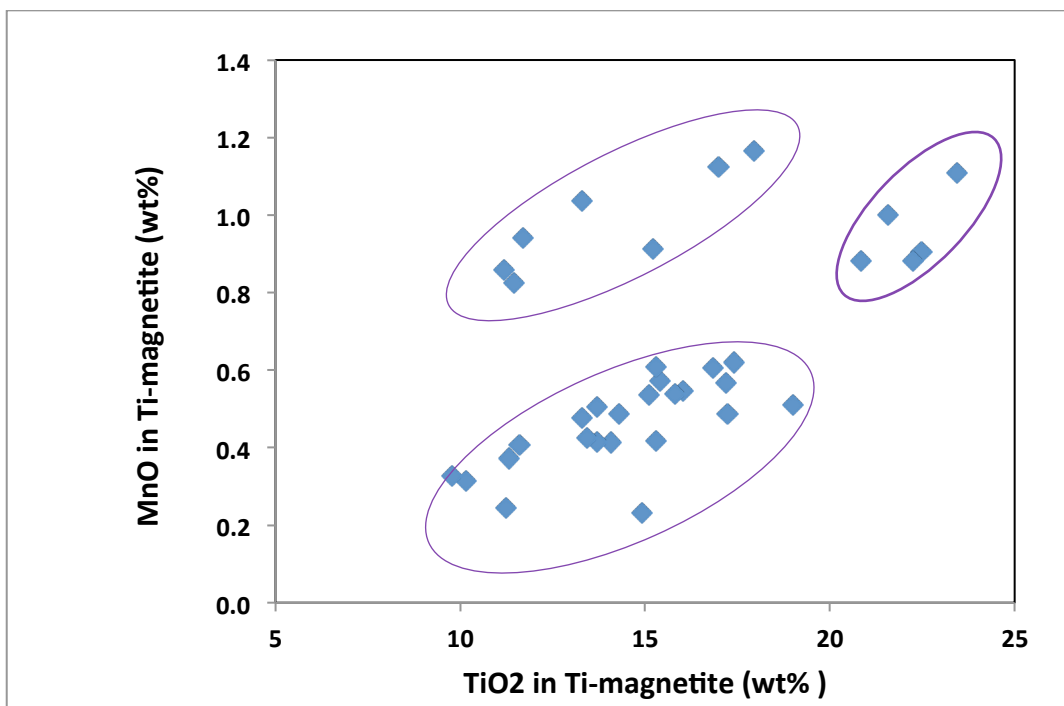


Fig. 70: TiO₂ versus MnO in titanomagnetite/magnetite showing the presence of more compositional populations. More detailed petrographic and chemical investigations are needed to correlate compositions to petrography and compositional re-equilibrations of the titanomagnetite compositions.

Laser ICP-MS compositions of ilmenite.

Concentrations of Nb are low in ilmenite and analysis by EMP should be supported by an additional method. The mean of 51 spot analyses by LA-ICP-MS shows an average of 385 ppm Nb and 0.06 wt% Nb₂O₅ in the ilmenite, very similar to the results obtained by EMP. The observed EMP concentrations of Nb can therefore be used for calculation of the primary proportion of ilmenite in the Franklin sill and dyke rocks from the Steensby Land region.

Observed compositions relative to specifications for ilmenite

It is not entirely clear how compositions vary with the petrographic groups of ilmenite. So far the EMP analyses suggest that all ilmenites with the exception of Cr₂O₃ in a few grains (Appendix 1) satisfy the compositional criteria forwarded to GEUS (Table 7).

Table 7: Critical compositional values of ilmenite

TiO ₂ : 45-55 wt%	by definition
FeO >20:	by definition
Fe ₂ O ₃ : <20	by definition
FeO:Fe ₂ O ₃ : >1	by definition
Cr ₂ O ₃ <0.3:	< 0.04
V ₂ O ₅ :	<0.23 wt %
CaO:	av. 0.08 wt%
MgO:	av. 0.38 wt%
MnO:	<1.35 wt%
Nb ₂ O ₅ :	<0.06 wt%
Al ₂ O ₃ :	av. 0.06 wt%

Concentrates of ilmenite that contain grains from both primary liquidus grains, exsolved titanomagnetite grains as well as grains crystallised during the alteration and recrystallization of the basalts at subliquidus conditions. At any given locality the bulk composition of an ilmenite concentrate will reflect the relative proportions of these very different types of ilmenite grains.

The March 31st PPT presentation also showed a summary of EMPA data for ilmenite. The median composition of the ilmenite grains analysed by EMP are probably better approximations to the bulk composition of ilmenite concentrates (Table 8).

Table 8: Median compositions of ilmenite compared to pigment specs for ilmenite

Oxide	wt. % in Ilmenite	key specs (pigment)
SiO ₂	0.02	
TiO ₂	49.29	45-55
Al ₂ O ₃	0.04	
Cr ₂ O ₃	<0.01	<0.1
FeO	42.76	>20
Fe ₂ O ₃	6.41	<20
MnO	0.75	
NiO	0.01	
MgO	0.20	
CaO	0.06	<1
FeO:Fe ₂ O ₃	6.60	>1

Bulk rock compositions

The major element bulk compositions and norms of 21 samples of sill and dyke rocks from the TiO₂-rich Franklin magmatism are shown in Appendix 3. The calculation of CIPW norms allows estimates of the primary contents and ratios of titanomagnetite and ilmenite in the basaltic sill and dyke rocks, and thus estimates of the proportion of ilmenite formed by exsolution from titanomagnetite. CIPW-norms are calculated at Fe₂O₃/FeO = 0.10, 0.15, and 0.2.

The Franklin magmatism is tholeiitic with and characterized by elevated FeO*, TiO₂, P₂O₅ and low mg#. The evolved and Fe-rich character of the magmatism suggests a rifting related magmatism through thick crust (Dawes, 2006).

In addition to the pre-existing major element analyses the table includes new ICP trace element analyses. A test for the validity of the calculated norms is a mass balance for V and Nb assuming that all V was originally hosted in titanomagnetite and that all Nb followed Ti in ilmenite and titanomagnetite. The trace element modelling (Appendix 4) validates the calculated normative proportions of titanomagnetite, magnetite and ilmenite in the investigated samples.

Evaluation of primary magnetite and ilmenite content and proportions

CIPW-norms are calculated from the major element compositions of magmatic rocks and provide end-member mineral proportion for the rock forming minerals of the sill and dyke rocks. The bulk compositions are basaltic and the mineralogy of the primary rocks is well represented by the norms, as long as the oxidation state and Fe₂O₃/FeO* (FeO* = all Fe as FeO) is known within acceptable limits.

CIPW-norms have been calculated on a volatile free basis at Fe₂O₃/FeO* set at 0.1, 0.15 and 0.2. Increasing Fe₂O₃/FeO* increases the proportions of modelled magnetite and quartz in the norms. It is therefore important for the evaluation of the proportions of ilmenite that can be supplied from the Steensby Land sills and dykes to constrain the Fe₂O₃/FeO* ratio at which the normative proportions of magnetite and ilmenite are calculated.

Bulk rock concentrations of V and Nb are modelled on the basis of the average contents in magnetite and ilmenite and the normative proportion of the two phases (Appendix 4). The calculated proportions on the basis of the three oxidation scenarios (Fe₂O₃/FeO* = 0.1, 0.15 and 0.2) clearly demonstrate that the norms of the samples, including their exsolved ilmenite, must be calculated at Fe₂O₃/FeO* = 0.2 (Table 9). Errors on modelled bulk rock contents of V and Nb are on average 9 and 2%, respectively, relative to the measured bulk V and Nb of the samples. At Fe₂O₃/FeO* = 0.1 the relative errors on modeled V and Nb have increased to 77 and 8 %, respectively.

Table 9: Calculated V and Nb in bulk rocks on basis of V and Nb in titanomagnetite and ilmenite, respectively, and normative proportions of magnetite and ilmenite.

Fe ₂ O ₃ /FeO*	0.20		0.15		0.10	
	ppm	%	ppm	%	ppm	%
Average V (ppm)	370		299		228	
Average deviation	-34	-9	-105	-35	-176	-77
Average Nb (ppm)	29		29		28	
Average deviation	-1	-2	-1	-5	-2	-8

The V₂O₅ and Nb₂O₅ contents of liquidus titanomagnetite and ilmenite are modelled for evaluation of the maximum titanomagnetite/ilmenite ratio in the Franklin basalts prior to hydrous alteration and for evaluation of the process responsible for the high ilmenite/magnetite ratio of the Steensby Land beach deposits. The proportion of normative ilmenite is controlled by TiO₂ and the proportion of titanomagnetite is controlled by the Fe₂O₃/FeO* ratio and the primary composition of ilmenite. The primary titanomagnetite is on basis of experimental evidence assumed have contained ~24 wt. % TiO₂ prior to exsolution of ilmenite and the proportion of titanomagnetite can be reconstructed by adding 0.82 proportions of normative ilmenite to calculated normative magnetite. The concentrations of V₂O₅ and Nb₂O₅ of the resulting “primary” proportions of titanomagnetite (TiMt₂₄) and ilmenite (Ilm₂₄) are then calculated from the bulk concentrations of V and Nb in the analysed samples and compared to observed concentrations of V₂O₅ and Nb₂O₅ in titanomagnetite and ilmenite (Table 10 and Appendix 4).

Table 10: Calculated V in titanomagnetite and Nb in ilmenite on the basis of normative proportions of TiMt₂₄ and ilm₂₄

Fe ₂ O ₃ /FeO*	0.20		0.15		0.10	
	Calc.	Obs.	Calc.	Obs.	Calc.	Obs.
Average V (ppm)	5122	6539	6823	6539	10236	6539
Average V ₂ O ₅ wt. %	0.80	-	1.06	-	1.60	-
Average Nb (ppm)	564	-	480	-	418	-
Average Nb ₂ O ₅ wt. %	0.08	0.06	0.07	0.06	0.06	0.06

The calculated titanomagnetite decreases from 8.44 wt% to 4.22 wt. % as Fe₂O₃/FeO* decreases from 0.2 to 0.1. Calculated average contents of V₂O₅ in titanomagnetite increases from 0.8 to 1.6 and Nb₂O₅ in ilmenite decreases from 0.8 to 0.6 as Fe₂O₃/FeO* decreases from 0.2 to 0.1. The estimated liquidus concentrations of V₂O₅ and Nb₂O₅ are ~1 wt % V₂O₅ and ~0.06 wt. % Nb₂O₅. The concentrations of V₂O₅ in titanomagnetite compares to those calculated assuming Fe₂O₃/FeO* = 0.15 in the CIPW-norm calculation. The Franklin basaltic sills and dykes of the Thule District had primary ration between titanomagnetite and ilmenite of 0.70 to 1.45 and very similar to common tholeiitic magmatism. The strong dominance of ilmenite in the now collected samples reflects, besides exsolution of ilmenite, late-magmatic to subsolidus dissolution processes that reduced the content of magnetite.

Ilmenite made available by erosion

Regional evaluation

The volumes of sills in the Steensby land, the tonnage of originally contained ilmenite and the tonnages of ilmenite made available for sedimentation are estimated in Table 11. The calculation is based on the areas of individual blocks (Table 1, Fig. 71). In order to maintain conservative estimates the density of the basaltic rocks is set to 2.6. A low density of the host rocks is chosen to account for the presence of hydrated phases in the sill and dyke rocks (full data in Appendix 5).

Table 11: Estimate of primary ilmenite, remaining ilmenite and eroded ilmenite in Steensby Land

<i>Block</i>	<i>Booth Sund block</i>	<i>Moriusaq block</i>	<i>Total</i>
Area, km ²	360	414	774
Thickness (km)*	0.4	0.4	0.4
Vol. frac. Sills**	0.3	0.3	0.3
Eroded fraction***	0.4	0.4	0.4
Density, rock kg/m ³	2600	2600	2600
m ³ /km ³		1.00E+09	
kg/Gt		1.00E+12	
Total volume, km ³	144.1	165.65	309.75
Total mass source rock, Gt	112	129	242
<i>Scenario A, 9 wt. % ilmenite in source****</i>			
Wt.% ilmenite in source	9	9	9
Total mass ilmenite, Gt	10	11.6	22
Contained ilmenite, Gt	6	7.0	13
Eroded ilmenite, Gt	4.0	4.7	8.7
<i>Scenario B, 7 wt. % ilmenite in source****</i>			
Wt.% ilmenite in source	7	7	7
Total mass ilmenite, Gt	8	9	17
Contained ilmenite, Gt	5	5	10
Eroded ilmenite, Gt	3	4	7
<i>Scenario C, 5 wt. % ilmenite in source****</i>			
Wt.% ilmenite in source	5	5	5
Total mass ilmenite, Gt	6	6	12
Contained ilmenite, Gt	3	4	7
Eroded ilmenite, Gt	2	3	5

* *Conservative estimate of the thickness of the succession hosting the sills*

** *Estimate of the stratigraphic proportion of sill material (Dawes, 2006)*

*** Estimate of the proportion of the 400 m thick and sill-bearing section that has been eroded

**** Ilmenite content of host rocks evaluated on basis of normative composition, petrographic observations and backscatter images. Observed contents of ilmenite vary from app. 5 to 9 wt% and 7 wt % is a probable average for the ilmenite content of the source rocks.

Only a 0.4 km section of Dundas Formation is assumed in the calculations even though the formation is up to 1000 m in thickness with as much as 300 m of sill. The reduced thickness is chosen as a constraint as the thickness of eroded Dundas Formation in postglacial times is not known with certainty. The total volume of sill material may be higher than here estimated.

Ilmenite is supplied not only from sills, but also from the related Franklin dykes. The potential tonnage of ilmenite hosted in the dykes is estimated in Table 12. The estimates operate with two different scenarios as the erosion depth in postglacial times is unknown. The two scenarios envisage erosion of dykes to a depth of 100 and 500 meters, respectively.

Table 12: Estimated mass of ilmenite contained in dykes

Western block (Booth Sound block)

East-West (km)	40	40
Integrated dyke width (km)*	0.2	0.2
vertical section (km)**	0.1	0.5
Volume of dike rock (km ³)	0.8	4
mass of dyke rock (Gt)	2.08	10.4
Contained ilmenite (Gt)***	0.104	0.52

Eastern block (Moriuaq block)

East-West (km)	40	40
Integrated dyke width (km)*	0.2	0.2
vertical section (km)**	0.1	0.5
Volume of dike rock (km ³)	0.8	4
mass of dyke rock (Gt)	2.08	10.4
Contained ilmenite (Gt)***	0.104	0.52

Total ilmenite contained in dykes (Gt) 0.208 1.040

* Summed up total thickness of dykes in the block

** Height of dyke section included in calculation

*** Assumes 0.05 wt. % ilmenite in dyke rocks.

Northern Moriusaq block

The width, length and thicknesses of individual sills removed by erosion have been extrapolated into the valley. Volumes of eroded sill material are model from these constraints.

Model 1

From watershed to fault between Dundas and Qaanaaq formations (blue quadrant in Fig. 71)

Table 13: Calculated volume of sill eroded in E-W valley 10 km north of Moriusaq. summary of calculations in Appendix 5

<i>Sill number (up section)</i>	<i>1</i>	<i>2</i>	<i>3</i>	<i>4</i>	<i>5</i>
Length parallel to coast, km	12	12	12	12	12
Width parallel to Granville Fj., km	5	5.4	6.5	6.8	8
Sill thickness (m)*	20	20	20	20	20
Vol. sill now removed, km ³	1.2	1.296	1.56	1.632	1.92
<i>Sill number (up section)</i>	<i>6</i>	<i>7</i>	<i>8</i>	<i>9</i>	
Length parallel to coast, km	12	12	12	12	
Width parallel to Granville Fj., km	8.6	9.4	10	10.8	
Sill thickness (m)*	20	20	20	20	
Vol. sill now removed, km ³	2.064	2.256	2.4	2.592	

The tonnages of ilmenite made available for re-deposition in the coastal environment can then be calculated from the sill tonnages (see Appendix 5)

Table 14: Estimated supply of ilmenite from watershed to Qaanaaq fault (preferred scenario in bold and italics)

Total vol. eroded rock, km ³	16.92
Total mass eroded rock, Gt	43.99
Scenario A. 9 wt. % ilmenite in source Ilmenite introduced to Granville Fj., Gt	4.0
Scenario B. 7. wt. % ilmenite in source Ilmenite introduced to Granville Fj., Gt	3.1
Scenario C. 5 wt. % ilmenite in source Ilmenite introduced to Granville Fj., Gt	2.2
The calculation uses: 1) Density, rock kg/m ³ = 2600, 2) m ³ /km ³ = 1.00E+09 and 3) Kg/Gt = 1.00E+12	

Model 2

Moriusaq block from Watershed to north side of the valley. The model has been calculated as there is no clear evidence for the presence of sills in the eroded lower parts of the Dundas Formation north of the valley. Only the sills that prior to erosion occurred in the lower part of the blue Moriusaq box (Fig. 71) are included in this model.

Table 15: Calculated volumes of sills eroded in E-W valley 10 km north of Moriusaq between watershed and the north side of valley

<i>Sill number</i>	<i>1</i>	<i>2</i>	<i>3</i>	<i>4</i>	<i>5</i>
Length parallel to coast, km	12	12	12	12	12
Width parallel to Granville Fj., km	1.25	1.65	2.75	3.05	4.25
Sill thickness (m)*	20	20	20	20	20
Vol. sill now removed, km ³	0.3	0.396	0.66	0.732	1.02
<i>Sill number</i>	<i>6</i>	<i>7</i>	<i>8</i>	<i>9</i>	
Length parallel to coast, km	12	12	12	12	
Width parallel to Granville Fj., km	4.85	5.65	6.25	7.05	
Sill thickness (m)*	20	20	20	20	
Vol. sill now removed, km ³	1.164	1.356	1.5	1.692	

* Standardized thickness on basis of descriptions in field notes (P.R. Dawes). More detailed estimates require collection of profile and samples in the valley. Data and calculations in Appendix 5.

Tonnages of ilmenite made available for sedimentation from sills eroded between watershed of Moriusaq block and the northern limit of the E-W valley 10 km inland from Moriusaq are shown in Table 16.

Table 16 Estimated supply of ilmenite from watershed to north side of valley (preferred scenario in bold and italics)

Total vol. eroded rock, km ³	8.82
Total mass eroded rock, Gt	22.93
Scenario A. 9 wt. % ilmenite in source	
Ilmenite introduced to Granville Fj., Gt	2.1
Scenario B. 7. wt. % ilmenite in source	
Ilmenite introduced to Granville Fj., Gt	1.6
Scenario C. 5 wt. % ilmenite in source	
Ilmenite introduced to Granville Fj., Gt	1.1

The calculation uses: 1) Density, rock kg/m³ = 2600, 2) m³/km³ = 1.00E+09 and 3) Kg/Gt = 1.00E+12. Details in Appendix 5.

The calculations suggest a significant potential in the E-W valley north of Moriusaq and in adjacent shore deposits in Granville Fjord.

Moriusaq block south of watershed

Hillside behind Moriussaq, stretching from Granville fjord to Kap Abernathy. Rivers and streams discharge to the south.

Sills

The calculation of the amount of ilmenite originally contained in sills, remaining in sills, and made available for re-depositions along shore of Steensby Land in the vicinity of Moriusaq is based on the following constraints:

1. Area, km ²	2. 168
3. Thickness, accumulated (m)	4. 60
5. Density, rock kg/m ³	6. 2600
7. m ³ /km ³	8. 1.00E+09
9. kg/Gt	10. 1.00E+12
11. Total volume, km ³	12. 10.1
13. Total mass sills, Gt	14. 26.2
15. Fraction eroded	16. 0.4

Table 17: Calculations of ilmenite tonnages in the Moriusaq block south of the watershed.

Scenario	A	B	C
% ilmenite in source	9	7	5
Total ilmenite, Gt	2.4	1.8	1.3
Ilmenite remaining in sills, Gt	1.5	1.1	0.8
Ilmenite eroded from sills, Gt	0.9	0.7	0.5

Dykes

The calculation of the amount of ilmenite originally contained in dykes that could be available for re-depositions along shore of Steensby Land in the vicinity of Moriusaq is based on the following constraints:

1. Model	1	2
2. Total thickness of dykes (m)	150	150
3. Coast parallel length (km)	12	12
4. Depth to which dykes are eroded (m)	100	500
5. Vol. source rock, km ³	0.18	0.90
6. Mass source rock, Gt	0.5	2.3

Table 18: Calculated ilmenite in dykes in 6 scenarios

Scenario (Note <i>change in units</i>)	A1	A2	B1	B2	C1	C2
% ilmenite in source	9	9	7	7	5	5
Contained ilmenite, Mt	42	211	33	164	23	117

Total ilmenite for Moriusaq Block south of watershed:

Dependent on chosen model the amount of ilmenite that is likely derived for sills and dykes south of the watershed in the hills north of Moriusaq amounts to 500 to 1100 million tons.

Summary of calculated ilmenite

The preferred tonnages ilmenite calculated for the Steensby Land Sill Complex in southern Steensby Land include:

1. Ilmenite contained in sills prior to erosion: 17 Gt
2. Ilmenite remaining in sills after erosion: 10 Gt
3. Ilmenite available for sedimentation 7 Gt

The estimates are believed to be conservative as thickness of eroded Dundas Formation is limited to 400 m, as the density is set to 2.6 (compared with an expected density of sill rocks of ~3, and as an average thickness of 20 m has been used compared to the expected common thickness of 20-50 meter of the sills. The total tonnage of ilmenite freed for sedimentation may be underestimated by a factor of 2-3. An important result from this study is that 1/3 of the ilmenite present in the sediment at Pituffik is derived from alteration of titanomagnetite. Contradictory to this, it is noted that little information is available for the amount of ilmenite that may have been lost in currents along the shores.

References

Dawes, P.R. (1989). The Thule black sand province, North-West Greenland: investigation status and potential. Open File Series Grønlands Geologiske Undersøgelse 89/4, 17 pp.

Dawes, P.R. (1991). Geological map of Greenland, 1:500 000, Thule, Sheet 5. Geological Survey of Denmark and Greenland

Dawes, P.R. (1997). The Proterozoic Thule Supergroup, Greenland and Canada: history, lithostratigraphy and development. Geology of Greenland Survey Bulletin 174, 150 pp.

Dawes, P.R. (2006). Explanatory notes to the Geological map of Greenland, 1:500 000, Thule, Sheet 5. Geological Survey of Denmark and Greenland map series 2, 97 pp.

Appendices

Appendix 1: Franklin magmatism, Thule Distric. Ilmenite analyses

sample No.	EMP No.	Weight%									Calculated				Gei-kilite	pyro-phaniite	Hae-matite	V2O3	V2O5	V ppm	Nb2O5	Nb ppm
		SiO2	TiO2	Al2O3	Cr2O3	FeO	MnO	NiO	MgO	CaO	Fe2O3	FeO	Sum	Ilmenite								
166673_1_16	70	0.00	53.25	0.00	0.03	46.95	1.48	0.01	0.21	0.00	1.04	46.02	102.04	95.18	0.77	3.10	0.96	n.d.	n.d.	n.d.	n.d.	n.d.
166673_1_24	78	0.02	53.21	0.00	0.10	47.25	1.51	0.01	0.12	0.00	1.26	46.11	102.34	95.25	0.43	3.16	1.16	0.23	0.27	1689	0.02	140
166673_1_1	56	0.03	53.14	0.05	0.09	46.82	1.32	0.00	0.15	0.00	0.70	46.19	101.67	96.02	0.54	2.78	0.65	0.29	0.35	2167	0.11	741
166673_1_28	82	0.01	52.98	0.03	0.06	46.84	1.52	0.00	0.13	0.00	1.08	45.86	101.69	95.30	0.50	3.20	1.00	0.08	0.10	613	n.d.	n.d.
166673_1_6	60	0.00	52.76	0.00	0.07	46.93	1.80	0.00	0.11	0.00	1.68	45.42	101.85	94.26	0.41	3.78	1.54	0.26	0.32	1943	n.d.	n.d.
166673_1_20	74	0.01	52.73	0.02	0.07	47.41	1.27	0.01	0.24	0.00	1.90	45.70	101.94	94.71	0.89	2.66	1.74	0.03	0.03	187	0.06	426
212513_102	101	0.00	52.72	0.01	0.01	49.38	0.59	0.00	0.17	0.08	3.18	46.52	103.27	95.32	0.61	1.22	2.85	0.62	0.75	4618	0.02	147
166672_1_33	1	0.04	52.71	0.01	0.08	47.03	1.26	0.02	0.10	0.10	1.20	45.95	101.47	95.86	0.36	2.66	1.12	0.38	0.47	2869	0.02	105
212513_103	102	0.02	52.71	0.00	b.d.	49.73	0.73	0.00	0.15	0.06	3.70	46.40	103.77	94.67	0.54	1.51	3.29	0.51	0.61	3781	0.07	454
166673_1_19	73	0.03	52.39	0.03	0.07	47.37	1.59	0.03	0.12	0.00	2.32	45.28	101.86	94.08	0.45	3.35	2.12	0.11	0.14	844	0.04	301
212513_120	119	0.01	52.01	0.11	b.d.	49.35	0.52	0.05	1.28	0.05	5.98	43.97	103.98	89.15	4.63	1.06	5.16	n.d.	n.d.	n.d.	0.02	147
212556_14	14	0.00	51.88	0.03	b.d.	51.08	0.76	0.07	0.32	0.02	6.40	45.32	104.79	91.82	1.14	1.55	5.49	n.d.	n.d.	n.d.	0.04	273
212556_30	30	0.03	51.76	0.01	b.d.	48.42	1.74	0.02	0.10	0.11	4.25	44.60	102.62	92.18	0.38	3.64	3.79	n.d.	n.d.	n.d.	0.45	3174
166135_30	30	0.04	51.69	0.04	0.02	49.20	0.53	0.00	0.70	0.00	5.00	44.70	102.73	91.92	2.55	1.11	4.41	0.23	0.28	1748	0.06	440
166135_25	25	0.02	51.49	0.04	b.d.	49.63	0.95	0.00	0.14	0.05	5.04	45.10	102.83	93.05	0.50	1.99	4.46	0.05	0.06	366	0.07	468
166135_26	26	0.08	51.48	0.10	0.03	47.38	0.62	0.05	1.73	0.30	5.33	42.58	102.30	87.66	6.35	1.30	4.70	0.16	0.20	1203	0.01	49
212513_121	120	0.02	51.48	0.08	b.d.	50.20	0.44	0.01	0.57	0.20	5.95	44.84	103.59	91.85	2.07	0.90	5.18	n.d.	n.d.	n.d.	0.02	147
212556_13	13	0.00	51.48	0.03	b.d.	50.00	0.73	0.06	0.24	0.00	5.42	45.12	103.09	92.82	0.89	1.52	4.77	n.d.	n.d.	n.d.	0.09	657
212513_106	105	0.00	51.46	0.01	b.d.	49.93	0.64	0.00	0.17	0.14	5.11	45.33	102.85	93.54	0.61	1.33	4.52	0.18	0.21	1315	0.04	252
166624_1_74	45	0.03	51.43	0.03	b.d.	49.22	1.13	0.02	0.26	0.07	5.09	44.64	102.70	92.18	0.96	2.36	4.50	0.00	n.d.	n.d.	0.01	77
212513_109	108	0.05	51.42	0.07	b.d.	50.42	0.61	0.01	0.16	0.15	5.66	45.33	103.46	93.16	0.60	1.28	4.96	0.24	0.29	1816	0.03	224
166135_27	27	0.06	51.40	0.09	b.d.	47.37	0.44	0.00	2.54	0.33	6.81	41.25	102.91	84.01	9.22	0.92	5.85	0.15	0.18	1083	0.02	154
212556_49	49	0.01	51.40	0.04	b.d.	49.61	1.10	0.04	0.22	0.04	5.44	44.71	103.01	92.11	0.81	2.29	4.79	n.d.	n.d.	n.d.	0.17	1188
166135_22	22	0.08	51.35	0.02	b.d.	49.78	1.20	0.00	0.03	0.11	5.40	44.92	103.10	92.65	0.10	2.50	4.76	n.d.	n.d.	22	n.d.	n.d.
166135_17	17	0.04	51.30	0.05	b.d.	50.56	1.08	0.01	0.30	0.04	6.73	44.50	104.05	90.87	1.09	2.24	5.80	n.d.	n.d.	0	0.07	510
212513_118	117	0.02	51.30	0.09	b.d.	50.46	0.64	0.00	0.18	0.11	5.88	45.17	103.39	92.87	0.66	1.33	5.15	0.08	0.10	628	0.03	182
212513_95	94	0.02	51.29	0.01	b.d.	50.52	0.79	0.00	0.13	0.13	6.03	45.09	103.49	92.63	0.46	1.65	5.26	0.10	0.12	740	n.d.	n.d.
212513_119	118	0.02	51.27	0.04	b.d.	50.48	0.66	0.03	0.15	0.12	5.91	45.16	103.37	92.89	0.55	1.38	5.17	0.08	0.09	575	0.03	210
212513_108	107	0.03	51.19	0.03	b.d.	49.77	1.12	0.00	0.17	0.31	5.75	44.60	103.20	91.98	0.63	2.34	5.05	0.18	0.22	1352	0.06	391
212513_107	106	0.02	51.17	0.08	b.d.	51.49	0.65	0.08	0.22	0.02	7.25	44.96	104.46	91.65	0.81	1.33	6.21	0.18	0.22	1352	0.06	433
212513_104	103	0.02	51.10	0.04	b.d.	50.74	0.63	0.04	0.14	0.15	6.30	45.07	103.48	92.69	0.51	1.31	5.49	0.07	0.08	501	n.d.	n.d.
212556_25	25	0.02	51.09	0.05	b.d.	50.89	0.81	0.02	0.19	0.03	6.79	44.78	103.79	91.75	0.70	1.68	5.87	n.d.	n.d.	n.d.	0.06	440
212513_101	100	0.01	51.08	0.06	b.d.	49.77	0.47	0.08	0.70	0.21	6.18	44.21	102.99	91.05	2.58	0.97	5.40	0.16	0.19	1158	0.01	91
212556_44	44	0.06	51.06	0.00	b.d.	50.21	0.91	0.00	0.17	0.07	6.13	44.69	103.10	92.12	0.62	1.90	5.36	0.08	0.09	568	0.06	440
212513_99	98	0.04	51.04	0.05	b.d.	49.85	0.48	0.04	0.66	0.22	6.25	44.23	103.01	91.10	2.44	1.00	5.46	0.18	0.22	1360	0.04	252
212556_20	20	0.00	51.04	0.02	b.d.	50.18	0.85	0.00	0.17	0.02	6.04	44.74	102.88	92.32	0.61	1.77	5.30	n.d.	n.d.	n.d.	0.10	720
166135_2	2	0.01	51.03	0.04	b.d.	50.60	0.48	0.03	1.19	0.03	8.12	43.29	104.22	87.85	4.29	0.98	6.87	n.d.	n.d.	n.d.	0.10	713
212513_122	121	0.00	51.02	0.04	b.d.	50.65	0.58	0.02	0.13	0.13	6.21	45.06	103.20	92.88	0.48	1.21	5.43	n.d.	n.d.	n.d.	n.d.	n.d.
212556_45	45	0.05	50.96	0.03	b.d.	50.49	0.99	0.00	0.11	0.12	6.52	44.62	103.41	91.85	0.41	2.06	5.67	n.d.	n.d.	n.d.	0.03	231
166624_1_44	15	0.02	50.95	0.08	b.d.	49.70	1.19	0.00	0.13	0.04	5.90	44.39	102.69	91.86	0.46	2.49	5.19	0.22	0.26	1614	0.06	391
166135_5	5	0.03	50.94	0.06	b.d.	50.31	0.63	0.00	0.81	0.05	7.32	43.72	103.56	89.45	2.96	1.30	6.29	n.d.	n.d.	n.d.	0.04	273
166135_13	13	0.02	50.93	0.03	b.d.	51.24	0.56	0.02	0.50	0.01	7.67	44.34	104.07	90.48	1.81	1.16	6.54	n.d.	n.d.	n.d.	0.02	168
166135_18	18	0.05	50.93	0.08	b.d.	50.33	1.05	0.02	0.23	0.05	6.67	44.32	103.41	91.17	0.84	2.19	5.80	0.02	0.02	149	0.07	510
212556_47	47	0.03	50.89	0.00	b.d.	49.32	1.65	0.00	0.12	0.12	6.05	43.88	102.73	90.79	0.44	3.46	5.31	n.d.	n.d.	n.d.	0.07	489
212513_111	110	0.05	50.81	0.00	b.d.	49.99	1.50	0.00	0.03	0.11	6.53	44.11	103.15	91.04	0.13	3.14	5.70	0.22	0.26	1614	0.08	538
212556_42	42	0.00	50.81	0.00	b.d.	49.73	1.56	0.04	0.13	0.15	6.50	43.88	103.07	90.58	0.48	3.26	5.68	n.d.	n.d.	n.d.	0.06	426
166135_1	1	0.03	50.80	0.05	b.d.	51.05	0.62	0.12	0.40	0.01	7.45	44.35	103.82	90.87	1.45	1.28	6.40	0.09	0.11	672	n.d.	n.d.

Appendix 1: Franklin magmatism, Thule Distric. Ilmenite analyses

sample No.	EMP No.	Weight%									Calculated			Gei-kilitite	pyro-phaniite	Hae-matite	V2O3	V2O5	V ppm	Nb2O5	Nb ppm	
		SiO2	TiO2	Al2O3	Cr2O3	FeO	MnO	NiO	MgO	CaO	Fe2O3	FeO	Sum									Ilmenite
166135_35	35	0.00	50.80	0.08	b.d.	49.82	0.58	0.00	1.04	0.02	7.31	43.24	103.06	88.70	3.80	1.21	6.29	0.02	0.02	149	0.03	182
212556_8	8	0.02	50.80	0.06	b.d.	49.55	0.50	0.04	0.86	0.06	6.57	43.64	102.55	90.05	3.17	1.05	5.73	0.06	0.07	426	n.d.	n.d.
166135_32	32	0.00	50.76	0.04	0.03	50.25	1.28	0.00	0.15	0.17	6.85	44.09	103.36	90.84	0.55	2.66	5.95	n.d.	n.d.	n.d.	0.04	273
212513_105	104	0.00	50.72	0.05	b.d.	50.23	0.57	0.00	0.15	0.07	6.07	44.77	102.40	92.90	0.57	1.19	5.35	0.26	0.32	1973	0.02	168
243410_61	61	0.05	50.72	0.18	b.d.	47.56	0.40	0.03	1.23	0.18	5.06	43.01	100.85	90.02	4.60	0.85	4.54	0.39	0.48	2944	0.03	217
212556_39	39	0.02	50.65	0.01	b.d.	50.54	1.17	0.00	0.17	0.10	7.20	44.06	103.38	90.71	0.62	2.44	6.23	n.d.	n.d.	n.d.	0.03	217
166135_29	29	0.05	50.64	0.06	b.d.	49.07	0.86	0.06	0.48	0.11	5.84	43.82	101.91	91.25	1.78	1.81	5.17	0.17	0.20	1240	0.05	377
212513_117	116	0.02	50.63	0.05	b.d.	50.87	0.65	0.00	0.12	0.06	6.91	44.65	103.09	92.19	0.46	1.35	6.01	0.13	0.15	941	n.d.	n.d.
166135_8	8	0.04	50.61	0.04	b.d.	50.98	0.56	0.00	0.70	0.02	8.09	43.70	103.76	89.40	2.55	1.16	6.90	0.01	0.02	105	0.09	650
166135_10	10	0.03	50.56	0.04	0.01	51.17	0.55	0.04	0.45	0.03	7.85	44.11	103.66	90.49	1.64	1.14	6.72	0.04	0.05	329	0.03	210
166624_1_48	19	0.03	50.55	0.06	b.d.	49.89	0.87	0.09	0.57	0.02	7.02	43.57	102.78	90.00	2.09	1.81	6.10	0.04	0.05	321	0.10	664
212556_38	38	0.05	50.55	0.01	0.01	48.85	2.11	0.00	0.12	0.18	6.39	43.10	102.52	89.49	0.46	4.44	5.62	n.d.	n.d.	n.d.	n.d.	n.d.
166135_33	33	0.02	50.54	0.06	b.d.	50.94	1.02	0.05	0.13	0.11	7.51	44.18	103.63	90.92	0.48	2.13	6.47	0.03	0.04	254	n.d.	n.d.
166672_1_31	85	0.04	50.50	0.06	0.01	49.31	1.03	0.02	0.12	0.00	5.72	44.17	101.65	92.31	0.43	2.18	5.09	0.33	0.40	2443	0.02	154
166672_1_30	84	0.05	50.45	0.26	b.d.	48.66	1.07	0.02	0.09	0.00	5.04	44.12	101.10	92.84	0.34	2.28	4.55	0.22	0.27	1636	n.d.	n.d.
166135_15	15	0.05	50.43	0.04	b.d.	50.33	0.70	0.01	0.42	0.17	7.15	43.89	102.86	90.78	1.54	1.47	6.21	n.d.	n.d.	n.d.	0.06	405
212556_19	19	0.06	50.42	0.02	b.d.	51.17	1.05	0.03	0.11	0.05	7.87	44.08	103.69	90.66	0.40	2.19	6.76	n.d.	n.d.	n.d.	0.12	825
166135_9	9	0.02	50.33	0.04	b.d.	50.69	0.64	0.06	0.41	0.02	7.56	43.89	102.96	90.63	1.51	1.33	6.54	0.07	0.09	531	0.06	433
212556_9	9	0.04	50.28	0.03	b.d.	51.06	0.47	0.04	0.88	0.01	8.77	43.17	103.68	88.39	3.21	0.97	7.43	0.09	0.11	650	n.d.	n.d.
212513_92	91	0.00	50.27	0.03	b.d.	51.28	0.50	0.00	0.15	0.11	7.60	44.44	103.09	91.85	0.54	1.04	6.57	0.12	0.14	867	0.01	n.d.
212556_16	16	0.03	50.26	0.01	b.d.	51.05	0.82	0.00	0.18	0.11	7.80	44.04	103.24	90.89	0.67	1.72	6.72	n.d.	n.d.	n.d.	0.08	552
212556_5	5	0.30	50.24	0.06	b.d.	50.88	0.98	0.09	0.16	0.09	7.76	43.89	103.58	90.65	0.60	2.05	6.70	n.d.	n.d.	n.d.	0.03	182
166624_1_50	21	0.03	50.20	0.07	b.d.	49.46	0.72	0.00	0.42	0.03	6.44	43.67	101.56	91.24	1.55	1.53	5.68	0.20	0.24	1487	0.06	391
166135_6	6	0.04	50.19	0.04	0.02	51.10	0.82	0.00	0.52	0.08	8.59	43.37	103.66	89.08	1.92	1.70	7.31	n.d.	n.d.	n.d.	0.08	573
166624_1_75	46	0.00	50.15	0.05	b.d.	50.92	0.76	0.01	0.36	0.04	8.04	43.69	103.09	90.18	1.33	1.58	6.91	0.20	0.24	1457	n.d.	n.d.
212513_98	97	0.00	50.15	0.03	b.d.	51.14	0.94	0.00	0.11	0.05	7.99	43.95	103.22	90.75	0.40	1.97	6.88	n.d.	n.d.	n.d.	0.04	252
212556_28	28	0.03	50.14	0.05	b.d.	50.35	0.86	0.05	0.21	0.08	7.23	43.85	102.49	91.12	0.77	1.81	6.30	n.d.	n.d.	n.d.	0.07	517
212556_55	55	0.04	50.13	0.18	0.02	48.66	0.50	0.00	0.98	0.07	6.48	42.83	101.23	89.56	3.66	1.05	5.73	0.49	0.60	3691	n.d.	n.d.
166624_1_66	37	1.00	50.12	0.27	0.02	48.49	1.32	0.00	0.23	0.07	5.73	43.33	102.08	91.20	0.85	2.81	5.14	0.09	0.11	650	0.12	860
243410_58	58	0.01	49.98	0.22	b.d.	49.65	0.47	0.00	0.70	0.05	7.13	43.23	101.78	90.18	2.59	0.98	6.25	0.14	0.17	1016	0.02	105
212513_97	96	0.00	49.87	0.06	b.d.	50.65	0.77	0.00	0.12	0.05	7.54	43.86	102.27	91.38	0.43	1.61	6.57	0.11	0.13	792	0.08	524
212513_113	112	0.00	49.81	0.00	b.d.	50.08	1.06	0.02	0.05	0.12	7.16	43.63	101.85	91.28	0.19	2.24	6.29	0.22	0.26	1621	0.06	440
212556_27	27	0.00	49.78	0.01	b.d.	50.64	0.88	0.04	0.15	0.02	7.82	43.60	102.30	90.79	0.57	1.85	6.79	0.00	n.d.	n.d.	n.d.	n.d.
166671_1_94	65	0.00	49.71	0.06	b.d.	50.56	0.46	0.00	0.98	0.00	8.96	42.49	102.66	87.80	3.60	0.96	7.64	0.30	0.37	2249	n.d.	n.d.
212556_31	31	0.01	49.45	0.01	b.d.	50.86	0.94	0.00	0.17	0.15	8.49	43.22	102.44	90.06	0.62	1.98	7.33	0.00	n.d.	n.d.	0.01	42
212556_41	41	0.01	49.43	0.00	b.d.	50.22	1.64	0.00	0.12	0.08	8.50	42.57	102.35	88.74	0.45	3.46	7.34	0.00	n.d.	n.d.	0.07	454
166672_1_32	86	0.00	49.40	0.08	b.d.	50.04	0.99	0.00	0.16	0.00	7.68	43.13	101.43	90.56	0.61	2.10	6.73	0.16	0.20	1203	n.d.	n.d.
212556_33	33	0.02	49.27	0.04	b.d.	50.35	0.70	0.07	0.38	0.01	8.25	42.92	101.67	89.92	1.42	1.48	7.18	0.07	0.08	501	n.d.	n.d.
166671_1_93	64	0.00	49.24	0.09	b.d.	50.97	0.77	0.04	0.43	0.14	9.15	42.74	102.58	88.96	1.59	1.62	7.84	0.20	0.24	1494	0.06	426
243410_63	63	0.03	49.19	0.17	b.d.	49.23	0.55	0.06	0.80	0.07	7.75	42.25	100.87	89.01	3.01	1.17	6.81	0.33	0.41	2496	n.d.	n.d.
212556_12	12	0.03	49.15	0.01	b.d.	50.77	0.89	0.05	0.24	0.10	8.79	42.86	102.12	89.63	0.90	1.89	7.59	0.09	0.11	672	n.d.	n.d.
212556_51	51	0.04	48.63	0.26	b.d.	49.31	0.52	0.06	0.54	0.03	7.85	42.24	100.17	89.88	2.05	1.11	6.96	0.33	0.40	2443	n.d.	n.d.
166671_1_99	70	0.02	48.62	0.03	b.d.	51.94	0.98	0.00	0.04	0.11	10.31	42.66	102.76	89.04	0.15	2.06	8.75	0.16	0.20	1210	n.d.	n.d.
212556_52	52	0.05	48.57	0.30	b.d.	50.18	0.48	0.01	0.99	0.04	9.73	41.42	101.60	86.92	3.71	1.02	8.35	0.43	0.53	3243	n.d.	n.d.
166671_1_95	66	0.05	48.56	0.06	0.02	51.45	0.64	0.03	0.33	0.07	10.02	42.43	102.21	88.85	1.24	1.35	8.56	0.27	0.33	2025	0.02	119
243410_57	57	0.06	48.54	0.23	b.d.	49.76	0.59	0.03	0.52	0.05	8.48	42.13	100.62	89.33	1.97	1.26	7.44	0.35	0.42	2600	0.04	273
243410_62	62	0.03	48.10	0.29	b.d.	51.18	0.36	0.02	1.21	0.06	11.60	40.74	102.40	85.04	4.48	0.76	9.72	0.37	0.45	2750	0.01	91

Appendix 1: Franklin magmatism, Thule Distric. Ilmenite analyses

sample No.	EMP No.	Weight%									Calculated			Geilkilite	pyrophanite	Hae-matite	V2O3	V2O5	V ppm	Nb2O5	Nb ppm	
		SiO2	TiO2	Al2O3	Cr2O3	FeO	MnO	NiO	MgO	CaO	Fe2O3	FeO	Sum									Ilmenite
243410_56	56	0.04	47.77	0.29	0.02	51.36	0.46	0.06	0.72	0.03	11.29	41.20	101.88	86.75	2.71	0.98	9.56	0.39	0.47	2877	0.02	133
Min		0.00	47.77	0.00	0.01	46.82	0.36	0.00	0.03	0.00	0.70	40.74	100.17	84.01	0.10	0.76	0.65	0.00	0.02	0	0.01	0
Max		1.00	53.25	0.30	0.10	51.94	2.11	0.12	2.54	0.33	11.60	46.52	104.79	96.02	9.22	4.44	9.72	0.49	0.60	3691	0.45	3174
Mean*		0.04	50.74	0.06	0.04	49.89	0.87	0.02	0.39	0.08	6.49	44.05	102.74	91.10	1.44	1.82	5.64	0.17	0.21	1268	0.06	395
Median		0.02	50.80	0.04	0.03	50.20	0.77	0.01	0.21	0.06	6.57	44.09	102.86	91.04	0.77	1.62	5.73	0.15	0.20	1158	0.05	339
st. dev		0.11	1.13	0.07	0.03	1.22	0.37	0.03	0.41	0.07	2.12	1.16	0.89	2.17	1.50	0.79	1.78	0.124	0.146	918	0.06	406

* Mean and median values are maximum values as all V₂O₃ and Nb₂O₅ value below detection are omitted.

Appendix 2: Magnetite in Franklin basalts

sample	No.	SiO2	TiO2	Al2O3	Cr2O3	FeO	MnO	NiO	MgO	CaO	V2O3	V2O5	V ppm	Nb2O5	Nb ppm	Ulvöspinel	magnetite	New sum
243410_59	59	0.27	23.44	1.91	b.d.	68.47	1.11	0.00	0.02	0.05	0.53	0.65	3990	0.034	238	68.13	31.87	96.81 *
212556_54	54	0.08	22.47	2.98	0.04	68.78	0.91	0.00	0.01	0.07	0.51	0.62	3796	0.008	56	64.49	35.51	96.97 *
212556_53	53	0.12	22.24	2.13	0.05	69.99	0.88	0.06	0.00	0.04	0.45	0.54	3325	0.017	119	64.05	35.95	97.28 *
243410_64	64	0.50	21.57	1.71	b.d.	70.27	1.00	0.00	0.01	0.06	0.27	0.33	2025	0.011	0	63.26	36.74	96.95 *
166135_36	36	0.00	20.84	0.78	0.04	72.29	0.88	0.05	0.01	0.72	0.93	1.13	6942	b.d.	0	59.81	40.19	97.81 *
166135_31	31	0.08	18.99	1.40	b.d.	75.79	0.51	0.02	0.03	0.01	0.72	0.87	5372	b.d.	0	53.78	46.22	99.33
212513_100	99	0.11	17.95	1.61	0.06	76.54	1.17	0.08	0.11	0.33	1.32	1.60	9833	b.d.	0	50.17	49.83	100.67
166624_1_51	22	0.10	17.40	2.22	0.08	76.48	0.62	0.08	0.03	0.08	1.06	1.29	7950	b.d.	0	48.98	51.02	99.76
166624_1_49	20	0.44	17.23	1.32	0.05	77.95	0.49	0.01	0.08	0.24	1.13	1.37	8436	b.d.	0	48.84	51.16	100.60
166624_1_52	23	0.12	17.18	1.47	0.07	78.93	0.57	0.01	0.10	0.02	0.70	0.85	5253	0.015	105	47.81	52.19	101.34
212556_40	40	0.03	16.99	0.93	0.02	79.36	1.13	0.05	0.05	0.03	0.58	0.71	4341	b.d.	0	47.17	52.83	101.57
166135_23	23	0.20	16.84	0.80	0.03	78.35	0.61	0.00	0.07	0.24	0.72	0.88	5410	0.062	433	47.73	52.27	100.06
166624_1_70	41	0.07	16.02	1.48	0.01	79.42	0.55	0.02	0.01	0.06	0.69	0.84	5148	b.d.	0	44.83	55.17	100.66
166624_1_57	28	0.05	15.80	1.02	b.d.	79.19	0.54	0.01	0.00	0.07	1.11	1.35	8287	b.d.	0	44.70	55.30	99.75
166135_3	3	0.00	15.41	1.54	0.09	76.83	0.57	0.05	0.01	0.50	1.35	1.64	10080	b.d.	0	44.18	55.82	97.99
166135_19	19	0.69	15.30	0.81	0.05	76.70	0.61	0.10	0.00	1.28	0.87	1.06	6508	b.d.	0	44.73	55.27	98.52
212556_6	6	0.07	15.30	0.95	b.d.	80.17	0.42	0.00	0.01	0.14	0.61	0.75	4588	0.015	105	43.13	56.87	100.24
212513_94	93	0.13	15.20	0.76	0.05	79.15	0.91	0.01	0.03	0.27	1.70	2.06	12673	b.d.	0	43.22	56.78	99.68
166624_1_76	47	0.17	15.12	2.00	0.08	79.64	0.54	0.03	0.03	0.03	1.07	1.30	7980	0.013	91	42.36	57.64	100.74
166135_4	4	0.07	14.92	2.02	0.08	79.51	0.23	0.07	0.03	0.15	1.06	1.28	7891	0.004	28	41.88	58.12	100.21
212556_29	29	0.10	14.30	0.91	0.00	79.75	0.49	0.02	0.01	0.31	0.88	1.06	6546	0.012	84	40.79	59.21	99.16
212556_15	15	0.06	14.07	1.21	0.02	79.91	0.41	0.01	0.03	0.23	0.85	1.03	6366	b.d.	0	40.00	60.00	99.24
212556_37	37	0.09	13.70	0.89	b.d.	82.40	0.51	0.03	0.03	0.15	0.57	0.69	4274	b.d.	0	38.28	61.72	101.29
212556_36	36	0.40	13.69	0.97	b.d.	81.64	0.42	0.05	0.00	0.44	0.57	0.69	4222	0.015	105	38.72	61.28	101.02
212556_43	43	0.06	13.41	0.91	0.02	81.73	0.43	0.07	0.01	0.21	0.63	0.76	4700	0.002	0	37.80	62.20	100.34
212556_4	4	0.62	13.30	0.67	b.d.	81.47	1.04	0.00	0.01	0.53	0.80	0.97	5985	b.d.	0	37.91	62.09	101.12
166624_1_60	31	0.14	13.29	1.92	0.03	81.33	0.48	0.00	0.02	0.12	1.08	1.31	8077	0.017	119	37.22	62.78	100.75
212556_18	18	0.78	11.71	0.58	b.d.	82.25	0.94	0.00	0.00	0.74	0.67	0.81	4991	b.d.	0	33.74	66.26	100.70
166624_1_61	32	0.07	11.59	1.87	0.04	82.26	0.41	0.08	0.02	0.06	1.68	2.04	12583	0.023	161	32.66	67.34	100.07
212556_17	17	0.63	11.46	0.57	b.d.	83.88	0.83	0.02	0.03	0.54	0.62	0.76	4663	0.046	322	32.52	67.48	101.77
212556_7	7	0.08	11.33	0.79	b.d.	83.89	0.37	0.02	0.00	0.16	0.91	1.10	6785	0.033	231	31.97	68.03	100.50
212556_3	3	0.39	11.23	0.99	b.d.	83.44	0.24	0.03	0.01	0.40	1.03	1.25	7726	0.010	70	31.96	68.04	100.51
212556_21	21	0.80	11.19	0.60	0.00	81.25	0.86	0.04	0.03	0.89	0.30	0.36	2204	0.021	147	32.69	67.31	99.36
166624_1_53	24	0.16	10.17	1.15	0.01	85.03	0.31	0.05	0.03	0.09	0.93	1.12	6912	b.d.	0	28.60	71.40	101.01
166671_1_101	72	0.08	9.76	1.18	b.d.	85.06	0.33	0.03	0.04	0.00	1.35	1.63	10050	0.023	161	27.51	72.49	100.53
166671_1_98	69	0.07	9.39	1.06	0.01	86.27	0.29	0.03	0.01	0.05	1.27	1.54	9497	0.002	14	26.27	73.73	101.34
averages		0.21	14.62	1.23	0.03	77.14	0.60	0.03	0.02	0.26	0.86	1.04	6539	0.190	74			

* The five first analyses have low sums. It is not clear why, but may be due to underestimation of the content of haematite component as a consequence of alteration

Appendix 3: Major and trace elements and CIPW-norms of Thule basalts

GGU#	165809	166135	166143	166147	166161	166163	166170	166171	166624	166630	166693	212513	212544	212556	243410	243557	166671	166672	166673	243558	243559
type	dyke 2	sill 2	dyke 2	dyke 2	sill 2	sill 2	dyke 2	sill 2	dyke 2	dyke 2	dyke 2	sill 2	dyke 2	sill 2	sill 2	sill 2	sill 2				
Bulk rock major element composition																					
SiO ₂	48.12	48.31	48.53	48.64	49.42	48.88	48.93	49.66	47.55	47.52	48.36	48.54	48.37	49.24	49.07	48.61	48.62	48.19	45.12	49.97	49.52
TiO ₂	5.21	5.08	4.49	4.79	5.18	3.68	4.05	3.80	5.19	5.25	4.77	3.75	4.67	4.48	5.34	4.85	3.99	4.51	5.82	4.13	4.51
Al ₂ O ₃	12.06	12.5	14.02	13.94	12.66	12.36	12.23	13.85	12.37	12.31	12.56	12.69	12.33	12.45	12.54	12.7	12.33	11.5	10.18	12.74	12.57
Fe ₂ O ₃	3.48	2.82	2.5	2.8	4.14	3.08	5.46	2.99	2.99	2.7	3.99	2.69	3.88	3.49	5	4.11	2.29	0.99	2.35	1.95	3.56
FeO	10.95	11.29	9.42	9.56	8.14	11.31	9.55	9.16	11.45	11.33	9.37	11.76	10.28	10.78	8.05	9.47	9.13	12.58	11.99	11.26	9.73
MnO	0.14	0.13	0.12	0.12	0.13	0.15	0.14	0.15	0.21	0.19	0.18	0.17	0.13	0.16	0.14	0.19	0.18	0.21	0.2	0.2	0.15
MgO	5.24	5.07	4.77	4.81	5.26	5.83	5.55	5.45	5.52	5.29	5.28	5.67	4.82	4.55	6.01	5.57	7.75	7.08	8.4	5.31	5.02
CaO	8.13	8.41	8.35	8.38	6.96	9.04	8.45	9.21	8.91	9.31	8.32	8.21	7.87	6.82	8.88	8.93	10.57	8.86	11.12	9.27	8.6
Na ₂ O	2.61	2.62	2.78	2.79	2.88	2.51	2.34	2.51	2.77	2.68	2.97	2.65	3.28	2.89	2.24	2.72	2.58	2.22	1.88	2.29	2.79
K ₂ O	1.42	0.72	1.4	1.27	1.76	0.78	0.64	0.46	0.734	0.555	1.558	1.04	1.32	1.94	0.7	0.676	0.595	0.765	0.623	1.097	1.46
P ₂ O ₅	0.5	0.46	0.47	0.45	0.56	0.3	0.35	0.38	0.461	0.476	0.549	0.32	0.54	0.49	0.49	0.518	0.429	0.434	0.149	0.413	0.4
LOI	1.65	2.18	2.12	1.9	2.05	1.8	1.56	1.63	1.9	1.78	1.69	2.29	2.14	2.14	1.19	1.77	1.68	2.63	2.27	1.57	1.21
sum	99.51	99.59	98.97	99.45	99.14	99.72	99.25	99.25	100.055	99.391	99.597	99.78	99.63	99.43	99.65	100.114	100.144	99.969	100.102	100.2	99.52
FeO*	14.08	13.83	11.67	12.08	11.87	14.08	14.46	11.85	14.14	13.76	12.96	14.18	13.77	13.92	12.55	13.17	11.19	13.47	14.10	13.01	12.93
mg#	0.40	0.40	0.42	0.42	0.44	0.43	0.41	0.45	0.41	0.41	0.42	0.42	0.39	0.37	0.46	0.43	0.55	0.49	0.52	0.42	0.41
Recalculated to 100% volatile free with preserved Fe₂O₃																					
SiO ₂	49.17	49.59	50.11	49.86	50.90	49.92	50.09	50.87	48.44	48.68	49.39	49.79	49.62	50.61	49.84	49.43	49.38	49.51	46.12	50.66	50.37
TiO ₂	5.32	5.22	4.64	4.91	5.34	3.76	4.15	3.89	5.29	5.38	4.87	3.85	4.79	4.60	5.42	4.93	4.05	4.63	5.95	4.19	4.59
Al ₂ O ₃	12.32	12.83	14.48	14.29	13.04	12.62	12.52	14.19	12.60	12.61	12.83	13.02	12.65	12.80	12.74	12.91	12.52	11.81	10.41	12.92	12.79
Fe ₂ O ₃	3.56	2.89	2.58	2.87	4.26	3.15	5.59	3.06	3.05	2.77	4.08	2.76	3.98	3.59	5.08	4.18	2.33	1.02	2.40	1.98	3.62
FeO	11.19	11.59	9.73	9.80	8.38	11.55	9.78	9.38	11.67	11.61	9.57	12.06	10.54	11.08	8.18	9.63	9.27	12.92	12.26	11.42	9.90
MnO	0.14	0.13	0.12	0.12	0.13	0.15	0.14	0.15	0.21	0.19	0.18	0.17	0.13	0.16	0.14	0.19	0.18	0.22	0.20	0.20	0.15
MgO	5.35	5.20	4.93	4.93	5.42	5.95	5.68	5.58	5.62	5.42	5.39	5.82	4.94	4.68	6.10	5.66	7.87	7.27	8.59	5.38	5.11
CaO	8.31	8.63	8.62	8.59	7.17	9.23	8.65	9.43	9.08	9.54	8.50	8.42	8.07	7.01	9.02	9.08	10.73	9.10	11.37	9.40	8.75
Na ₂ O	2.67	2.69	2.87	2.86	2.97	2.56	2.40	2.57	2.82	2.75	3.03	2.72	3.36	2.97	2.28	2.77	2.62	2.28	1.92	2.32	2.84
K ₂ O	1.45	0.74	1.45	1.30	1.81	0.80	0.66	0.47	0.75	0.57	1.59	1.07	1.35	1.99	0.71	0.69	0.60	0.79	0.64	1.11	1.49
P ₂ O ₅	0.51	0.47	0.49	0.46	0.58	0.31	0.36	0.39	0.47	0.49	0.56	0.33	0.55	0.50	0.50	0.53	0.44	0.45	0.15	0.42	0.41
sum	100.00	100.00	100.00	100.00	100.00	100.00	100.00	100.00	100.00	100.00	100.00	100.00	100.00	100.00	100.00	100.00	100.00	100.00	100.00	100.00	100.00
FeO*	14.39	14.20	12.05	12.38	12.22	14.38	14.81	12.14	14.41	14.10	13.24	14.55	14.13	14.31	12.75	13.39	11.37	13.84	14.42	13.20	13.16

Appendix 3: Major and trace elements and CIPW-norms of Thule basalts

GGU#	165809	166135	166143	166147	166161	166163	166170	166171	166624	166630	166693	212513	212544	212556	243410	243557	166671	166672	166673	243558	243559
type	dyke 2	sill 2	dyke 2	dyke 2	sill 2	sill 2	dyke 2	sill 2	dyke 2	dyke 2	dyke 2	sill 2	dyke 2	sill 2	sill 2	sill 2	sill 2				
Traces by ICP-MS (ppm)																					
Sc	31.59	27.96	26.49	26.60	30.68	34.43	31.68	33.60	30.81	28.99	24.63	30.14	25.07	22.22	28.55	23.95	33.64	30.90	37.53	26.81	24.41
Ti	3.48	3.33	2.89	3.05	3.27	2.27	2.44	2.31	3.19	3.16	2.78	2.08	2.60	2.49	2.91	2.73	2.49	2.75	3.39	2.31	2.44
V	453.89	416.98	367.45	412.80	436.30	451.13	451.21	402.11	463.29	441.50	376.58	416.11	363.72	328.98	411.30	370.17	452.20	374.48	438.04	324.18	325.05
Cr	41.17	52.82	68.77	68.61	116.02	105.83	65.69	146.30	57.89	52.84	30.20	66.06	46.40	23.56	112.66	45.68	334.86	206.59	296.85	91.24	46.31
Mn	0.16	0.15	0.13	0.13	0.13	0.16	0.15	0.15	0.16	0.13	0.12	0.16	0.13	0.15	0.12	0.12	0.13	0.15	0.14	0.13	0.13
Co	49.22	49.13	38.90	40.34	37.13	48.44	47.33	38.28	45.87	44.25	43.68	43.43	38.84	43.16	53.15	54.63	45.40	49.43	52.22	50.15	45.33
Ni	100.76	104.07	84.76	80.57	91.74	100.40	95.90	79.97	98.04	92.25	99.38	86.51	82.89	79.73	92.68	108.88	171.62	166.52	201.86	56.88	47.37
Cu	304.98	239.36	272.30	300.51	246.53	276.89	261.32	302.41	247.96	273.99	264.40	262.26	257.16	248.71	275.15	241.71	255.02	177.81	200.87	150.86	119.56
Zn	153.61	156.01	133.54	130.63	109.57	109.85	120.59	113.24	148.68	128.34	116.37	118.50	120.07	164.04	133.74	138.13	95.90	158.52	177.12	143.97	92.33
Ga	27.50	28.64	28.43	28.09	29.08	24.35	25.58	27.48	26.55	27.14	27.88	24.89	27.85	28.85	27.88	27.35	26.31	25.23	21.51	25.19	26.40
Rb	46.49	25.13	43.42	31.61	52.80	22.44	17.58	9.03	21.47	13.02	32.50	35.06	34.84	50.86	13.62	19.09	12.90	22.02	16.08	27.28	37.99
Sr	460.74	492.99	464.59	474.06	400.63	333.22	344.32	336.37	479.33	495.61	546.83	336.35	416.61	401.70	454.95	605.60	446.19	455.69	389.02	486.60	549.46
Y	48.55	47.41	46.29	46.42	51.73	39.05	43.19	47.34	42.06	43.81	47.71	39.79	53.83	51.71	46.53	45.48	37.50	41.68	25.73	41.49	43.23
Zr	451.71	341.57	416.95	405.99	458.53	259.73	305.04	317.16	362.51	389.93	429.64	267.49	464.50	448.52	409.32	412.35	324.38	347.75	213.76	337.47	363.47
Nb	34.89	35.50	28.39	28.18	33.51	20.70	24.87	23.81	30.58	31.94	37.81	21.50	32.92	35.10	30.16	37.14	24.09	33.78	22.21	30.71	33.03
Cs	0.24	0.23	0.26	0.19	0.11	0.31	0.32	0.25	0.50	0.46	0.15	0.45	0.22	0.51	0.12	2.17	0.27	0.50	0.37	0.53	0.70
Ba	178.31	181.40	318.62	338.62	314.62	320.50	174.98	121.46	186.45	138.66	273.71	466.78	298.24	841.33	144.17	255.76	124.55	194.53	124.13	357.53	494.63
La	31.99	33.60	28.31	27.24	32.11	19.30	22.69	21.60	26.68	28.58	35.87	19.52	32.98	38.52	25.95	35.58	23.86	31.24	15.35	32.22	34.98
Ce	86.15	86.76	76.32	73.75	88.05	50.90	59.34	58.81	70.92	75.51	91.65	51.89	87.72	95.85	72.32	89.93	66.88	79.57	39.03	78.67	85.63
Pr	13.20	12.61	11.63	11.16	13.43	7.49	8.88	8.94	10.61	11.41	13.11	7.94	13.65	13.79	11.50	13.10	10.28	11.55	5.94	11.43	12.08
Nd	61.39	58.72	55.50	53.10	63.52	36.15	42.34	42.71	50.21	52.94	60.01	37.52	63.26	63.19	54.98	59.16	48.40	53.01	27.77	51.35	54.20
Sm	14.41	13.91	13.28	12.80	15.41	9.06	10.37	10.92	11.79	12.69	13.77	9.43	15.21	15.07	13.44	13.79	11.36	12.19	6.93	11.81	12.36
Eu	4.41	4.24	4.17	3.99	4.59	2.84	3.20	3.46	3.74	3.83	4.20	2.97	4.55	4.64	4.11	4.26	3.57	3.77	2.37	3.62	3.78
Gd	14.16	13.49	12.89	12.62	14.71	9.28	10.70	11.30	11.57	12.34	13.66	9.80	14.70	14.61	13.02	13.20	10.70	12.20	7.05	11.75	11.96
Tb	1.98	1.91	1.79	1.81	2.11	1.38	1.59	1.68	1.68	1.74	1.89	1.41	2.12	2.06	1.84	1.86	1.51	1.68	1.02	1.63	1.70
Dy	10.33	10.19	9.68	9.50	11.06	7.81	8.71	9.21	8.68	9.07	9.59	7.86	11.16	10.78	9.77	9.57	7.85	8.77	5.47	8.53	8.74
Ho	1.85	1.78	1.75	1.72	1.96	1.45	1.60	1.74	1.58	1.64	1.71	1.47	2.01	1.93	1.74	1.72	1.42	1.56	0.99	1.54	1.58
Er	4.62	4.32	4.38	4.36	4.88	3.76	4.18	4.51	3.90	4.15	4.21	3.87	4.94	4.74	4.34	4.25	3.51	3.89	2.43	3.82	3.97
Tm	0.62	0.57	0.57	0.57	0.66	0.52	0.57	0.62	0.51	0.56	0.56	0.52	0.65	0.63	0.59	0.56	0.46	0.50	0.31	0.52	0.53
Yb	3.39	3.27	3.32	3.30	3.74	3.04	3.31	3.63	2.98	3.13	3.22	3.10	3.74	3.63	3.37	3.19	2.64	2.91	1.83	2.98	3.03
Lu	0.51	0.45	0.47	0.47	0.52	0.44	0.48	0.52	0.42	0.43	0.44	0.45	0.54	0.49	0.46	0.45	0.37	0.41	0.26	0.43	0.43
Hf	11.25	8.83	10.19	10.11	11.44	6.64	7.75	7.98	8.86	9.68	10.33	6.65	11.35	10.96	9.96	10.21	7.96	8.87	5.77	8.50	8.96
Ta	2.24	2.26	1.85	1.85	2.11	1.38	1.60	1.57	1.94	2.00	2.37	1.35	2.02	2.13	1.92	2.26	1.64	2.04	1.46	1.91	2.02
Pb	3.03	4.52	4.37	3.74	3.50	3.02	2.71	1.47	1.69	1.75	4.66	8.38	5.60	10.04	3.59	2.94	1.59	6.29	6.78	8.36	4.02
Th	2.72	3.41	2.79	2.73	2.79	1.76	2.13	1.73	2.14	2.46	3.77	1.92	3.16	4.92	2.67	3.90	1.79	3.07	1.61	3.40	3.83
U	0.88	0.92	0.81	0.81	0.86	0.52	0.60	0.60	0.66	0.80	1.06	0.57	0.96	1.15	0.80	1.02	0.62	0.67	0.45	0.83	1.01

Appendix 3: Major and trace elements and CIPW-norms of Thule basalts

GGU#	165809	166135	166143	166147	166161	166163	166170	166171	166624	166630	166693	212513	212544	212556	243410	243557	166671	166672	166673	243558	243559
type	dyke 2	sill 2	dyke 2	dyke 2	sill 2	sill 2	dyke 2	sill 2	dyke 2	dyke 2	dyke 2	sill 2	dyke 2	sill 2	sill 2	sill 2	sill 2				
CIPW-norm (wt-%)																					
Fe₂O₃/FeO* = 0.20																					
Quartz	3.64	5.79	3.49	3.87	4.86	3.49	6.13	6.37	2.88	4.18	1.46	2.52	1.48	3.51	7.51	4.51	1.01	4.19	0.00	6.00	3.56
Plagioclase	39.97	43.51	46.60	46.51	42.06	42.24	41.83	47.54	43.37	43.61	42.42	43.14	43.92	40.85	41.78	44.25	42.80	38.92	34.11	41.14	41.81
Orthoclase	8.57	4.37	8.57	7.68	10.76	4.73	3.90	2.78	4.43	3.37	9.40	6.32	8.04	11.76	4.20	4.08	3.55	4.61	3.78	6.56	8.81
Diopside	16.81	15.58	14.08	14.11	12.08	19.08	15.77	15.11	18.40	19.35	17.88	16.05	17.36	13.05	15.46	17.00	23.96	18.33	30.23	18.33	18.82
Hypersthen	15.07	15.19	13.43	13.43	14.82	17.97	18.86	15.98	15.15	13.60	14.01	19.22	14.28	16.29	15.45	15.23	16.31	19.70	14.87	14.82	13.11
Olivine	0.00	0.00	0.00	0.00	0.00	0.00	0.00	0.00	0.00	0.00	0.00	0.00	0.00	0.00	0.00	0.00	0.00	0.00	0.73	0.00	0.00
Ilmenite	10.12	9.89	8.81	9.33	10.14	7.14	7.90	7.39	10.05	10.22	9.27	7.29	9.10	8.76	10.33	9.38	7.69	8.77	11.28	7.94	8.72
Magnetite	4.64	4.57	3.89	3.99	3.94	4.64	4.78	3.91	4.64	4.54	4.28	4.68	4.55	4.61	4.12	4.32	3.67	4.45	4.64	4.25	4.25
Apatite	1.18	1.09	1.14	1.07	1.34	0.72	0.83	0.90	1.09	1.14	1.30	0.76	1.27	1.16	1.16	1.23	1.02	1.02	0.35	0.97	0.95
Total	100.00	99.99	100.01	99.99	100.00	100.01	100.00	99.98	100.01	100.01	100.02	99.98	100.00	99.99	100.01	100.00	100.01	99.99	99.99	100.01	100.03
Fe₂O₃/FeO* = 0.15																					
Quartz	2.75	4.91	2.74	3.11	4.12	2.54	5.20	5.63	1.99	3.25	0.66	1.63	0.62	2.60	6.72	3.69	0.31	3.35	0.00	5.19	2.74
Plagioclase	40.00	43.54	46.63	46.54	42.09	42.31	41.86	47.57	43.40	43.68	42.44	43.17	43.94	40.85	41.81	44.27	42.83	38.95	34.14	41.16	41.81
Orthoclase	8.57	4.37	8.57	7.68	10.76	4.73	3.90	2.78	4.43	3.37	9.40	6.32	8.04	11.82	4.20	4.08	3.55	4.61	3.78	6.56	8.81
Diopside	16.93	15.69	14.18	14.22	12.14	19.22	15.87	15.16	18.48	19.52	17.96	16.11	17.48	13.16	15.58	17.12	24.09	18.39	30.41	18.44	18.96
Hypersthen	16.97	17.06	15.04	15.03	16.44	19.87	20.85	17.60	17.08	15.43	15.76	21.18	16.13	18.19	17.13	16.99	17.75	21.53	13.44	16.52	14.82
Olivine	0.00	0.00	0.00	0.00	0.00	0.00	0.00	0.00	0.00	0.00	0.00	0.00	0.00	0.00	0.00	0.00	0.00	0.00	3.10	0.00	0.00
Ilmenite	10.12	9.91	8.81	9.33	10.16	7.14	7.90	7.41	10.05	10.22	9.27	7.31	9.12	8.76	10.33	9.38	7.69	8.79	11.30	7.96	8.72
Magnetite	3.48	3.44	2.91	3.00	2.96	3.48	3.60	2.94	3.48	3.41	3.20	3.52	3.42	3.47	3.09	3.25	2.75	3.33	3.48	3.19	3.19
Apatite	1.18	1.09	1.14	1.07	1.34	0.72	0.83	0.90	1.09	1.14	1.30	0.76	1.27	1.16	1.16	1.23	1.02	1.04	0.35	0.97	0.95
Total	100.00	100.01	100.02	99.98	100.01	100.01	100.01	99.99	100.00	100.02	99.99	100.00	100.02	100.01	100.02	100.01	99.99	99.99	100.00	99.99	100.00
Fe₂O₃/FeO* = 0.10																					
Quartz	1.86	0.00	2.00	2.35	3.36	1.65	0.00	0.00	1.05	2.37	0.00	0.73	0.00	1.67	5.92	2.85	0.00	2.46	0.00	0.00	1.92
Plagioclase	40.02	43.56	46.66	46.57	42.11	42.34	41.88	47.64	43.46	43.70	42.44	43.20	43.97	40.91	41.83	44.30	42.85	38.95	34.14	41.19	41.84
Orthoclase	8.57	4.37	8.57	7.68	10.76	4.73	3.90	2.78	4.43	3.37	9.46	6.32	8.04	11.82	4.20	4.08	3.55	4.67	3.78	6.56	8.81
Diopside	17.00	15.79	14.23	14.27	12.22	19.33	15.91	15.29	18.63	19.64	18.09	16.20	17.48	13.24	15.64	17.18	24.21	18.51	30.60	18.50	19.08
Hypersthen	18.92	18.94	16.65	16.70	18.06	21.78	22.87	19.18	18.94	17.29	16.70	23.13	17.14	20.13	18.84	18.79	17.76	23.36	11.97	18.30	16.56
Olivine	0.00	0.00	0.00	0.00	0.00	0.00	0.00	0.00	0.00	0.00	0.00	0.00	0.68	0.00	0.00	0.00	1.08	0.00	5.52	0.00	0.00
Ilmenite	10.12	9.91	8.81	9.34	10.16	7.14	7.90	7.41	10.07	10.22	9.27	7.31	9.12	8.76	10.33	9.40	7.71	8.79	11.30	7.96	8.74
Magnetite	2.32	2.29	1.94	2.00	1.97	2.32	2.39	1.96	2.32	2.28	2.13	2.35	2.28	2.31	2.06	2.16	1.83	2.23	2.32	2.13	2.13
Apatite	1.18	1.09	1.14	1.07	1.34	0.72	0.83	0.90	1.09	1.14	1.30	0.76	1.30	1.16	1.16	1.23	1.02	1.04	0.35	0.97	0.95
Total	99.99	99.98	100.00	99.98	99.98	100.01	99.98	100.00	99.99	100.01	99.99	100.00	100.01	100.00	99.98	99.99	100.01	100.01	99.98	99.99	100.03

Appendix 4: Modelling of V , V2O5 , Nb and Nb2O5 contents of Franklin basalts

Based on norms in appendix 3

GGU#	165809	166135	166143	166147	166161	166163	166170	166171	166624	166630	166693	212513	212544	212556	243410	243557	166671	166672	166673	243558	243559
type	dyke 2	sill 2	dyke 2	dyke 2	sill 2	sill 2	dyke 2	sill 2	dyke 2	dyke 2	dyke 2	sill 2	dyke 2	sill 2	sill 2	sill 2	sill 2				

Modelled liquidus $TiMt_{24}$ and ilm_{24} on basis of CIPW-norms in Table YYY

Assumes $TiMt_{24}$ = normative magnetite + 0.82 proportion normative ilmenite.

$Fe_2O_3/FeO^* = 0.20$

$TiMt_{24}$	8.44	8.32	7.08	7.26	7.17	8.44	8.70	7.12	8.44	8.26	7.79	8.52	8.28	8.39	7.50	7.86	6.68	8.10	8.44	7.74	7.74
ilm_{24}	6.32	6.14	5.62	6.06	6.91	3.34	3.98	4.18	6.25	6.50	5.76	3.45	5.37	4.98	6.95	5.84	4.68	5.12	7.48	4.46	5.24
$TiMt_{24}/ilm_{24}$	1.34	1.35	1.26	1.20	1.04	2.53	2.19	1.70	1.35	1.27	1.35	2.47	1.54	1.68	1.08	1.35	1.43	1.58	1.13	1.74	1.48

$Fe_2O_3/FeO^* = 0.15$

$TiMt_{24}$	6.33	6.26	5.30	5.46	5.39	6.33	6.55	5.35	6.33	6.21	5.82	6.41	6.22	6.32	5.62	5.92	5.01	6.06	6.33	5.81	5.81
ilm_{24}	7.27	7.09	6.42	6.87	7.73	4.29	4.95	5.00	7.20	7.42	6.65	4.42	6.32	5.91	7.80	6.72	5.44	6.06	8.45	5.34	6.10
$TiMt_{24}/ilm_{24}$	0.87	0.88	0.82	0.79	0.70	1.48	1.32	1.07	0.88	0.84	0.88	1.45	0.99	1.07	0.72	0.88	0.92	1.00	0.75	1.09	0.95

$Fe_2O_3/FeO^* = 0.10$

$TiMt_{24}$	4.22	4.17	3.53	3.64	3.59	4.22	4.35	3.57	4.22	4.15	3.88	4.28	4.15	4.20	3.75	3.93	3.33	4.06	4.22	3.88	3.88
ilm_{24}	8.22	8.03	7.22	7.70	8.54	5.24	5.94	5.80	8.17	8.35	7.52	5.38	7.25	6.87	8.64	7.63	6.21	6.96	9.40	6.21	6.99
$TiMt_{24}/ilm_{24}$	0.51	0.52	0.49	0.47	0.42	0.81	0.73	0.61	0.52	0.50	0.52	0.79	0.57	0.61	0.43	0.52	0.54	0.58	0.45	0.62	0.55

Mass balance for V and Nb in bulk rocks as collected

$Fe_2O_3/FeO^* = 0.20$ (preferred)

																					%		
																					mean	dev.	
V (ppm), calculated	399	392	338	349	353	371	387	325	398	393	367	375	383	384	367	371	313	374	410	353	360	370	
calc-meas.	-55	-25	-30	-64	-83	-80	-64	-77	-65	-48	-9	-41	20	55	-44	1	-140	-1	-28	29	35	-34	-9
Nb (ppm)	33	32	29	30	32	24	27	24	33	33	30	25	30	29	33	30	25	29	36	26	29	29	
calc-meas.	-2	-3	0	2	-1	4	2	1	2	1	-8	3	-3	-6	3	-7	1	-5	14	-4	-5	-1	-2

$Fe_2O_3/FeO^* = 0.15$

V (ppm)	323	319	274	284	290	295	310	262	322	320	297	299	310	310	300	301	252	301	334	284	291	299	
calc-meas.	-131	-98	-94	-128	-147	-156	-141	-140	-141	-122	-80	-117	-54	-19	-112	-69	-200	-74	-104	-40	-34	-105	-35
Nb (ppm)	32	31	28	29	32	23	26	24	32	32	29	24	29	28	32	30	24	28	35	26	28	29	
calc-meas.	-3	-4	-1	1	-2	3	1	0	1	0	-8	2	-4	-7	2	-7	0	-6	13	-5	-5	-1	-5

Appendix 4: Modelling of V, V2O5, Nb and Nb2O5 contents of Franklin basalts

Appendix 4 continued

GGU#	165809	166135	166143	166147	166161	166163	166170	166171	166624	166630	166693	212513	212544	212556	243410	243557	166671	166672	166673	243558	243559	
type	dyke 2	sill 2	dyke 2	dyke 2	sill 2	sill 2	dyke 2	sill 2	dyke 2	dyke 2	dyke 2	sill 2	dyke 2	sill 2	sill 2	sill 2	sill 2					
<i>Fe₂O₃/FeO* = 0.10</i>																						
V (ppm)	247	243	210	219	225	219	231	198	247	246	227	223	235	234	232	230	193	229	258	214	222	228
calc-meas.	-207	-174	-157	-194	-211	-232	-220	-204	-216	-196	-150	-193	-128	-95	-179	-140	-260	-146	-180	-110	-103	-176
Nb (ppm)	31	31	27	29	31	22	25	23	31	31	29	23	28	27	32	29	24	27	35	25	27	28
calculated - measured	-4	-5	-1	0	-2	2	0	-1	0	-1	-9	2	-5	-8	1	-8	0	-7	12	-6	-6	-2

Based on measured averages:

Magnetite: 6538 ppm V and 74 ppm Nb (Table xx)

Ilmenite: 945 ppm V and 291 ppm Nb (Table xx)

Modelled liquidus V in titanomagnetite and Nb in ilmenite

Based on normative proportion of TiMt₂₄ and Ilm₂₄ and bulk rock V and Nb.

All V in titanomagnetite and all Nb in ilmenite

																						obs.	
																						mean	ave
<i>Fe₂O₃/FeO* = 0.20</i>																							
V (ppm)	5375	5013	5190	5685	6084	5342	5187	5651	5486	5343	4834	4885	4392	3921	5485	4708	6770	4624	5187	4191	4202	5122	6539
V ₂ O ₅ wt. %	0.84	0.78	0.81	0.89	0.95	0.83	0.81	0.88	0.86	0.83	0.75	0.76	0.69	0.61	0.86	0.73	1.06	0.72	0.81	0.65	0.66	0.80	
Nb (ppm)	553	578	505	465	485	621	625	569	490	492	656	623	613	705	434	636	515	660	297	689	631	564	
Nb ₂ O ₅ wt. %	0.08	0.08	0.07	0.07	0.07	0.09	0.09	0.08	0.07	0.07	0.09	0.09	0.09	0.10	0.06	0.09	0.07	0.09	0.04	0.10	0.09	0.08	0.06
<i>Fe₂O₃/FeO* = 0.15 (preferred)</i>																							
V (ppm)	7166	6660	6938	7561	8099	7123	6887	7515	7315	7114	6466	6495	5843	5209	7314	6258	9035	6179	6916	5584	5599	6823	6538
V ₂ O ₅ wt. %	1.12	1.04	1.08	1.18	1.26	1.11	1.07	1.17	1.14	1.11	1.01	1.01	0.91	0.81	1.14	0.98	1.41	0.96	1.08	0.87	0.87	1.06	
Nb (ppm)	480	501	442	410	433	483	503	476	425	430	569	486	521	593	387	553	443	557	263	575	541	480	
Nb ₂ O ₅ wt. %	0.07	0.07	0.06	0.06	0.06	0.07	0.07	0.07	0.06	0.06	0.08	0.07	0.07	0.08	0.06	0.08	0.06	0.08	0.04	0.08	0.08	0.07	0.06
<i>Fe₂O₃/FeO* = 0.10</i>																							
V (ppm)	10750	10005	10407	11341	12169	10684	10373	11272	10972	10640	9714	9729	8765	7825	10970	9416	13577	9227	10374	8362	8385	10236	6539
V ₂ O ₅ wt. %	1.68	1.56	1.62	1.77	1.90	1.67	1.62	1.76	1.71	1.66	1.52	1.52	1.37	1.22	1.71	1.47	2.12	1.44	1.62	1.30	1.31	1.60	
Nb (ppm)	425	442	393	366	392	395	419	410	374	383	503	399	454	511	349	487	388	485	236	494	472	418	
Nb ₂ O ₅ wt. %	0.06	0.06	0.06	0.05	0.06	0.06	0.06	0.06	0.05	0.05	0.07	0.06	0.06	0.07	0.05	0.07	0.06	0.07	0.03	0.07	0.07	0.06	0.06

Table 1: Regional estimate, both sides of Granville Fjord
 Red polygons in map (Fig. 68)

Western block, map scale 1:500k (Booth Sund block)

Block name	Area (mm ²)*	Area (km ²)	calculated volume of sill rock
a	462	115.5	13.86
b	72	18	2.16
c	50	12.5	1.5
d	132	33	3.96
e1	115	28.75	3.45
e2	230	57.5	6.9
f	380	95	11.4
subtotal area		360	43.23
			0
			0

Eastern block, map scale 1:500k (Moriusaq block)

Block name	Area (mm ²)*	Area (km ²)	calculated volume of sill rock
g	930	232.5	27.9
h	449.5	112.375	13.485
i	77	19.25	2.31
j	16	4	0.48
k	184	46	5.52
subtotal area		414	49.695

*measured in map

Table 2: Estimate of primary ilmenite, remaining ilmenite and eroded ilmenite. Eroded ilmenite available for deposition in sediments.

	Booth Sund block	Moriusaq block	Total
Area, km ²	360	414	774
Thickness (km)*	0.4	0.4	0.4
Vol. frac. Sills**	0.3	0.3	0.3
Eroded fraction***	0.4	0.4	0.4
Density, rock kg/m ³	2600	2600	2600
m ³ /km ³		1.00E+09	
kg/Gt		1.00E+12	
Total volume, km ³	144.1	165.65	309.75
Total mass source rock, Gt	112	129	242
Scenario A, 9 wt. % ilmenite in source****			
Wt.% ilmenite in source	9	9	9
Total mass ilmenite, Gt	10	11.6	22
Contained ilmenite, Gt	6	7.0	13
Eroded ilmenite, Gt	4.0	4.7	8.7
Scenario B, 7 wt. % ilmenite in source****			
Wt.% ilmenite in source	7	7	7
Total mass ilmenite, Gt	8	9	17
Contained ilmenite, Gt	5	5	10
Eroded ilmenite, Gt	3	4	7
Continued			
Appendix 5, Table 2 continued			
Scenario C, 5 wt. % ilmenite in source****			
Wt.% ilmenite in source	5	5	5
Total mass ilmenite, Gt	6	6	12
Contained ilmenite, Gt	3	4	7
Eroded ilmenite, Gt	2	3	5

* conservative estimate of the succession hosting the sills

** Conservative estimate of the stratigraphic proportion of sill material (Dawes, 2006)

*** Estimate of the proportion of the 400 m thick and sill-bearing section that has been eroded

**** Ilmenite content of host rocks evaluated on basis of normative composition, petrographic observations and backscatter images.

Observed contents of ilmenite vary from app. 5 to 9 wt% and 7 wt % is a probable average for the ilmenite content of the source rocks.

Table 3: Estimated mass of ilmenite contained in dykes**Western block (Booth Sound block)**

East-West (m)	40	40
Integrated dyke width (m)*****	0.2	0.2
vertical section (m)*****	0.1	0.5
Volume of dike rock (km ³)	0.8	4
mass of dyke rock (Gt)	2.08	10.4
Contained ilmenite (Gt)*****	0.104	0.52

Eastern lock (Moriusaq block)

East-West (m)	40	40
Integrated dyke width (m)*****	0.2	0.2
vertical section (m)	0.1	0.5
Volume of dike rock (km ³)	0.8	4
mass of dyke rock (Gt)	2.08	10.4
Contained ilmenite (Gt)	0.104	0.52

Total ilmenite contained in dykes (Gt)

	0.208	1.040
--	-------	-------

***** Added up total thickness of dykes in the block

***** height of dyke section includede in calculation

***** Assumes 0.05 wt% ilmenite in dyke rocks.

Table 4: Ilmenite in valley draining westwards into Granville Fj.**Model 1: Volume between the north-sloping hillside and the Qaanaaq Fault***Blue square in map (M)*

Sill number	1	2	3	4	5	6	7	8	9
Length parallel to coast, km	12								
Width parallel to Granville Fj., km	5	5.4	6.5	6.8	8	8.6	9.4	10	10.8
Sill thickness (m)*	20	20	20	20	20	20	20	20	20
Vol. sill now removed, km ³	1.2	1.296	1.56	1.632	1.92	2.064	2.256	2.4	2.592
Total vol. eroded rock, km^{3**}	16.92								
Total mass eroded rock, Gt	43.99								
Scenario A. 9 wt. % ilmenite in source									
Ilmenite introduced to Granville Fj., Gt	3.96								
Scenario B. 7. wt. % ilmenite in source									
Ilmenite introduced to Granville Fj., Gt	3.08								
Scenario C. 5 wt. % ilmenite in source									
Ilmenite introduced to Granville Fj., Gt	2.20								

* Standardised thickness on basis of descriptions in field notes (P.R. Dawes). More detailed estimates require collection of profile and samples in the valley.

**Calculation using: 1) Density, rock kg/m³ = 2600, 2) m³/km³ = 1.00E+12, and kg/Gt = 1.00E+12.

Table 5: Ilmenite in valley draining westwards into Granville Fj.**Model 2: volume between the north-sloping hillside and northern limit of the valley floor**

South of stippled line, no evidence that the sills extended all the way to the fault to the Qaanaaq formation in postglacial times.

Sill number	1	2	3	4	5	6	7	8	9
Length parallel to coast, km	12								
Width parallel to Granville Fj., km	1.25	1.65	2.75	3.05	4.25	4.85	5.65	6.25	7.05
Sill thickness (m)*	20	20	20	20	20	20	20	20	20
Vol. sill now removed, km ³	0.3	0.396	0.66	0.732	1.02	1.164	1.356	1.5	1.692
Total vol. eroded rock, km³	8.82								
Total mass eroded rock, Gt	22.93								
Scenario A. 9 wt. % ilmenite in source									
Ilmenite introduced to Granville Fj., Gt	2.06								
Scenario B. 7 wt. % ilmenite in source									
Ilmenite introduced to Granville Fj., Gt	1.61								
Scenario C. 5 wt. % ilmenite in source									
Ilmenite introduced to Granville Fj., Gt	1.15								

* Standardised thickness on basis of descriptions in field notes (P.R. Dawes). More detailed estimates require collection of profile and samples in the valley.

**Calculation using: 1) Density, rock kg/m³ = 2600, 2) m³/km³ = 1.00E+12, and kg/Gt = 1.00E+12.

Valley draining westwards into Granville Fj.

South of stippled line: volume between the north-sloping hillside and northern limit of the valley floor (no evidence that the sills extended all the way to the fault to the Qaanaaq formation)

Sill number	1	2	3	4	5	6	7	8	9
Length parallel to coast, km	12								
Width parallel to Granville Fj., km	1.25	1.65	2.75	3.05	4.25	4.85	5.65	6.25	7.05
Sill thickness (m)*	20	20	20	20	20	20	20	20	20
Vol. sill now removed, km ³	0.3	0.396	0.66	0.732	1.02	1.164	1.356	1.5	1.692
Density, rock kg/m ³	2600								
m ³ /km ³	1.000E+09								
kg/Gt	1.00E+12								
Total vol. eroded rock, km³	8.82								
Total mass eroded rock, Gt	22.93								
Scenario A. 9 wt. % ilmenite in source									
Ilmenite introduced to Granville Fj., Gt	2.1								
Scenario B. 7 wt. % ilmenite in source									
Ilmenite introduced to Granville Fj., Gt	1.6								
Scenario C. 5 wt. % ilmenite in source									
Ilmenite introduced to Granville Fj., Gt	1.1								

* Standardized thickness on basis of descriptions in field notes (P.R. Dawes). More detailed estimates require collection of profile and samples in the valley.

Checked by Troels Nielsen
April 7th, 2017

Table 6: Estimate of eroded ilmenite from hillside behind Moriussaq, stretching from Granville Fjord to Kap Abernathy

Sills		Dykes		
Area, km ²	168	Total thickness dykes, m	150	
Thickness, accumulated (m)	60	Coast parallel length, km	12	
Density, rock kg/m ³	2600	Depth of dykes, m	100	500
m ³ /km ³	1.00E+09	Vol. source rock, km ³	0.18	0.90
kg/Gt	1.00E+12	Mass source rock, Gt	0.5	2.3
Total volume, km ³	10.1			
Total mass sills, Gt	26.2	Scenario A, 9 wt.% ilm (NB change of units!)		
Fraction eroded	0.4	Contained ilmenite, Mt	42	211
Scenario A. 9 wt. % ilmenite in source		Scenario B, 7 wt.% il		
Total ilmenite, Gt	2.4	Contained ilmenite, Mt	33	164
Ilmenite remaining in sills, Gt	1.4			
Ilmenite eroded from sills, Gt	0.9	Scenario C, 5 wt.% il		
		Contained ilmenite, Mt	23	117
Scenario B. 7 wt. % ilmenite in source				
Total ilmenite, Gt	1.8			
Ilmenite remaining in sills, Gt	1.1			
Ilmenite eroded from sills, Gt	0.7			
Scenario C. 5 wt. % ilmenite in source				
Total ilmenite, Gt	1.3			
Ilmenite remaining in sills, Gt	0.8			
Ilmenite eroded from sills, Gt	0.5			

Checked by Troels Nielsen
April 7th, 2017